



**A STUDY OF VIBRATION ATTENUATION OF SHEAR
BUILDINGS UNDER DYNAMIC LOADS USING TLCDS**

LUCAS BORCHARDT GHEDINI

UNIVERSIDADE DE BRASÍLIA

FACULDADE DE TECNOLOGIA

DEPARTAMENTO DE ENGENHARIA CIVIL E AMBIENTAL

BRASÍLIA/DF

JANEIRO - 2023

UNIVERSIDADE DE BRASÍLIA
FACULDADE DE TECNOLOGIA
DEPARTAMENTO DE ENGENHARIA CIVIL E AMBIENTAL

**A STUDY OF VIBRATION ATTENUATION OF SHEAR
BUILDINGS UNDER DYNAMIC LOADS USING TLCDS**

LUCAS BORCHARDT GHEDINI

ORIENTADOR: LINEU JOSÉ PEDROSO

DISSERTAÇÃO DE MESTRADO EM ESTRUTURAS E CONSTRUÇÃO CIVIL

PUBLICAÇÃO: E.DM – 01A/23

BRASÍLIA/DF

JANEIRO - 2023

UNIVERSIDADE DE BRASÍLIA
FACULDADE DE TECNOLOGIA
DEPARTAMENTO DE ENGENHARIA CIVIL E AMBIENTAL

**A STUDY OF VIBRATION ATTENUATION OF SHEAR BUILDINGS
UNDER DYNAMIC LOADS USING TLCDS**

LUCAS BORCHARDT GHEDINI

DISSERTAÇÃO DE MESTRADO SUBMETIDA AO DEPARTAMENTO DE ENGENHARIA CIVIL E AMBIENTAL DA FACULDADE DE TECNOLOGIA DA UNIVERSIDADE DE BRASÍLIA COMO PARTE DOS REQUISITOS NECESSÁRIOS PARA A OBTENÇÃO DO GRAU DE MESTRE EM ESTRUTURAS E CONSTRUÇÃO CIVIL.

APROVADA POR:



Prof. Lineu José Pedroso, Dr. Ing. (ENC/UnB)

ORIENTADOR



Prof. José Luis Vital de Brito, DSc. (ENC/UnB)

EXAMINADOR INTERNO



Paulo Marcelo Vieira Ribeiro, DSc. (Universidade Federal de Pernambuco (UFPE))

EXAMINADOR EXTERNO

BRASÍLIA/DF, 30 DE JANEIRO DE 2023

FICHA CATALOGRÁFICA

GHEDINI, LUCAS BORCHARDT

A Study of Vibration Attenuation of Shear Buildings Under Dynamic Loads Using TLCDS. [Distrito Federal] 2023.

xx, 113p., 210x297 mm (ENC/FT/UnB, Mestre, Estruturas e Construção Civil, 2023).

Dissertação de Mestrado – Universidade de Brasília, Faculdade de Tecnologia.

Departamento de Engenharia Civil e Ambiental

- | | |
|-------------------------------|------------------------|
| 1. Structural Dynamics | 2. Vibration Control |
| 3. Tuned Liquid Column Damper | 4. Parametric Analysis |
| I. ENC/FT/UnB | II. Título (Mestre) |

REFERÊNCIA BIBLIOGRÁFICA

Ghedini, Lucas Borchardt (2023). **A Study of Vibration Attenuation of Shear Buildings Under Dynamic Loads Using TLCDS**. Dissertação de Mestrado em Estruturas e Construção Civil, Publicação E.DM-01A/23, Departamento de Engenharia Civil e Ambiental, Universidade de Brasília, Brasília-DF, 113p.

CESSÃO DE DIREITOS

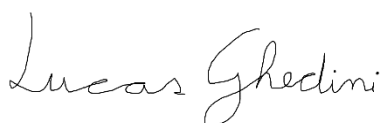
AUTOR: Lucas Borchardt Ghedini

TÍTULO: A STUDY OF VIBRATION ATTENUATION OF SHEAR BUILDINGS UNDER DYNAMIC LOADS USING TLCDS

GRAU: Mestre

ANO: 2023

É concedida à Universidade de Brasília permissão para reproduzir cópias desta dissertação de mestrado e para emprestar ou vender tais cópias somente para propósitos acadêmicos e científicos. O autor reserva outros direitos de publicação e nenhuma parte dessa dissertação de mestrado pode ser reproduzida sem autorização por escrito do autor.



Lucas Borchardt Ghedini

SHVP TR 1, QD 1, CJ 3, CS 15

72005-098 Brasília-DF - Brasil.

lbghedini@gmail.com

ACKNOWLEDGEMENTS

First and foremost, I would like to praise and thank God, the Almighty, who has granted countless blessings, knowledge, and opportunities for me to get where I am.

I would like to thank my family. It would have been impossible to finish my studies without their unwavering support over the past few years. I value the love and encouragement they provided me.

My mother, for caring for me with the love that only a mother knows.

My father, for teaching me not only good things but also the harsh truths of life.

My sister, for showing me the real concept of family.

My most profound appreciation goes to my advisor, Prof. Lineu José Pedroso. The completion of this master's degree would not have been possible without your guidance and support. I would like to express my deepest gratitude for believing in me, for the insightful conversations we've had along the way and for providing invaluable direction throughout my master's program.

I would also like to thank:

My friends who were there for me when I needed it. Shout-out goes to D7 and Mario.

All members and students of PECC, for the opportunity we had to socialize and help each other. Shout-out goes to Rafael and Maurício.

The people in my life who encouraged me and provided me with valuable feedback.

CNPq for providing financial support in the form of a master's scholarship.

Last but not least, I'd like to express my gratitude to all who somehow participated in my journey to get here. Shout-out goes to Fernando, for the comprehension in the final stretch of this race.

“Everything is theoretically impossible until it is done.”

Robert A. Heinlein

RESUMO

ESTUDO DA ATENUAÇÃO DE VIBRAÇÃO DE SHEAR BUILDINGS SOB CARGAS DINÂMICAS USANDO TLCDS

Autor: Lucas Borchardt Ghedini

Orientador: Lineu José Pedroso, Dr. Ing

Programa de Pós-graduação em Estruturas e Construção Civil

Brasília, Janeiro de 2023.

O problema da escassa área de construção nas principais e populosas cidades do mundo levou ao uso de edifícios altos na era moderna. Isso serve como uma forma de destinar mais espaço para residências, comércio, empreendedorismo e negócios. O uso de materiais leves e de alta resistência, juntamente com técnicas de construção avançadas, levaram a um aumento incrível no número de edifícios altos, que tendem a ser estruturas esbeltas, flexíveis e levemente amortecidas. Por causa disso, eles são muito sensíveis às excitações ambientais, como ventos e terremotos. Isso também faz com que esses tipos de estrutura se tornem mais suscetíveis aos problemas causados por vibrações indesejadas, que podem induzir falha estrutural, desconforto aos ocupantes e mau funcionamento dos equipamentos. Mesmo pequenas vibrações, muitas vezes sem oferecer risco à integridade estrutural de uma edificação, podem causar extremo incômodo e desconforto aos seus habitantes. Assim, torna-se importante a busca por formas práticas e eficazes de reduzir esses problemas relacionados à vibração na forma de, por exemplo, dispositivos capazes de controlar as vibrações da estrutura. O funcionamento de um dispositivo passivo está focado em absorver parte da energia da estrutura à qual está acoplado e dissipar essa energia por mecanismos próprios. Um desses dispositivos é o amortecedor de coluna líquida sintonizado (TLCD), que consiste em um tubo em forma de U parcialmente preenchido com água. Parte da energia absorvida do sistema principal vibratório é dissipada pelo movimento do líquido no interior do tubo. A eficiência do TLCD na redução da vibração estrutural é analisada neste trabalho. A análise na busca de seus parâmetros ideais é feita por métodos numéricos e analíticos, como a análise paramétrica. Pacotes de software como o DynaPy são usados para realizar simulações, gerar dados, modelar estudos de caso e analisar situações que aproximam exemplos práticos e cenários da vida real, como excitações sísmicas. Parâmetros ótimos do TLCD são apresentados via mapa de resposta para reduzir a resposta permanente máxima da estrutura à excitação harmônica e para reduzir a resposta rms da estrutura à excitação sísmica. A variação dos parâmetros do TLCD apresentados pelo mapa de resposta está diretamente relacionada com a força atuante na estrutura. Porém, verifica-se que, independentemente da força atuante, existe uma faixa de frequência ideal para sintonizar o TLCD onde se encontram as maiores reduções na resposta primária do sistema. A partir dos parâmetros ideais da coluna de líquido determinados pela análise paramétrica, foram obtidas reduções de resposta estrutural de aproximadamente 60%. Este trabalho também ilustra as múltiplas funcionalidades do Dynapy como ferramenta para aprendizagem e ensino de dinâmica de estruturas.

Palavras-chave: Dinâmica Estrutural, Controle de Vibração, Amortecedor de Coluna Líquida Sintonizado, Análise Paramétrica, DynaPy

ABSTRACT

A STUDY OF VIBRATION ATTENUATION OF SHEAR BUILDINGS UNDER DYNAMIC LOADS USING TLCDS

Author: Lucas Borchardt Ghedini

Advisor: Lineu José Pedroso, Dr. Ing.

Graduate Program in Structures and Civil Construction

Brasilia, January 2023.

The problem of scarce construction area in the main and highly populated cities of the world has led to the use of tall buildings in the modern era. This serves as a way to allocate more space for homes, commerce, entrepreneurship and business. The use of lightweight and high strength materials along with advanced construction techniques have led to an incredible rise in the number of tall buildings, which tend to be slender, flexible and lightly damped structures. Because of that, they are very sensitive to environmental excitations such as winds and earthquakes. This also causes these types of structure to become more susceptible to the problems caused by unwanted vibrations, which could induce structural failure, occupant discomfort and malfunction of equipment. Even small vibrations, often times not offering risk to a building's structural integrity, can cause extreme nuisance and discomfort to its inhabitants. Thus, it becomes important to search for practical and effective ways to reduce these vibration-related problems in the form of, for example, devices capable of controlling structure vibrations. The functioning of a passive device is focused on absorbing part of the energy of the structure to which it is coupled and dissipating this energy by its own mechanisms. One of these devices is the tuned liquid column damper (TLCD), which consists of a U-shaped tube partially filled with water. Part of the energy absorbed from the vibrating main system is dissipated by the movement of the liquid inside the tube. In this work, the efficiency of the TLCD in reducing structural vibration is analyzed. The analysis in the search for its ideal parameters is made by numerical and analytical methods, such as a parametric analysis. Software packages like DynaPy are used to perform simulations, generate data, model case studies and analyze situations that approximate practical examples and real-life scenarios, such as seismic excitations. Optimal TLCD parameters are presented via response map for reducing the structure's maximum permanent response to harmonic excitation and for reducing the structure's rms response to seismic excitation. The variation of the TLCD parameters presented by the response map is directly related to the force acting on the structure. However, it is verified that regardless of the acting force, there is an ideal frequency range to tune the TLCD where the greatest reductions in the primary system response are found. From the ideal liquid column parameters determined by the parametric analysis, structural response reductions of approximately 60% were achieved. This work also illustrates Dynapy's multiple features as a tool for learning and teaching structural dynamics.

Keywords: Structural Dynamics, Vibration Control, Tuned Liquid Column Damper, Parametric Analysis, DynaPy

Table of Contents

1. Introduction	1
1.1 Problem context.....	1
1.2 Objectives	3
1.3 Methodology.....	4
1.4 Scope and limitations	4
1.5 Contributions	4
1.6 Organization	5
2. Bibliographical Review	6
2.1 Generalities about types and classification of damping devices	6
2.2 Succinct literature review about TLCDS	20
2.3 Some aspects of studies and research in the nuclear area that contribute to the advance of knowledge about TLCDS	25
2.3.1 Initial aspects	25
2.3.2 The different types of unsteady flow in pipelines	28
2.3.3 Experimental devices for the study of unsteady flow in pipelines at CEA France	28
2.3.4 Some conclusions obtained through the experimental results reported above and which are directly transportable to TLCDS studies	34
3. Theoretical Foundation.....	37
3.1 Mathematical formulation of the Shear Building.....	37
3.2 TLCDS model.....	39
3.3 Structure-TLCD model.....	42
3.4 Equivalent and parametric mathematical formulation for an SDOF structure with a TLCDS.....	45
3.4.1 Tuned liquid column damper.....	45
3.4.2 TLCDS coupled to the structure	45
3.4.3 Parametric equations	46
4. Solution Methods.....	47
4.1 Central Difference Method.....	47
4.2 Newmark Method	48
4.3 Runge-Kutta Method	48
4.4 Nonlinearity Treatment	49
5. Computational Aspects.....	50
5.1 An Overview of DynaPy	50
5.2 DynaPy Architecture and Methodology	53

5.3 Step-by-Step Mode	55
6. Results	58
6.1 Validations.....	58
6.1.1 Analytical and numerical solution in the time domain.....	58
6.1.2 Frequency analysis through a harmonic excitation	62
6.2 Parametric Analyses	65
6.2.1 Mass ratio (μ) and tuning ratio (γ).....	66
6.2.2 Damping ratio (ζf).....	67
6.2.3 Analysis of a surface point	69
6.3 Case study, simulations, and practical applications	71
6.3.1 Case study 1.....	71
6.3.2 Case study 2.....	74
6.3.3 Extra simulation for case study 2	81
6.3.4 Multiple PTLCD.....	83
7. Conclusions and future perspectives	88
7.1 Conclusions	88
7.2 Perspectives and recommendations for future works	89
References	90
Appendix	100

Table of Figures

Figure 1-1 - Yachthouse Residence Club (source: Gazeta do Povo (2020)).....	1
Figure 1-2 - Water displacement due to a building's oscillation during a storm (source: https://youtu.be/3YXrOFr4H9Q , accessed on January 16 2023).....	2
Figure 1-3 - Various types of dynamic loads acting on an offshore wind turbine (Colherinhas, 2020 apud Batista, 2022 - adapted).....	3
Figure 1-4 - A simple scheme of the TLCD	4
Figure 2-1 - Summary of active and passive systems (Lago et al., 2015).....	9
Figure 2-2 - (a) Simple pendulum and (b) multiple-stage pendulum (Yamazaki et al., 1992).....	10
Figure 2-3 - “Allied Bank” tower (left) and schemes with elevations (right) (Banavalkar, 1990).....	11
Figure 2-4 - Buildings containing TMD and analyzed by Tamura (Tamura et al., 1995)	12
Figure 2-5 - Widespread location of instrumentation in CFSMP buildings (Bashor et al., 2012).....	13
Figure 2-6 - Modeling of a system with one degree of freedom and TMDs (Chang 1999)	14
Figure 2-7 - Bidirectional liquid column damper (Lee and Min, 2011).....	15
Figure 2-8 - Schematic representation of the TVMD (Ikago et al., 2012)	15
Figure 2-9 - Diagram with DSF connectors (left) and diagram of TMDs distributed with DSF cavities (right) (Moon 2011)	16
Figure 2-10 - Shear building and SSI model (Liu et al., 2008).....	17
Figure 2-11 - Stresses at Shinjuku Center building under seismic action (Aono et al., 2011).....	18
Figure 2-12 - Concepts 1 and 2 for damped bracing (Smith and Willford, 2007)	18
Figure 2-13 - Arrangement for a U-tube of a V ² type TMD (Vickery et al., 2001)	19
Figure 2-14 - Concept of the story with pendulum isolator (Tatemichi et al., 2004).....	19
Figure 2-15 - Front view of the embossed LCD (ELCD) utilized (Park et al. 2018).....	20
Figure 2-16 - (a) Simplified secondary sodium circuit, located between the secondary pump and the steam generator where the transient originates (explosive Na-H ₂ O reaction) and (b) the simplified representation of a pressurized TLCD also in oscillatory flow caused by oscillations of a building under dynamic actions	27
Figure 2-17 - Test section of the Gascogne experimental test rig (Gibert, 1988, 1989)	29
Figure 2-18 - Isometric representation of the hydraulic system of the Claudia test rig (Velez et al., 2015)	30
Figure 2-19 - Numerical (TRANSPECTRO-1D) and experimental evolution of pressure in the pressure transducer (P)	31

Figure 2-20 - SAFRAN circuit, representing a simplified scale model of a PWR reactor	32
Figure 2-21 - DIPLODOCUS model: (a) preliminary test device using vibrating membranes as a variable pressure source and (b) simplified schematic of the device...	33
Figure 2-22 - Illustration of the Rio test rig: (a) piston-pressurizer view, (b) pressurizer-piston view and (c) simplified schematic of the device	34
Figure 3-1 - Two-story building in the shear building model (Mendes, 2018).....	37
Figure 3-2 - Shear building model for a multiple-story structure (Mendes, 2018).....	38
Figure 3-3 - Configuration of the tuned liquid column damper	39
Figure 3-4 - Single degree of freedom structure with a TLCD (Mendes, 2018a, adapted)	42
Figure 3-5 - Structure-TLCD system with multiple stories (Mendes, 2018a, adapted) .	43
Figure 3-6 - Multiple parallel TLCDs (Mendes, 2018).....	43
Figure 3-7 - Structure with TLCD attached.....	46
Figure 5-1 - Structure tab of the DynaPy software.....	50
Figure 5-2 - TLCD tab of the DynaPy software.....	51
Figure 5-3 - DynaPy's dynamic response screen	52
Figure 5-4 - Comparison of the dynamic responses with and without a PTLCD for a five-story shear building in resonance (Freitas, 2017).....	52
Figure 5-5 - Comparison of the dynamic responses with and without a PTLCD for a one-story shear building submitted to the El Centro earthquake (Freitas, 2017).....	53
Figure 5-6 - DynaPy's flowchart.....	54
Figure 5-7 - Inputs Summary tab.....	55
Figure 5-8 - Assembly tab	56
Figure 5-9 - Equation of Motion tab.....	56
Figure 5-10 - Explanation of the central difference method in the Solution tab.....	57
Figure 5-11 - Outputs tab containing many plot options.....	57
Figure 6-1 - Free vibration and no damping (plotted in Excel).....	58
Figure 6-2 - Free vibration with damping (plotted in Excel)	59
Figure 6-3 - Forced vibration and no damping (plotted in Excel).....	60
Figure 6-4 - Forced vibration with damping (plotted in Excel)	61
Figure 6-5 - Comparison between analytical and numerical solutions (plotted in Excel)	61
Figure 6-6 - Frequency analysis for an SDOF system for different values of damping (MATLAB [®] /Excel)	62
Figure 6-7 - Frequency analysis in DynaPy	64

Figure 6-8 - Frequency analysis for the uncoupled and the coupled structure-TLCD systems (MATLAB [®] /Excel).....	65
Figure 6-9 - Surfaces relating the response ratio (λ) to the parameters of mass ratio (μ) and tuning ratio (γ), considering different values of aspect ratio: (a) $\alpha = 0.60$ (b) $\alpha = 0.70$ (c) $\alpha = 0.80$ e (d) $\alpha = 0.90$	66
Figure 6-10 - Colormap relating the response ratio (λ) to the mass ratio (μ) and the tuning ratio (γ), considering different values of aspect ratio (α): (a) $\alpha = 0.60$ (b) $\alpha = 0.70$ (c) $\alpha = 0.80$ e (d) $\alpha = 0.90$	67
Figure 6-11 - Surfaces relating the TLCD damping ratio (ζf) to the mass ratio (μ) and tuning ratio (γ) parameters, considering different values of aspect ratio (α): (a) $\alpha = 0.60$ (b) $\alpha = 0.70$ (c) $\alpha = 0.80$ e (d) $\alpha = 0.90$	68
Figure 6-12 - Colormap relating the TLCD damping ratio (ζf) to the mass ratio (μ) and the tuning ratio (γ), considering different values of aspect ratio (α): (a) $\alpha = 0.60$ (b) $\alpha = 0.70$ (c) $\alpha = 0.80$ e (d) $\alpha = 0.90$	69
Figure 6-13 - Example of validation for a response ratio (λ) of 0.70, an aspect ratio of 0.70, a mass ratio of (μ) 0.01 and a tuning ratio of 0.85	70
Figure 6-14 - Time responses for the structure with and without TLCD (MATLAB [®] /Excel)	71
Figure 6-15 - Structure input data.....	72
Figure 6-16 - PTLCD input data.....	72
Figure 6-17 - Response of each story of the building without PTLCD (plotted in DynaPy)	73
Figure 6-18 - Response of each story of the building with PTLCD (plotted in DynaPy)	73
Figure 6-19 - (a) Five-story shear building with TLCD attached to the fifth story and (b) time history of ground acceleration for the El Centro earthquake	74
Figure 6-20 - Surfaces relating the structure displacement response ratio (λ) for the El Centro earthquake to the parameters of mass ratio (μ) and tuning ratio (γ), considering different values of aspect ratio (α): (a) $\alpha = 0.60$ (b) $\alpha = 0.70$ (c) $\alpha = 0.80$ e (d) $\alpha = 0.90$	76
Figure 6-21 - Colormap relating the structure response ratio (λ) for the El Centro earthquake to the parameters of mass ratio (μ) and tuning ratio (γ), considering different values of aspect ratio (α): (a) $\alpha = 0.60$ (b) $\alpha = 0.70$ (c) $\alpha = 0.80$ e (d) $\alpha = 0.90$	77
Figure 6-22 - Surfaces relating the TLCD damping ratio (ζf) to the mass ratio (μ) and tuning ratio (γ) parameters, considering different values of aspect ratio (α): (a) $\alpha = 0.60$ (b) $\alpha = 0.70$ (c) $\alpha = 0.80$ e (d) $\alpha = 0.90$	78
Figure 6-23 - Colormap relating the TLCD damping ratio (ζf) to the mass ratio (μ) and tuning ratio (γ) parameters, considering different values of aspect ratio (α): (a) $\alpha = 0.60$ (b) $\alpha = 0.70$ (c) $\alpha = 0.80$ e (d) $\alpha = 0.90$	79
Figure 6-24 - Time response of the top of the structure (x_5) with the mass ratio variation of the ideal TLCD designed from the response map (plotted in Excel)	80

Figure 6-25 - Time response of the top of the structure (x_5) with the aspect ratio variation for the TLCD with a fixed mass ratio of 5% and designed from the response map (plotted in Excel).....	81
Figure 6-26 - Both responses superposed (plotted in DynaPy).....	81
Figure 6-27 - Structure-PTLCD system analyzed and modelled in DynaPy	82
Figure 6-28 - Reduction achieved in the TLCD response (plotted in DynaPy)	83
Figure 6-29 - Damper arrangements: a) only one damper, b) two dampers, c) three dampers and d) four dampers	84
Figure 6-30 - Comparison between the response of a building with and without dampers subjected to a sinusoidal resonant load (plotted in DynaPy).....	85
Figure 6-31 - System response with diaphragm additions (plotted in DynaPy).....	86

List of tables

Table 2-1 - Types of passive control devices and how they work (Mendes, 2018)	6
Table 6-1 - Comparison between the analytical and numerical frequencies of an SDOF	62
Table 6-2 - Comparison between the analytical and numerical frequencies of an MDOF	65
Table 6-3 - Maximum structure responses with and without TLCD and the corresponding λ	71
Table 6-4 - Mass ratio variation of the ideal TLCD designed from the response map ..	79
Table 6-5 - Aspect ratio variation for the TLCD with a fixed mass ratio of 5% and designed from the response map	80
Table 6-6 - Damper specifications.....	84
Table 6-7 - Percentage reductions in displacements	85
Table 6-8 - Water column displacements with and without diaphragms	86
Table 6-9 - Percentage reductions in displacements with diaphragm	87

List of Acronyms and Abbreviations

AMD - Active Mass Dampers

AVSD - Active Variable Stiffness Devices

BLD - Bi-Directional Liquid Column Damper

CEA - Commissariat of Atomic Energy (in French)

CEN - Center of Nuclear Studies (in French)

CFD - Computational Fluid Dynamics

DEDR - Division of Studies and Reactor Development (in French)

DEMT - Department of Mechanical and Thermal Studies (in French)

ELCD - Embossment Liquid Column Damper

FNR - Fast Neutron Reactor

FSI - Fluid-Structure Interaction

GDFE - Group of Dynamics and Fluid-Structure (in Portuguese)

LCVA - Liquid Column Vibration Absorber

LEVS - Laboratory of Structures, Vibrations and Earthquakes (in French)

MDOF - Multiple Degree of Freedom

MMD - Multiple Mass Dampers

PLCD - Pressurized Liquid Column Damper

PTLCD - Pressurized Tuned Liquid Column Damper

PWR - Pressurized Water Reactor

SC - Secondary Circuit

SDOF - Single Degree of Freedom

SG - Steam Generator

TLA - Tuned Liquid Attenuators

TLCBD - Tuned Liquid Column Ball Damper

TLCD - Tuned Liquid Column Damper

TLCSL - Tuned Liquid Column and Sloshing Damper

TLD - Tuned Liquid Damper

TMD - Tuned Mass Damper

TSD - Tuned Sloshing Damper

TVMD - Tuned Viscous Mass Damper

List of Symbols

A - Cross-sectional area of the TLCD

A_c - TLCD diaphragm area

B - Horizontal length of liquid in the TLCD

C - Damping coefficient

c_d - Damping coefficient of the fluid due to localized head loss

c_{dk} - Constant part of the fluid damping coefficient due to localized head loss

$c_{d\dot{x}}$ - Correction factor for the fluid damping coefficient due to localized head loss

c_f - Damping coefficient of the fluid

c_{feq} - Equivalent linear damping coefficient of the fluid

c_k - Constant part of the fluid damping coefficient due to distributed losses

c_S or C_S - Damping coefficient of the structure

$c_{\dot{x}}$ - Correction factor for the fluid damping coefficient due to distributed losses

d or D - Diameter

e - Approximation error between the nonlinear and the equivalent linear functions

E - Modulus of elasticity of the material

f - Flow friction coefficient

f_0 or F_0 - Amplitude of external force

$f(t)$ - force acting over time

F - External force

F_D - Damping forces

g - Gravity acceleration

h - Height

I - Moment of inertia of the cross section

K - Stiffness

k_{air} - Air chamber stiffness coefficient

k_f - Stiffness coefficient of the fluid

k_S or K_S - Stiffness coefficient of the structure

L - Total length of liquid in the TLCD

M - Mass

m_f - Mass of the fluid
 m_s or M_s - Mass of the structure
 P - External force or air pressure inside the gas chamber
 P_0 - Amplitude of external force
 P_{feq} - Equivalent dynamic load applied on the TLCD
 P_{seq} - Equivalent dynamic load applied on the structure
 R_e - Reynold's number
 t - Time
 T - Natural period of the system
 U_m - Maximum velocity of the flow
 V_f - Volume of the fluid
 x or X - Displacement of the system
 \dot{x} or \dot{X} - Velocity of the system
 \ddot{x} or \ddot{X} - Acceleration of the system
 X_m - Piston displacement
 x_f - Vertical fluid displacement
 \dot{x}_f - vertical velocity of the fluid
 \ddot{x}_f - Vertical fluid acceleration
 \ddot{x}_g - Ground acceleration
 x_s - Horizontal displacement of the structure
 \dot{x}_s - Horizontal velocity of the structure
 \ddot{x}_s - Horizontal acceleration of the structure
 Z - Height of the air column
 Δh - Fluid head loss due to diaphragm
 ΔP_f - Pressure drop of the fluid
 Δt - Time step
 Δt_{cr} - Critical time step
 α - Aspect ratio
 β - Frequency ratio
 γ - Tuning ratio or specific weight of the fluid

ε - Absolute roughness of the TLCD tube
 ζ - Damping ratio
 ζ_f - TLCD damping ratio
 ζ_s - Structure damping ratio
 θ - Phase angle
 λ - Response ratio
 μ - Mass ratio
 ν - Kinematic viscosity
 ν_f - Kinematic viscosity of water
 ξ - Head loss coefficient
 ρ_f - Specific mass of water/fluid
 τ - Time
 ω - Circular frequency
 ω_n - Natural frequency
 ω_d - Damped frequency
 ω_e - Excitation frequency
 ω_f - Natural frequency of the TLCD
 ω_s - Natural frequency of the structure
 Ω - Natural frequency of the coupled system
 $[A]$ - Matrix representation
 $\{A\}$ - Vector representation
 $[C_f]$ - Fluid damping generic submatrix
 $[C_s]$ - Generic structure damping submatrix
 $[K_f]$ - Generic fluid stiffness submatrix
 $[K_s]$ - Generic structure stiffness submatrix
 $[M_f]$ - Generic fluid mass submatrix
 $[M_{fs}]$ - Generic fluid-structure mass coupling submatrix
 $[M_s]$ - Generic structure mass submatrix
 $[M_{sf}]$ - Generic structure-fluid mass coupling submatrix
 $[0]$ - Null submatrix

- $\{P_f\}$ - Subvector of the equivalent dynamic load applied on the TLCD
- $\{P_s\}$ - Subvector of the equivalent dynamic load applied on the structure
- $\{X_f\}$ - Generic fluid displacement subvector
- $\{X_s\}$ - Generic structure displacement subvector
- $\{\dot{X}_f\}$ - Generic fluid velocity subvector
- $\{\dot{X}_s\}$ - Generic structure velocity subvector
- $\{\ddot{X}_f\}$ - Generic fluid acceleration subvector
- $\{\ddot{X}_s\}$ - Generic structure acceleration subvector
- $\{\phi\}$ - Eigenvector

1. Introduction

1.1 Problem context

The problem of scarce construction area in the main and highly populated cities of the world has led to the use of tall buildings in the modern era. This serves as a way to allocate more space for homes, commerce, entrepreneurship and business. The use of lightweight and high strength materials along with advanced construction techniques have led to an incredible rise in the height of buildings, thus originating the famous skyscrapers.

One of them, the Yachthouse Residence Club, can be seen in Figure 1-1. It is located in Balneário Camboriú, Santa Catarina, Brazil, known for being a city of luxury and called the Brazilian Dubai. Often times, where there is luxury, there are imposing and very expensive buildings. At 281 m (922 ft), it is one of the tallest residential buildings in Latin America and it is known as the Brazilian Twin Towers.



Figure 1-1 - Yachthouse Residence Club (source: Gazeta do Povo (2020))

Skyscrapers, as the name suggests, are very tall buildings, while also tending to be slender, flexible and lightly damped structures. Because of that, they are very sensitive to environmental excitations such as winds, ocean waves and earthquakes. This also causes these types of structure to become more susceptible to the problems caused by unwanted vibrations, which could induce structural failure, occupant discomfort and malfunction of equipment. Even small vibrations, often times not offering risk to a building's structural integrity, can cause extreme nuisance and discomfort to its inhabitants. An example of this can be seen in Figure 1-2 -Figure 1-2, which shows the water displacement of a small swimming pool in a penthouse due to the building's oscillation during a storm.



Figure 1-2 - Water displacement due to a building's oscillation during a storm (source: <https://youtu.be/3YXrOFr4H9Q>, accessed on January 16 2023)

The building in which the penthouse is located is also in the city of Balneário Camboriú. During a storm, the wind in this coast beach city can reach speeds of over 100 km/h (62.5 mph), causing tall buildings to oscillate due to its force. In tropical storms, the wind velocity can even surpass 140 km/h (87.5 mph). Thus, it becomes important to search for practical and effective ways to reduce or suppress these vibration-related problems, leading to studies and researches in the field of structural control.

Towers are another type of structure affected by dynamic loads. They can serve numerous purposes, but one in particular has experienced a large growth due to the pursuit of other sources of energy. The advantages of green and renewable energy generate science and governmental incentives, which in turn motivates the industry to create devices capable of harvesting the seemingly endless energy of nature. The tower shaped structures capable of harvesting the power of wind are called wind turbines. Depending on their location, these slender structures need to be able to support strong winds, ocean waves and currents, vortices, earthquakes or even a combination of two or more of them. Since the ones capable of providing energy at a competitive price are also very large and expensive, it becomes imperative that very little goes wrong during their life span. Figure 1-3 illustrates the different dynamic loads that can act on an offshore wind turbine.

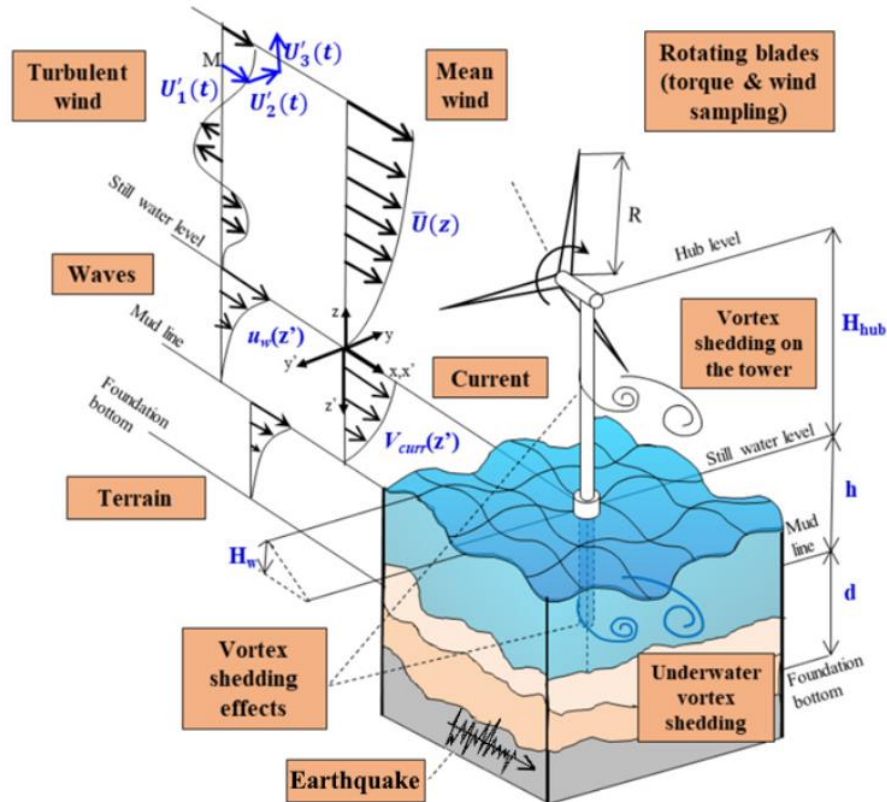


Figure 1-3 - Various types of dynamic loads acting on an offshore wind turbine (Colherinhas, 2020 apud Batista, 2022 - adapted)

Given this problem, the use of devices capable of reducing the susceptibility of those structures to dynamic loads becomes necessary. This is done through the use of control devices capable of preventing structural damage in structures by controlling their vibrations. Countless control technologies have been developed and studied to guarantee structural safety during great amplitude responses due to wind or seismic action. These devices are designed to dampen, isolate, and act over unwanted vibrations so that the structure stays inside the range specified by its designer for a safe use.

1.2 Objectives

The main objective of this work is to study and analyze the vibration attenuation achieved in shear buildings under dynamic loads by using a damping device called tuned liquid column damper (TLCD), which is the damper utilized in this work and exemplified in Figure 1-4. The specific objectives are:

- i. Model the structure and the TLCD in the programs DynaPy and MATLAB[®] to obtain their responses numerically and run different case studies.
- ii. Evaluate the relevant parameters of the TLCD that influence its performance in attenuating the structure response due to different excitations.
- iii. Show the many applications that DynaPy has in the study of structural dynamics and implement new features to aid in this matter, such as a Step-by-Step mode.



Figure 1-4 - A simple scheme of the TLCD

1.3 Methodology

The methodology consists in:

- i. Study the different systems analyzed: structure and TLCD, both uncoupled, and then both of them coupled.
- ii. Model the systems in the programs mentioned above in the objectives section.
- iii. Validate the numerical solutions obtained.
- iv. Do parametric analyses and run extensive simulations to understand the influence of the relevant parameters of the TLCD that affect the vibration attenuation of the structure.
- v. Present the results in a way that covers many variations of the problem for different scenarios.

1.4 Scope and limitations

The scope of this work comprises the study of structures modelled by the shear building theory and the study of TLCDs and pressurized tuned liquid column dampers (PTLCDs) modelled numerically through differential equations of motion. The shear building model considers only the translational degrees of freedom and ignores others, such as the rotational ones. Regarding the dynamic loads considered in the analyses, only harmonic excitations and random vibrations in the form of seismic excitations were used.

The TLCD model in the version of DynaPy used in this work has some limitations, such as the coupling with the structure only occurring at the top story. Another limitation of this model is that it is not possible to add multiple TLCDs of different properties or in different orientations, i.e., the multiple TLCDs have the exact same geometry and the liquid inside each one of them moves along the same direction.

No experimental tests were performed and no specific software was employed, such as Computational Fluid Dynamics (CFD), although data from those sources was and can be used to support future validations and results. Regarding the many different fields and possibilities in the study of structural dynamics, DynaPy is still an incomplete software and has room to grow and include many more features.

1.5 Contributions

This dissertation is a contribution made to the Department of Civil Engineering at the University of Brasília, within the scope of the Group of Dynamics and Fluid-Structure (GDPE, in Portuguese), as a continuation of previous work in the field of TLCDs by, but not limited to, Pedroso (1992b), Freitas (2017), Mendes (2018), Oliveira (2021). The following contributions were made:

- i. A review of the coding and functionalities of DynaPy, which, in many aspects, weren't sufficiently tested.

- ii. Validations, tests and qualifications of the program were made in order to ensure conviction and confidence in the results obtained.
- iii. A new feature was added to DynaPy in the form of the Step-by-Step mode, along with some interface improvements.
- iv. A parametric study was done in the form of surfaces that show the relevant parameters of the TLCD that affect the response of the structure.
- v. Inclusion of a frequency sweep showing both the uncoupled and the coupled structure-TLCD system.

1.6 Organization

This work is organized as follows:

Chapter 1 introduces the theme of this dissertation. It presents the problem to be studied, the fundamentals that motivate it, the methodology adopted in the study, as well as the general and specific objectives. It also contains the scope and limitations of the work and the contributions of the study.

Chapter 2 is a literature review about the most relevant studies in the area of Tuned Dampers. The main contributions of each author in the context of the present work are considered.

Chapter 3 explains the theory and the mathematical aspects involved in modelling each system presented in this study. It presents the theoretical basis of the studied problem, the dominant equations and the conceptual basis for the problem.

Chapter 4 presents the solution methods and the equations used to solve the equations of motion numerically. It also contains the simplifications adopted and the numerical schemes and methods for solution.

Chapter 5 briefly describes the programming language of one of the software used for the dynamic study in this work - DynaPy. It explains how it works and shows images of the software's interface, as well as some results obtained.

Chapter 6 presents the results and discussions of the analyses carried out for the TLCDs models used. Different case studies are analyzed and modeled in DynaPy.

Chapter 7 presents the conclusions, perspectives and recommendations for future works.

2. Bibliographical Review

2.1 Generalities about types and classification of damping devices

The control devices are classified in passive, active, semi active, and hybrid systems. Passive control devices are systems which do not require an external power source, being able to work normally in an eventual power outage. These devices impart forces that are developed in response to the motion of the structure, for example, base isolation, viscoelastic dampers, tuned mass dampers, etc., aiming to dissipate the structure's energy to which it is connected. This is done by absorbing a portion of the energy the structure has during an oscillation, thanks to the relative movement between them. Table 2-1 shows some of the main passive control devices and how they dissipate the structure's vibration energy.

Table 2-1 - Types of passive control devices and how they work (Mendes, 2018)

Passive device	How it works
Tuned Mass Dampers (TMD)	A mass is attached to the structure by a spring-damper system; the damper of the system dissipates the energy.
Tuned Liquid Dampers (TLD)	Similar to the TMD, but liquid is used instead of a mass. Dissipation of energy occurs in orifices of plates or screens placed inside the tube or tank. When a pipe or tube is utilized, the device is called a tuned liquid column damper (TLCD).
Metallic Yield Dampers	Energy dissipation occurs by inelastic deformation of the metal (yielding).
Friction Dampers	The friction caused by the relative motion dissipates energy.
Viscoelastic Dampers	Shear deformation in the system causes energy dissipation.
Viscous Fluid Dampers	Uses a piston with fluid and orifices inside it. The vibration of the structure forces the piston's movement, dissipating energy.
Base Isolation	Flexible devices positioned between the superstructure and the foundation, reducing wave propagation to it from a seismic event.

The most commonly used passive device is the Tuned Mass Damper, which is based on the inertial secondary system principle, and consists of a mass attached to the building through a spring and a dashpot. In order to be effective, its parameters need to be optimally tuned to the building dynamic characteristics, thus imparting indirect damping through modification of the combined structural system.

Like a TMD, a tuned liquid damper/tuned sloshing damper (TSD) imparts indirect damping to the structure, reducing its response. It consists of a tank partially filled with liquid. The energy dissipation occurs through various mechanisms: viscous action of the fluid, wave breaking, contamination of the free surface with beads, and container geometry and roughness. Unlike a TMD, however, a TSD has an amplitude dependent transfer function which is complicated by nonlinear liquid sloshing and wave breaking.

The TLDs can be broadly classified into two categories: shallow-water and deep-water dampers. This classification is based on the ratio of the water depth to the length of the tank in the direction of the motion. A ratio of less than 0.15 is representative of the shallow water case. In the shallow water case, the TLD damping originates primarily from energy dissipation through the action of the internal fluid's viscous forces and from wave breaking. For the deep-water damper, baffles or screens are needed to enhance damping. The damping mechanism is therefore dependent on the amplitude of the fluid motion, wave breaking patterns, and screen configuration. The deep-water damper has one drawback in the fact that a large portion of water does not participate in sloshing and adds to the dead weight. At an intermediate level of fill depth, the container can be utilized for building water supply. If the existing water tanks are not utilized, the large space occupied by water containers may, in some cases, require a part of the building roof. However, most practical installations of TLDs use many smaller tanks so as to maximize the effective mass of liquid engaged in sloshing (Yalla and Kareem, 2000).

TLDs were proposed in the late 1800s where the frequency of motion in two interconnected tanks tuned to the fundamental rolling frequency of a ship was successfully utilized to reduce this component of motion (Den Hartog, 1956). Initial applications of TLDs for structural applications were proposed by Kareem and Sun (1987); Modi et al. (1987) and Fujino et al. (1988).

Tuned liquid column dampers are a special type of TLDs relying on the motion of the column of liquid in a U-tube-like container to counteract the forces acting on the structure, with damping introduced through a valve/orifice in the liquid passage (Sakai et al. 1989). The damping is amplitude dependent since the valve/orifice constricts the dynamics of the liquid in a nonlinear way.

The passive devices are tuned to work in a specific frequency of the structure, generally its fundamental frequency. However, this becomes a problem when the structure no longer oscillates in that frequency. This can occur due to a nonlinear behavior from the structure or in seismic events, since earthquakes have a frequency range and not a single frequency (Thenozhi and Yu, 2013).

Active devices come as a solution to this problem, controlling vibrations by making use of sensors connected to the structure, to the damping devices and sensors that measure the excitation signal. With all the information and thanks to an algorithm, the system generates an opposite signal that activates dampers positioned in strategic locations to reduce the structure's vibration. Active control systems are driven by an externally applied force which tends to oppose unwanted vibrations. The control force is generated depending on the feedback of the structural response. Examples of such systems include Active Mass Dampers (AMDs). One of the disadvantages of the active devices is that they demand a high amount of power supply. In case of a power outage, possibly caused by a critical event like an earthquake, the system becomes inactive. Owing to the uncertainty of the power supply during extreme conditions, passive systems are generally

avored over active systems. According to Pestana (2012), the use of this type of device varies according to local engineering practice and customs.

As an alternative, semi active control devices act as a middle ground, with energy requirements orders of magnitude less than typical active control systems and, at the same time, are able to sense and use the structure's movement to develop an opposite movement. These systems do not impart energy into the system and thus maintain stability at all times, for example, variable orifice dampers, electro-rheological dampers, etc. A paper by Symans and Constantinou (1999) provides a review on semi-active devices for seismic protection of structures. Another alternative is to use a system that puts together both passive and active devices, known as the hybrid control device. The name implies the combined use of active and passive systems or passive and semi-active systems.

Regarding damping systems and damping devices, Lago et al. (2015) describes and characterizes them in a succinct manner. The following excerpts are from the work of Lago et al. (2015).

The first category of passive dampers is normally an integral part of primary systems. They are positioned in ideal locations (e.g., in reinforcement systems) to reduce dynamic building movement. The force generated by these devices is a function of the rate of change of strains over time and the relative damping arising from the phase shift between force and displacement. There are different types of devices that belong to this category and, among them, the most important are: viscous, viscoelastic, hysterical, frictional and electromagnetic storms.

The second category of passive systems is based on the inertial and restorative force created by an additional mass, usually positioned on top of a building. There are two main categories of devices belonging to this family: Tuned Mass Dampers and Tuned Liquid Dampers. In TMD, the mass is supported by an appropriate mechanical system that allows it to move out of phase with the fundamental period of the building. In the TLD, the mass is composed of moving water, and it is even possible to use the building's water supply source (for example, water tanks located near the top of the building). In the case of a rectangular tank, its dimensions and the water level define the "sloshing" frequencies of the TSD.

Unlike passive systems that are tuned to work over a narrow range of load conditions, active systems perform more efficiently over a wider range. There are many different types of active devices, but the most prominent are active mass dampers and active variable stiffness devices (AVSD). Similar to passive dampers, these active devices work through the same dissipation principles based, respectively, on mass and material. However, its properties are adjusted from a computer control system. While they hold great promise as a better solution for auxiliary damping in tall buildings, their applications have been limited due to high costs and reliability issues. It is believed that further research on these devices may lead to increases in their use. Figure 2-1 summarizes the types of systems.

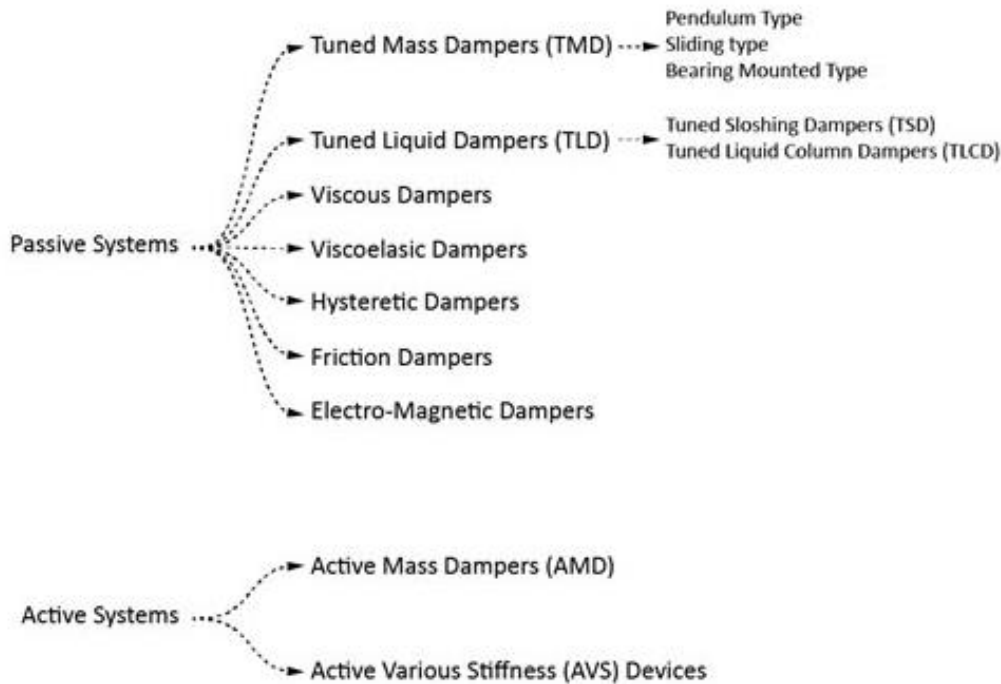


Figure 2-1 - Summary of active and passive systems (Lago et al., 2015)

In order to obtain a broad understanding of the types of dampers used to control vibrations in tall buildings, the various devices and solutions used were searched in the literature. The writing of this section is based on and contains excerpts from the work of Lago et al. (2015), which consists of a synthesis of different attenuating devices present in the literature.

There are a large number of studies conducted in tall buildings and with damping technologies and, because of this, it would be almost impossible to review all available publications on the subject. Therefore, a highlight is presented of some of the main aspects of research related to tall buildings and damping technologies, without trying to be an exhaustive and complete review on the subject.

Regarding the practical considerations for vibration control of tall buildings with mass dampers made in “Performance of tuned mass dampers under wind loads” (Kwok and Samali, 1995), the selection of the optimal vibration control system is a function of several factors including: efficiency, compactness and weight, capital cost, operating cost, maintenance and security requirements. Mass dampers are generally the most used system in one of the following forms: passive, active and hybrid. The article analyzes these systems with particular reference to large scale verifications. For passive tuned mass dampers, several design considerations need to be taken into account to achieve an economical solution. First, the additional mass on top of the building cannot exceed one to two percent of the building's modal mass. Another practical aspect involves moving additional mass even during small excitations. The easiest way to get this is with a pendulum. However, this requires a lot of space; this is why alternative solutions have been proposed (such as inverted pendulums or multistage pendulums, as can be seen in Figure 2-2).

Another important aspect is that these systems can be fine-tuned after the characteristics of the building are known (i.e., when the building is complete). In the case of large mass

movements, it is necessary to install safety devices to limit movement. In most cases, these passive systems can also be designed to operate as active systems, with hydraulic servo actuators and/or servo motors as the driven mechanisms. An important aspect to be considered with these devices is the additional requirements for safety measures in order to control the generated forces.

The advantage of an active system is the lower mass and greater additional damping provided, which can be 10% or more compared to 3-4% for a passive system. However, this ends up generating an increase in costs in the system. A passive system can reach up to one percent of the construction cost, while an active system costs up to two percent (with higher maintenance costs as well). Observing the properties of both systems, the ideal case would be to have a hybrid system, which takes advantage of passive and active systems. This system would work as passive or active depending on the loading conditions. When greater damping and motion control is required, active systems are generally used. For low damping and movement control, passive systems are used. These systems, despite being more expensive than passive ones due to the presence of an active damper, achieve considerable savings in operating and maintenance costs. To take all these factors into account, parametric studies are the best means of selecting the most suitable vibration control system. These, together with experimental tests, will provide the most appropriate tools.

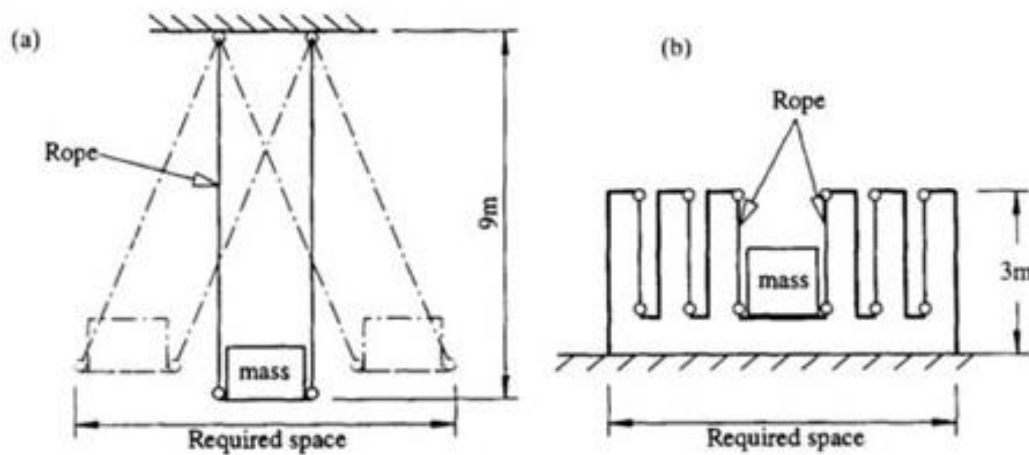


Figure 2-2 - (a) Simple pendulum and (b) multiple-stage pendulum (Yamazaki et al., 1992)

The work of “Structural systems to improve wind induced dynamic performance of high rise Buildings” (Banavalkar, 1990) deals with modifying the shape of the vibrational mode without significantly affecting the overall stiffness of the building. Therefore, the focus is on modifying the mass and damping of the building. The author attempts to optimize the shape of the building mode to reduce floor acceleration in two different case studies, shown in Figure 2-3, and illustrates how adding damping can be an effective means of achieving this goal.

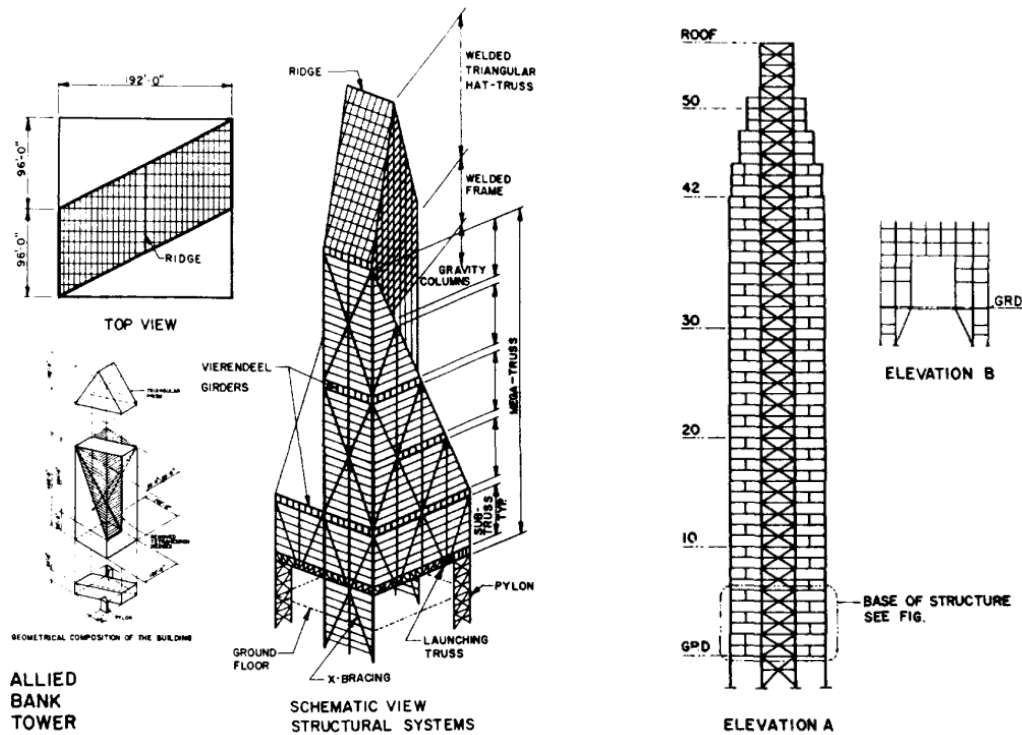


Figure 2-3 - “Allied Bank” tower (left) and schemes with elevations (right) (Banavalkar, 1990)

Modal properties are very important parameters that must be estimated in the design of tall buildings. Studies were carried out to determine a better estimate of these properties by monitoring buildings, as shown in “Field observations on modal properties of two tall buildings under strong wind” (Au et al., 2012). The authors describe how two tall buildings in Hong Kong are analyzed during typhoon and monsoon events. The recorded accelerations of buildings are used to identify the modal properties of the building. 30-minute intervals and a fast Bayesian frequency domain method are used to determine the natural frequencies, damping ratio, and mode shapes. Comparison between different events shows that the procedure is an effective way to identify the natural frequencies, while the damping rate estimates show more dispersion.

Large scale measurements have always been considered important aspects to validate TMD device designs. One of the first works on this subject was written by Tamura et al. in 1995 (“Effectiveness of tuned liquid dampers under wind excitation”). The article describes an experimental full-scale measurement program that was conducted to prove the efficiency of TLDs. Building performance was measured under wind vibration, with and without the installation of TLDs. Four structures (three towers and a hotel) were analyzed, as shown in Figure 2-4. From data analysis, the authors found that the efficiency of TLDs depends on their mass (compared to the mass of the building) and the damping of the sloshing movement. In general, a larger mass provides more damping in the building, damping the movement of sloshing is considered ideal. This damping can be easily controlled with floating particles, baffles, nets and other means.

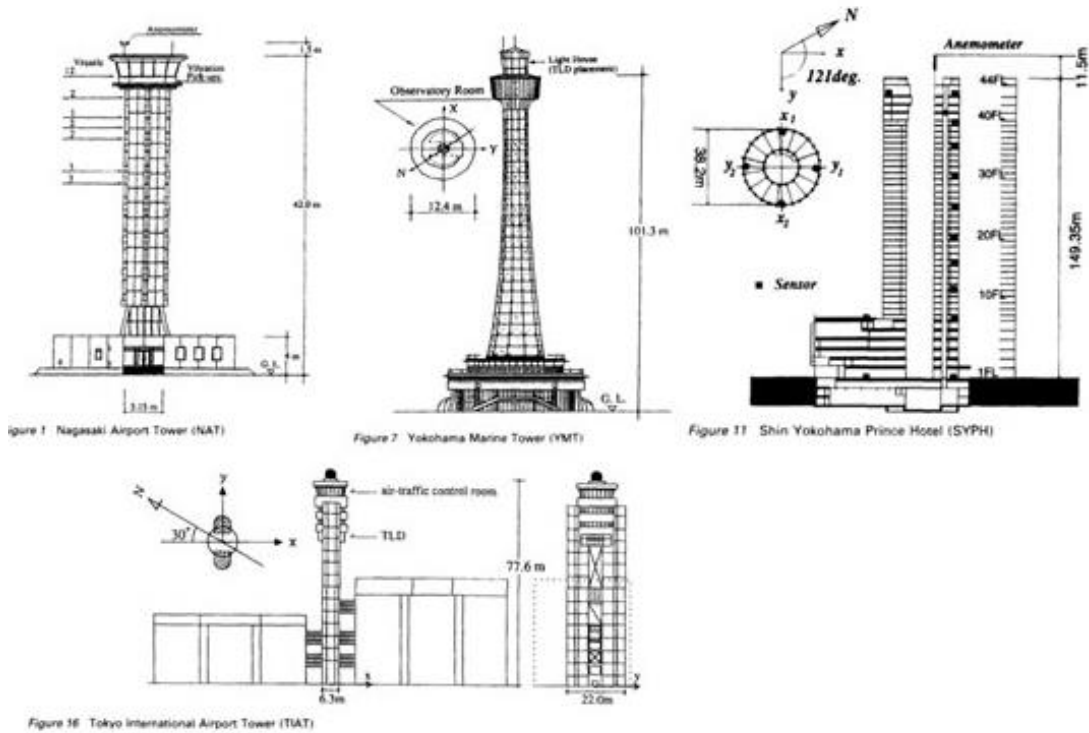


Figure 2-4 - Buildings containing TMD and analyzed by Tamura (Tamura et al., 1995)

Reliability in estimating building acceleration and dynamic properties is an important topic as, in most cases, it is a design factor for tall buildings. For these reasons, in “Full-scale performance evaluation of tall buildings under wind” by Bashor et al. (2012), the importance of large-scale monitoring is emphasized especially with regard to the Chicago Full-Scale Monitoring Program (CFSMP). This program monitors three Chicago buildings under a wide variety of wind environment conditions utilizing instrumentation such as the ones shown in Figure 2-5. The results show significant dispersions due to different factors and, among them, the most important are: temperature effects, characteristics of the wind-induced response and errors in the analysis technique used. In particular, damping estimation is less effective than natural frequency calculation. As a consequence, the authors suggest that these results need to be analyzed in a meaningful way and that the variability needs to be carefully evaluated.

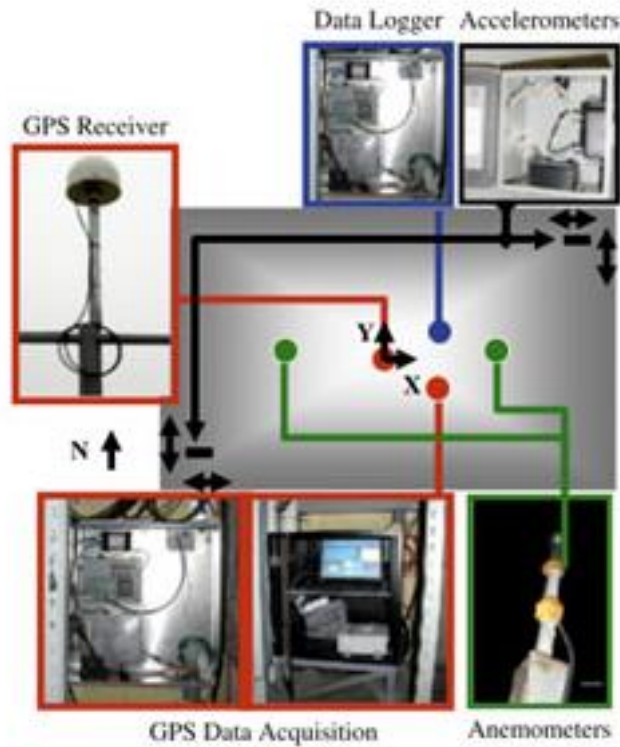


Figure 2-5 - Widespread location of instrumentation in CFSMP buildings (Bashor et al., 2012)

In “Mass Dampers and their Optimal Designs for Building Vibration Control”, Chang (1999) describes the control performance of three different damper devices: tuned mass dampers, tuned liquid column dampers and liquid column vibration absorbers (LCVA), shown in Figure 2-6. The comparison of the three systems was carried out theoretically from the point of view of a system with one degree of freedom. Two sets of different formulas are proposed and tested under wind excitation and white noise seismic excitation. The results show that the mass damper performance is a function of the efficiency index (i.e., the mass ratio between the TMD and the building) and that the TMD control performance is always better than the LCVA and TLCD. Furthermore, the performance of the LCVA is better than the TLCD performance when the vertical to horizontal area ratio of the mass damper is greater than one. When the ratio is less than one, the TLCD performs better than the LCVA.

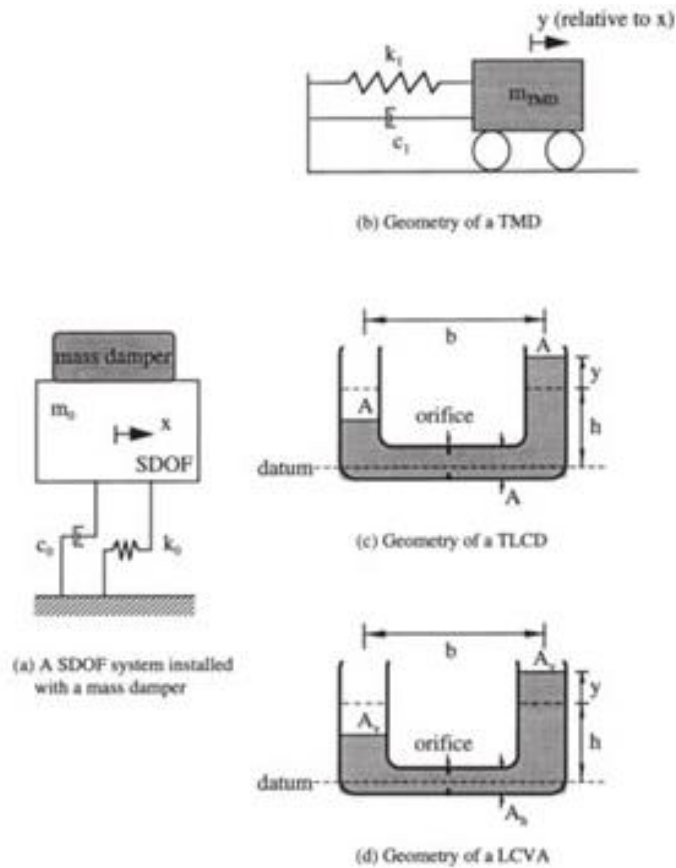


Figure 2-6 - Modeling of a system with one degree of freedom and TMDs (Chang 1999)

A new type of liquid damper, shown in Figure 2-7, is introduced in the article “Reducing acceleration response of a SDOF structure with Bi-directional Liquid Damper” (Lee and Min, 2011). Buildings vibrate in directions along the wind and perpendicular to it. Even though simultaneous vibration in both directions is unusual, changes in wind direction and torsional vibration would require the installation of dampers in two orthogonal directions. The authors present a vibration absorber that can alone control two different vibration modes at the same time. The so-called Bi-Directional Liquid Column Damper (CF) is similar to a conventional TLCD, in which in one direction the water column is used as a mass damper system and in the other direction the vertical columns are used as “sloshing” type shock absorbers. By proposing a methodology, the authors also validate the proposed scheme with tests on a vibrating table for a one-story shear model. They assert the importance of fine tuning in both directions to avoid the adverse effect of the interaction between the two systems.

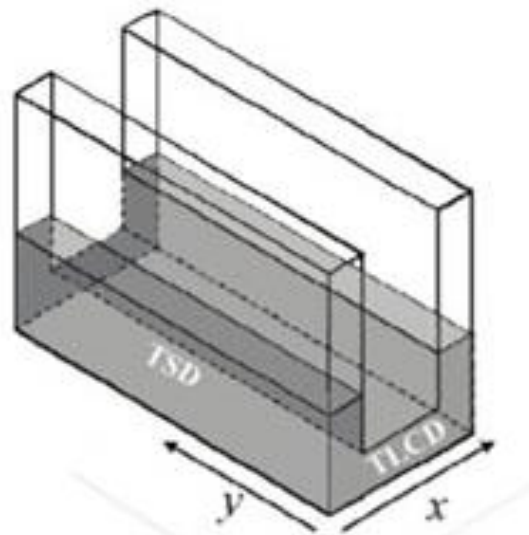


Figure 2-7 - Bidirectional liquid column damper (Lee and Min, 2011)

Ikago et al. (2012) in their article “Seismic Control Design of Tall Buildings using Tuned Viscous Mass Dampers” presents a new tuned mass damper system that can be effective for wind and earthquake induced vibrations. The system uses a rotating viscous mass damper with a spring connection to the main building. This system, called a Tuned Viscous Mass Damper (TVMD) and shown in Figure 2-8, allows the creation of a large apparent mass that would be more efficient for earthquake vibration control. The authors also propose a simple response estimation method that is useful for the design of structures with TVMDs.

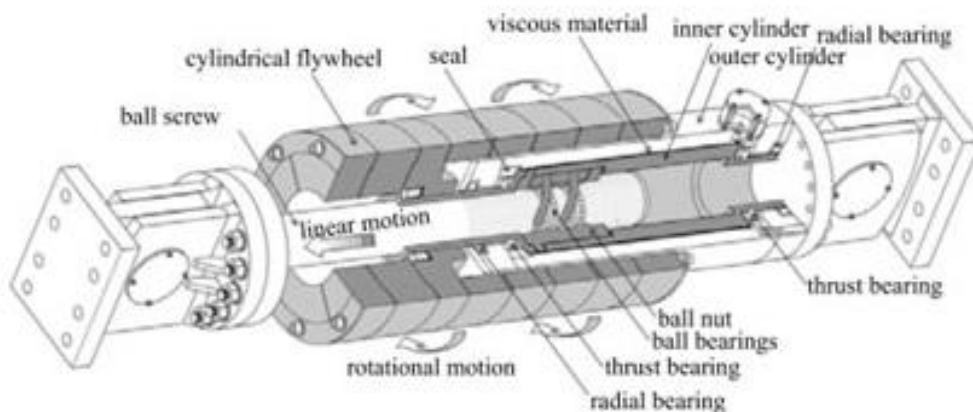


Figure 2-8 - Schematic representation of the TVMD (Ikago et al., 2012)

An innovative structural design solution strategy for tall buildings and damping devices was proposed by Moon (2011) in his article “Structural Design of Double Skin Facades as Damping Devices for Tall Buildings”. The author describes a new damping strategy configuration that takes advantage of double skin facade systems (DSF), currently very common in tall buildings. Two different solutions are studied and are shown in Figure 2-9. The first considers the modification of the connectors between the main structure and the facade. They have very low stiffness and additional damping. Although it is a very promising structural solution, this system has serious problems with facade vibration. The second is investigated to overcome these problems and uses small masses in the facade cavities. Therefore, this technique is similar to a TMD, but with the advantage of utilizing

unused space in the building. Furthermore, this second system would allow for greater reliability than a standard TMD, as there are more masses it can also be used to obtain better control of the higher vibration modes.

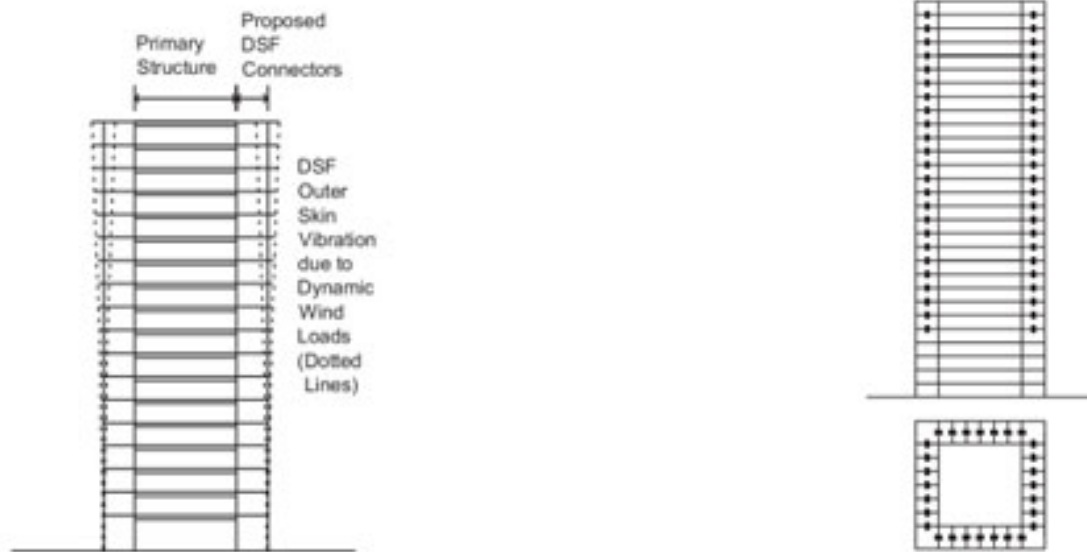


Figure 2-9 - Diagram with DSF connectors (left) and diagram of TMDs distributed with DSF cavities (right) (Moon 2011)

One of the first studies on soil-structure interaction (SSI) in tall buildings with damping devices was proposed by Liu et al. (2008) in their article “Wind-induced vibration of high-rise building with tuned mass damper including soil-structure interaction”. A model for a shear building and SSI is shown in Figure 2-10. The authors state the importance of understanding the implications of having more flexible and less shock absorbing structures built on flexible soils. For these reasons, they developed a mathematical model in the time domain to consider the soil-structure interaction of tall buildings subjected to wind loads. Several numerical examples were conducted to attest the validity of the model. The results demonstrate that the soil-structure interaction cannot be ignored for low stiffness soils; otherwise, the induced response will be overestimated and the effectiveness of TMD underestimated. As a consequence, TMDs are more effective in suppressing vibration in soils with higher stiffness.

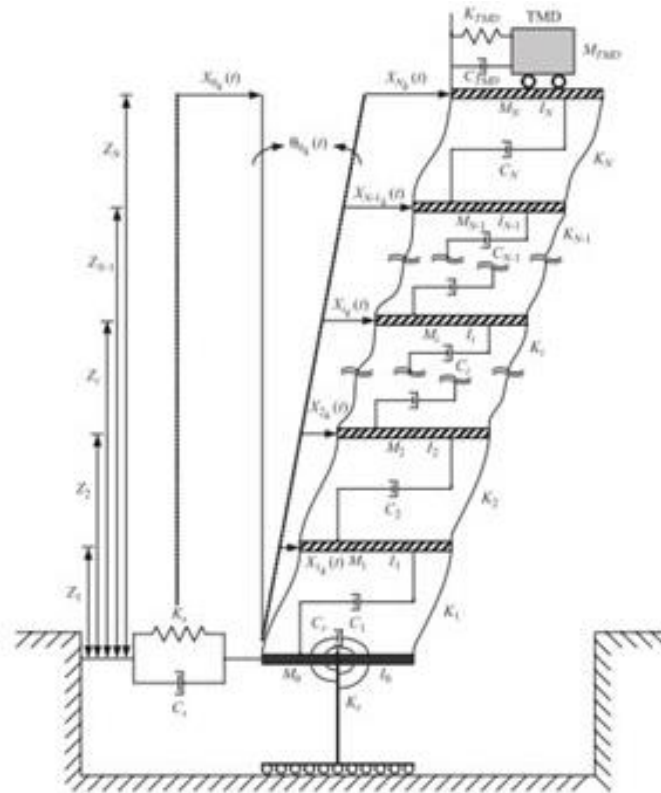


Figure 2-10 - Shear building and SSI model (Liu et al., 2008)

The article “Seismic retrofit of high-rise building with deformation-dependent oil-dampers” (Aono et al., 2011) deals with the problem of ground movement for long periods in existing skyscrapers in Japan. To overcome this problem, the authors suggest that the most advantageous solution is to use a strain-dependent oil damper and that eliminates the additional reinforcement requirements in the areas where these devices are installed (which is typical when other devices are used). In fact, this damper limits its force when the deformation of the structure approaches the limit. The proposed solution was used in a 54-story building in Japan (Shinjuku Center Building). Dynamic analyzes on long-period earthquakes were performed and compared with the response observed during the 2011 earthquake off the Pacific coast of Tohoku. The results show good agreement between the model and the actual response. Figure 2-11 shows the oil dampers and the stresses at Shinjuku Center building under seismic action.

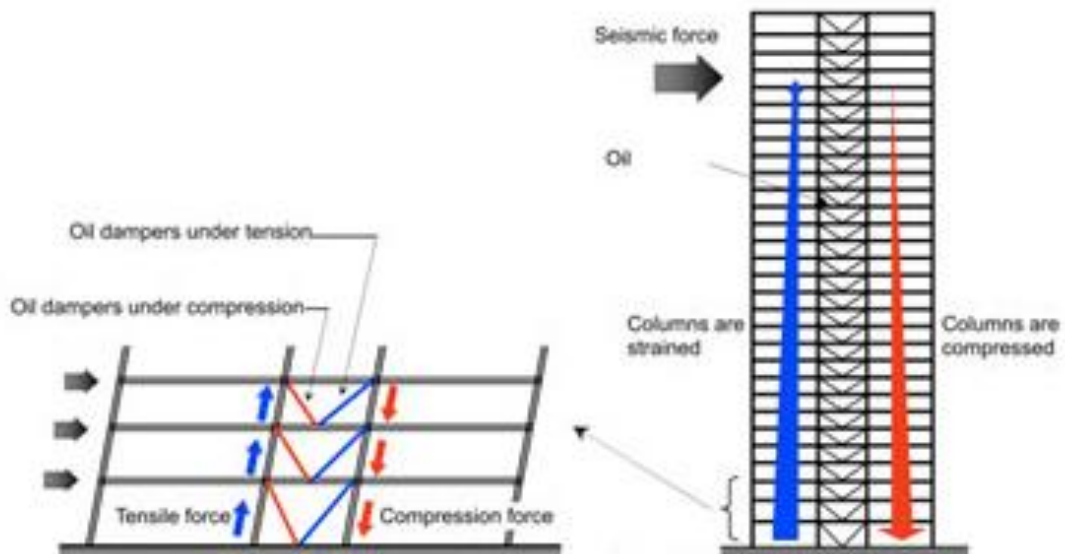


Figure 2-11 - Stresses at Shinjuku Center building under seismic action (Aono et al., 2011)

In “The Damped outrigger concept for tall buildings” (Smith and Willford, 2007), the authors describe a new philosophy for the design of tall buildings with additional damping systems. This consists of inserting shock absorbers into the bracing of a building. One of the main advantages of this system is to increase damping (around 5 to 10%) and reduce inherent damping variability. Viscous dampers are used as damping devices and two different configurations are proposed: dampers in the connection of the external column with the bracing and dampers in the coupling beams, shown in Figure 2-12. Along with these innovative solutions, the authors provide a blueprint for designing tall buildings that adopt this technology. The article concludes with an example of a building that is under construction (when the article was published) using this technique.

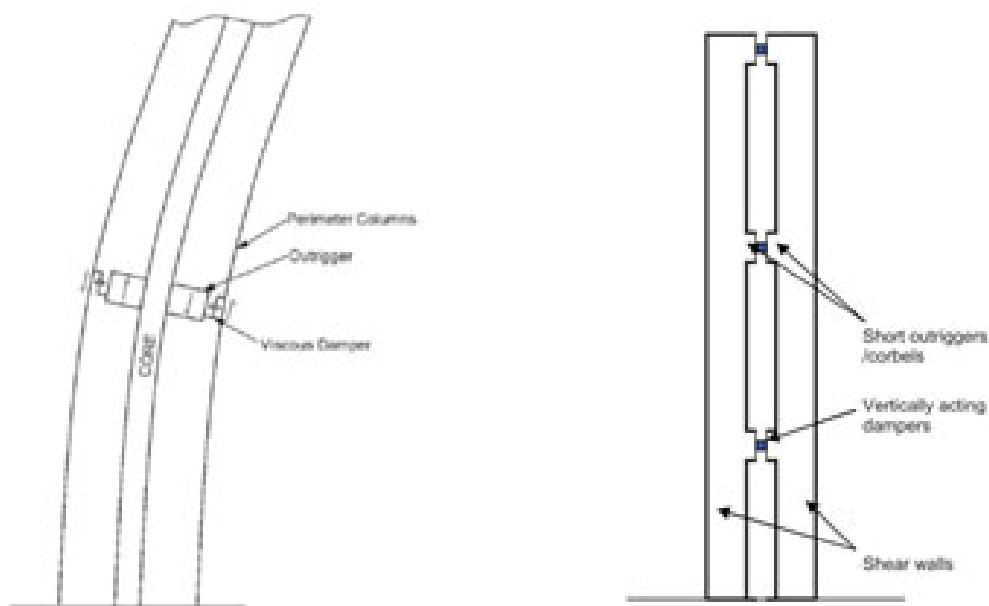


Figure 2-12 - Concepts 1 and 2 for damped bracing (Smith and Willford, 2007)

Nonlinear tuned mass attenuator devices are compared with linear ones in the article “The behavior of simply nonlinear tuned mass dampers” by Vickery et al. (2001). Two simple

and commonly used nonlinear forms are discussed: dry friction and "velocity squared" (V^2), shown in Figure 2-13. To compare the linear TMD with the non-linear one, the latter must be linearized. The linearization assumption is that the individual cycles are sinusoidal with a slowly varying amplitude that follows the Rayleigh shape associated with a narrow-band Gaussian process. These assumptions were verified with a real simulation in the non-linear time domain for a sample application. The results show that the velocity squared TMD significantly reduces movements with little cost in performance compared to the ideal linear TMD. Instead, friction TMD only performs well around the design point.

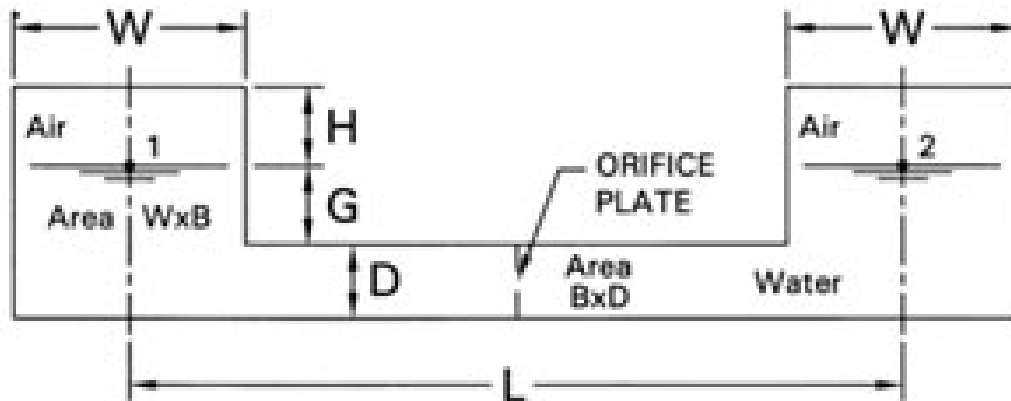


Figure 2-13 - Arrangement for a U-tube of a V^2 type TMD (Vickery et al., 2001)

The article by Tatemichi et al. ("A Study on Pendulum Seismic Isolators for High-Rise Buildings", 2004) deals with a type of seismic isolation device in tall buildings: the so-called nonparallel cantilever system. A concept of a story with pendulum isolator is shown in Figure 2-14. This system is considered suitable for tall buildings because it offers longer periods and is not influenced by the weight of the building, unlike the standard isolation device solution (e.g., rubber bearing). In fact, the period of the system only depends on the length of the suspended system. The authors suggest that a possible application of this technology is for the insulation of individual floors. Furthermore, a conceptual scheme for skyscrapers is proposed and tested on a small scale. The results show the system's potential, although additional studies need to be carried out before a full-scale application can be made.

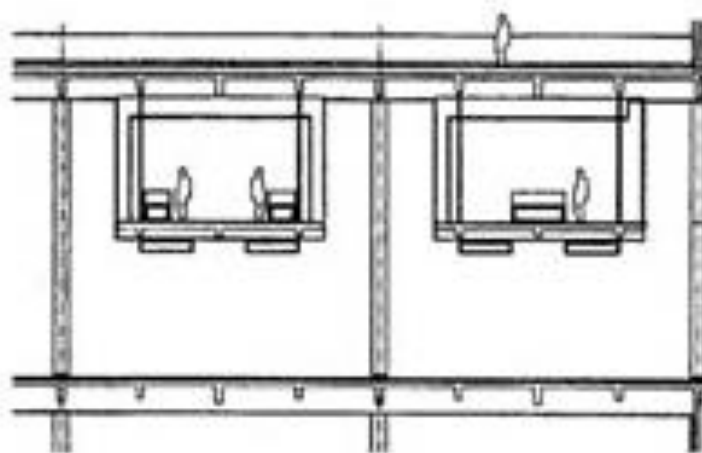


Figure 2-14 - Concept of the story with pendulum isolator (Tatemichi et al., 2004)

Vibration control using a Liquid Column Damper (LCD) containing reliefs on its internal walls, shown in Figure 2-15, is analyzed by Park et al. (2018). The results show that the embossed LCD has a damping rate up to 2.7 times higher than the traditional LCD. It also has an acceleration reduction of up to 20% more compared to the LCD, in addition to having a more stable behavior throughout the used frequency range.

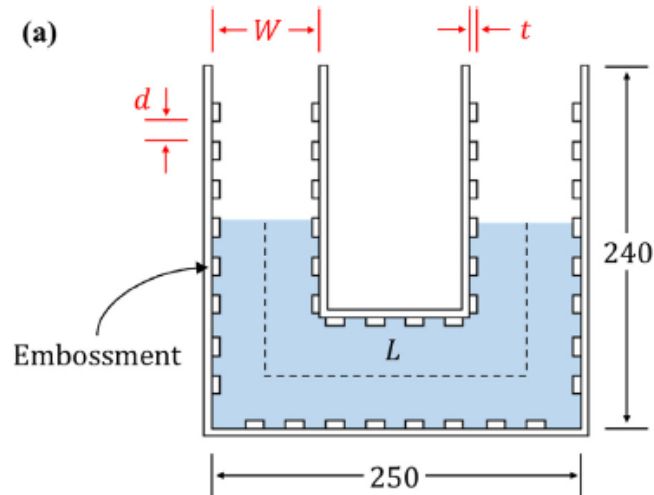


Figure 2-15 - Front view of the embossed LCD (ELCD) utilized (Park et al. 2018)

2.2 Succinct literature review about TLCDS

The current trend toward buildings of ever increasing heights and the use of lightweight, high strength materials, and advanced construction techniques have led to increasingly flexible and lightly damped structures. Understandably, these structures are very sensitive to environmental excitations such as wind, ocean waves and earthquakes. This causes unwanted vibrations inducing possible structural failure, occupant discomfort, and malfunction of equipment. Hence it has become important to search for practical and effective devices for suppression of these vibrations (Yao, 1972).

The study of structural dynamics in general is in a fairly consolidated state, having many classic texts in the literature, such as Clough and Penzien (2003), Chopra (1995), Blevins (1990), Tedesco et al. (1999), Naudascher and Rockwell (2005). All of them have formulations for systems of single degree of freedom (SDOF) and multiple degree of freedom (MDOF), as well as analytical solutions for several distinct cases. The Group of Dynamics and Fluid-Structure (GDFE) from the University of Brasilia has many texts and researches in many fields of study, ranging from introductions to structural dynamics to specific damping methods and dynamic analysis of offshore wind turbines. These texts include Pedroso (1992b, 2000, 2003a, 2003b), Bomtempo (2017), Freitas (2017), and Mendes (2018).

The dynamics of a tuned liquid column damper type damper can be seen in Pedroso (1989), where the author presents formulas capable of describing the equation of motion of an oscillating column of incompressible fluid. Despite some differences between the model presented in this work and the model of a TLCD as we commonly understand it, it is possible to extrapolate the equations to the model under development, since the research in question was more oriented to the fluid in pipes of nuclear reactors. In fact, the studies conducted by Pedroso (1983, 1986) in his doctoral studies at the Center of Nuclear Studies (CEN, in French) of the Commissariat of Atomic Energy (CEA, in French), at Saclay, France, in the years of 1982 to 1986, on fluid columns (compressible

or not) and/or not pressurized, were characterized by pioneering works, not oriented to civil construction (attenuation of vibrations in tall buildings). They produced extraordinary results, which would later be used in this other sector, through independent and sometimes tortuous paths, since the theoretical, numerical and experimental studies of CEA had conclusively provided the importance of control parameters in these types of problems.

Several types of shock absorbers have been studied, developed and applied (Spencer and Nagarajaiah, 2003; Saaed et al., 2013) to reduce the vibration of the main system due to dynamic loads. The functioning of a passive device is focused on absorbing part of the energy of the structure to which it is coupled and dissipating this energy by its own mechanisms. Traditionally, the TLCD consists of a U-shaped tube partially filled with water. Part of the energy absorbed from the vibrating main system is dissipated by the movement of the liquid inside the tube. The performance of this liquid column device matches the traditional tuned mass damper and tuned liquid damper (Souza, 2003; Bigdeli and Kim, 2016). However, the TLCD still offers advantages such as low cost, absence of moving mechanical parts, relatively easy installation, adaptation to existing structures and simple maintenance (Yalla and Kareem, 2000).

For the tuned liquid column damper to present good efficiency in reducing the vibrations of the primary system to which it is connected, it is necessary to pay attention to the characteristics adopted for the attenuator, such as its operating frequency, its dimensions and its damping. Usually, the damping of the movement of the liquid column occurs during the liquid's passage through a diaphragm (Balendra et al., 1995). Also, to increase the performance of the TLCD, an electro valve that varies the opening of the diaphragm according to the response of the structure and the damper can be employed (Yalla and Kareem, 2000; Souza, 2003; La and Adam, 2018). The replacement of this diaphragm by metallic balls has also been studied to dissipate the energy of the fluid (Gur et al., 2015). In terms of reducing the structure response, as well as the liquid column response, there is a gain in performance.

The dimensions adopted for the liquid column directly influence the efficiency of the absorber. Studies were made on changing the cross section of the horizontal and vertical sections of the tube (Balendra et al., 1999; Hochrainer and Ziegler, 2006; Altay and Klinkel, 2018). Still, so that the TLCD can act in more than one direction, Lee et al. (2011) proposes a tuned liquid column and sloshing damper (TLCSD). Also, the tuned liquid multi-column damper has been developed (Coudurier et al., 2018), presenting good responses for the vibration control of floating wind turbines, structures subjected to simultaneous dynamic loads in several directions. In addition to this, the application case of the TLCD in wind turbines has been widely studied (Balendra et al., 1995; Colwell and Basu, 2009; Mensah and Osorio, 2014; Buckley et al., 2018; Hemmati et al., 2019). The liquid column damper is also of interest for reducing the response of tall buildings (Hochrainer and Ziegler, 2006; Min et al., 2005) and bridges (Shum et al., 2008). Specifically, the main dynamic load considered in these structures is due to the wind. Just like the random action of the wind, efforts have been applied to the dynamic analysis of structures with TLCD for the control of earthquake vibrations (Gosh and Basu, 2005; Chakraborty et al., 2012; Mendes et al., 2018; Espinoza et al., 2018). For a better performance of the damper, Gosh and Basu (2004) and Sonmez et al. (2016) propose a different composition, in which the TLCD is connected to the primary structure using an adaptive spring. In addition, to having greater malleability for the functioning of the attenuators, authors such as Hochrainer and Ziegler (2006) and Bhattacharyya et al. (2017) have evaluated the possibility of pressurizing the vertical section of the tube,

promoting additional stiffness to the attenuator and, consequently, changing the natural frequency of the TLCD. Both variations in the stiffness of the attenuator (springs and pressurized chambers) demonstrate the option to use this damper in a high frequency range, where the conventional TLCD has a performance loss.

The majority of earlier studies consisted of passive versions of the liquid damper, meaning that the designed damping characteristics are not controlled. The device is optimal at the design ranges of excitation frequencies but performs worse at other excitation frequencies. To answer this matter, semi-active and active systems were proposed. Lou et al. (1994) proposed an active system in which a baffle was placed inside the liquid damper. The orientation of the baffle changed the effective length of the damper, making it useful as a variable-stiffness damper.

Multiple Mass Dampers (MMDs) with natural frequencies distributed around the natural frequency of the primary system requiring control have been studied by Yalla and Kareem (2000). Such systems lead to smaller sizes of TLCDs, which improve their construction, installation and maintenance. More spatial distributions of the TLCDs in the structure are also possible due to the reduction in their size. There is a significant advantage in using multiple spatially distributed tuned dampers when compared to using a single damper. That is because, when strategically located, multiple dampers are more effective in mitigating the motions of buildings and other structures undergoing complex motions (Bergman et al. 1990).

Most structures under the influence of environmental loads experience both lateral and torsional motions. To deal with this, it is possible to use separate dampers, each oriented in a particular direction, or to simply utilize a bi-directional TLCD. Implementations in buildings have been proposed and reported by Shimizu and Teramura (1994) by using a new bi-directional tuned liquid damper with period adjustment equipment.

Balendra et al. (1995) studied the efficiency of TLCDs in the vibration control of many structures under random wind action. The authors evaluate the influence in the fluid's movement caused by a restriction inside a hole-shaped tube. It is noted that regardless of the structure's characteristics, the same reduction in the displacements and acceleration of the system can be achieved with a proper opening in the damper's restriction.

Shape adjustments have been proposed and studied by researchers, for example, a V-shaped TLCD (Gao et al., 1997). They try to find the optimal damper dimensions to achieve the highest possible reduction in the dynamic response of the structure. It is observed that the damper with the higher horizontal length to total length ratio is the one with a better reduction in the response for a small amplitude increase in the liquid movement. This is because the horizontal mass is the one that effectively acts on the structure. Another variation of the TLCD is also proposed, allowing the column cross-section to be non-uniform. The performance of this damper is compared to that of the TLCD and it is found to be as or even more effective. Other advantages obtained by changing the shape of the TLCD are the versatility and architectural adaptability, since its natural frequency is determined not only by the length of the liquid column but also by the area ratio of the horizontal and vertical portions of the tube (Hitchcock et al., 1997; Chang and Hsu, 1999).

Souza (2003) compares the efficiency between different types of dampers that make use of liquid to dissipate the vibration energy of the structure. These types of dampers are efficient in reducing the horizontal oscillation of structures subjected to dynamic loads. In the particular case of resonance excitation, the efficiency is greater. The results for the

Liquid Column Damper are similar to the other liquid dampers, but the LCD has some advantages: it requires less mass, has a steadier behavior, has a smaller reaction time, and offers greater flexibility to the designer.

Hochrainer and Ziegler (2006) studied the incorporation of a sealed pressurized gas chamber to both ends of the Liquid Column Damper. The main qualities of the LCD are maintained, but the addition of this mechanism enhances the performance of the Pressurized Liquid Column Damper (PLCD) when compared to the classic LCD. The authors propose the use of the pressurized chamber as an active control device to reduce the vibration peaks during the transient response, emphasizing that the PLCD is a promising alternative to the control devices due to its low cost and easy to install technology.

Shum et al. (2008) studied the use of PTLCDs in the reduction of vibration in long span cable-stayed bridges. Multiple PTLCDs are used under the deck of the bridge, so that applied loads on the deck are transferred to the damper, reducing lateral and torsional vibrations. The results show that this damping device is very effective for this particular application. Additionally, the PTLCD offers great flexibility to the designer in defining the geometric parameters and the natural frequency of the damper.

Tait (2008) proposes a pre-design method for a TLD with rectangular tank. The method linearizes the equations of motion and analyzes the system as if it were a simple mass-spring-damper equivalent model. The method was experimentally tested and it was concluded that it is capable of representing well the first vibration mode of the fluid. However, it cannot simulate the nonlinear behavior of the TLD and, consequentially, the dynamic response on the free surface of the fluid.

A hybrid TLD model is studied by Banerji and Samanta (2011). In this model, the TLD is rigidly connected to a TMD that is connected to the structure by a spring. The optimized system, which was also lighter than the original TLD, was capable of significantly reducing the structure's dynamic response, compared to the model of a simple TLD.

Pestana (2012) evaluates the efficiency of a TLD system in a reduced-scale frame and compares the results with a numerical simulation, obtaining great accuracy. The system undergoes different dynamic actions to verify its efficiency. It is observed that the frequencies of the damper and of the structure must be as close as possible to have a gain in the device's efficiency. The ratio between the liquid's horizontal length and total length must be limited by the available space and should be as high as possible.

Kenny et al. (2013) studies the optimization of many parameters of a TLCD, such as the tune ratio, the pressure loss coefficient, mass ratio, and length ratio. Experimental results with no dampening are compared to those of an optimized TLCD and a badly optimized one, revealing the importance of the optimization of this kind of damper.

Gur et al. (2015) evaluate the efficiency of a TLCD that had its orifice substituted by a metal ball that was free to move inside the horizontal portion of the tube, called a Tuned Liquid Column Ball Damper (TLCBD). The metal ball essentially acts as a mobile orifice that regulates the damper's liquid flow. After a parametric study related to the mass, the horizontal length of the damper, and intensity of excitation, it is observed a greater performance in the reduction of the structure's response when comparing the TLD and the TLCBD.

Bigdeli and Kim (2016) compare the performance between different types of the most used passive control devices by performing an experimental study. These devices include:

Tuned Mass Damper, Tuned Liquid Damper, Liquid Column Damper. The study evaluates the individual contributions of the mass and the damping of each device in the control of seismic vibrations. The LCD, compared to the TLD, has a larger share in the energy dissipation caused by its damping, and, in general, leads to a greater reduction in the structural vibration.

Freitas (2017) coded the software DynaPy to assist in the numerical study that evaluates the efficiency of TLCDs in structures modelled using the shear building theory. Multiple dampers are tested, as well as the incorporation of a pressurized chamber in the vertical portion of the TLCD. For a sine wave excitation, it is observed that a greater reduction in the structure's vibration response occurs when a control device with a higher mass is used. The addition of the pressurized chamber to the TLCD ends up helping in its design, since the damper's frequency now also becomes dependent of the pressure in the gas chamber and not just the length of the TLCD. Furthermore, the dynamic response of a shear building under a seismic excitation is numerically simulated. The results show that, despite a reduction of 42% in the maximum displacement, there has been a reduction in the efficiency of the control of the total response.

The vibration control using a Liquid Column Damper containing embossments on its inside walls is analyzed by Park et al. (2018). The results show that the LCD with embossments has a damping ratio of up to 2.7 times higher than the traditional LCD. It also has up to 20% more acceleration reduction than the LCD, while also having a steadier behavior in all the range of frequencies utilized.

Mendes (2018) studies the use of multiple pressurized tuned liquid column dampers in reducing the vibration caused by a seismic excitation in various system models utilizing soil-structure interaction. The interaction between the soil, the foundation, and the structure, together with the PTCLDs, is considered in many of them. They include tridimensional models of multiple-story structures, flexible base for the structure represented by impedance functions, and multiple PTLCDs arranged in a cross pattern. The variation in the structure response and the efficiency of the dampers due to the soil-structure interaction is evaluated by a parametric study of each system. The numerical study was performed developing a computational routine implemented into the software MATLAB. The results show the importance of considering the soil-structure interaction, due to the soil flexibility and its added damping effect in the system, reducing the response of the soil-structure-damper system when compared to the structure-damper system. The effects observed for rigid structures in flexible soil show that they are heavily influenced by it, while it is not as significant for flexible structures in a rigid soil.

Mendes et al. (2023) analyze the efficiency of the TLCD in reducing structural vibration by adopting numerical and analytical methods in the search for the ideal parameters of the liquid column. The equivalent linear model is considered for the U-shaped liquid column equation of motion with damping resulting from an orifice. A variation of TLCD parameters for two load types is investigated. Initially, a numerical study in conjunction with the analytical formulation for a sinusoidal load is adopted. Subsequently, the action of the El Centro earthquake through the recorded ground accelerations is considered in a case study. Optimal TLCD parameters are presented via response map for reducing the structure's maximum permanent response to harmonic excitation and for reducing the structure's rms response to seismic excitation with wide frequency and various amplitude. The variation of the TLCD parameters presented by the response map is directly related to the force acting on the structure. However, it is verified that regardless of the acting force, there is an ideal frequency range to tune the TLCD where the greatest reductions

in the primary system response are found. From the ideal liquid column parameters determined by the parametric analysis, structural response reductions of approximately 60% were achieved.

To conclude this succinct literature review, it is opportune to present, in the domain in question, the research activities that have been developed within the scope of the University of Brasília (UnB) by the Group of Dynamics and Fluid-Structure (GDFE) from PECC/ENC-FT, which has also been dedicated to several studies related to tuned liquid attenuators (TLAs), sloshing, water waves, etc. The more recent publications include: Sarmiento et al. (2020), Moraes et al. (2020), Mendes et al. (2023, 2019, 2018), Mendes (2018), Ghedini et al. (2019), Freitas and Pedroso (2018, 2017a, 2017b), Silva (2018), Silva et al. (2018), Pedroso (2016), among others.

2.3 Some aspects of studies and research in the nuclear area that contribute to the advance of knowledge about TLCDS

2.3.1 Initial aspects

Due to several phenomena present in the flow of the fluid column, which have not been adequately treated by many authors, many inaccuracies, discrepancies and dubious results, in several aspects, have been observed in the technical literature TLCDS. These problems, however, had been adequately addressed in similar phenomena in the tubular circuits of nuclear reactors.

Therefore, many studies and researches in the nuclear field with results immediately transferable to the field of knowledge of the TLCDS are no longer reported in international technical literature. This is due to the fact that nuclear technology is a sensitive, confidential sector, with severe restrictions on the disclosure of their results and the confidentiality of the research.

Even if the original motivation and orientation of these studies and researches were not aimed at the issue of using TLCDS in civil construction, they could have contributed significantly in boosting knowledge about the TLCDS. Unfortunately, the aforementioned restrictions did not allow these pioneering studies to have a greater dissemination in the scientific literature, reducing them to hermetic knowledge restricted to research centers involved with nuclear technology.

This section presents some experimental studies related to nuclear technology that contributed knowledge to the TLCDS study field. The Group of Dynamics and Fluid Structure of UnB (GDFE, in Portuguese) can benefit from it thanks to the existing relations with Nuclear Research Centers in France, with emphasis on the Commissariat of Atomic Energy (CEA, in French), today known as French Alternative Energies and Atomic Energy Commission, research centers in Saclay, Cadarache and Grenoble, described by Pedroso (1983, 2015).

Thus, several experimental studies in models, circuits (loops) and test rigs were conceived at the Center of Nuclear Studies (CEN, in French) in Saclay, of the Commissariat of Atomic Energy of France, at the Laboratory of Structures, Vibrations and Earthquakes (LEVS, in French) of the Department of Mechanical and Thermal Studies (DEMT, in French), of the Division of Studies and Reactor Development (DEDR, in French). These results are directly transportable to the problem involving TLCDS.

Academic texts on much of the research carried out at the time can be found in Gibert (1988). With the changes that occurred in CEA-France, many of these laboratories and

services began to have other names and were even subdivided into other units, such as the Tamaris Laboratory (see the annex on page 112), which became one of the large Test Laboratories (Platforms) from Saclay (CEA PARIS-SACLAY - *Les Plateformes de Simulation Et Modélisation* (2023)). Other web pages also allow access to the other laboratories and to the research and development units, namely: CEA PARIS-SACLAY - *Le CEA Paris-Saclay, Centre de Recherche Scientifique et d'Innovation* (2023), CEA - *From Research to Industry - Science and Technology for Tomorrow's* (2023), and a general access guide with information from the Paris-Saclay Center (CEA360 - *Centre Paris-Saclay - General Information Guide* (2023)).

In the 1970s and 1980s, in Europe and mainly in France, the development of nuclear technology in the area of nuclear reactors made extraordinary progress and two types of reactors became the subject of many research studies, namely: i) Fast Neutron Reactors (FNR) which is a nuclear reactor that uses fast neutrons as opposed to thermal neutrons, described in Bist (1978), Costa (1979), Sauvage (2004) and in the reference “*Les Reacteurs Nucleaires à Caloporteur Sodium*” (2014); ii) Pressurized Water Reactors (PWR).

These two types of reactors simulate, in the study, design, test and operation phases, hypothetical and real accident scenarios, events that are undesirable and that have been the subject of important studies to avoid or mitigate the harmful effects of these accidents.

At the time, technologies involving these two main types of nuclear reactors sought answers to problems that raised, among others, the following research questions:

i) In sodium-cooled reactors, the explosive sodium-water reaction can occur at the Steam Generator (SG) level as a result of a leak due to total or partial rupture of a water pipe in the SG, as described in Pedroso et al. (1990).

The gases produced by the reaction expand violently, producing pressure waves generated by the initial peak of pressure in the hydrogen bubble. The pressure waves travel through the SG and pass to the secondary circuit (SC) of the reactor, which was practically designed to work without pressure (below 10 Bars), a fact that can compromise the structural integrity of this circuit. After the most acute transient phase, the sodium column inside the secondary circuit of the reactor, located between the secondary pump, which has an argon sky (gas cavity), and the SG, will be subjected to damped oscillatory movements, reproducing what happens on a TLCD. Figure 2-16 relates the similarity of the two problems.

Figure 2-16a shows the secondary sodium circuit in a simplified way (depicted as a rectified circuit), located between the secondary pump and the steam generator where the explosive sodium-water ($\text{Na-H}_2\text{O}$) reaction takes place and the pressure transient is originated. A discontinuity of the pressure field caused by the presence of a localized pressure loss (singularity) is also qualitatively illustrated. After the initial and severe phase of the transient, the sodium column oscillates between the two expansion tanks containing argon, which function as a pressurizer (stiffness of a pressurized gas cavity), reproducing with great similarity what is observed in a pressurized TLCD. Figure 2-16b shows a simplified representation of a PTLCD in oscillatory flow caused by oscillations of a building under dynamic actions, such as wind, earthquakes, etc.

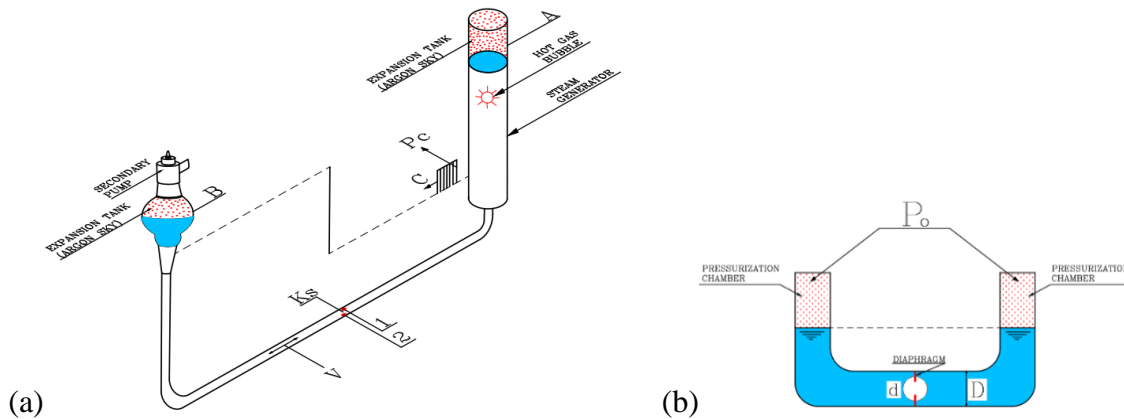


Figure 2-16 - (a) Simplified secondary sodium circuit, located between the secondary pump and the steam generator where the transient originates (explosive Na-H₂O reaction) and (b) the simplified representation of a pressurized TLCD also in oscillatory flow caused by oscillations of a building under dynamic actions

ii) In tubular circuits of pressurized water reactors, the appearance of pressure transients caused by planned or accidental maneuvers, as well as depressurization accidents, among others, cause the propagation of these pressure waves. They travel through these circuits and affect the internal elements and components of the reactor, in addition to a series of parallel phenomena that occur as the waves come and go, changing the properties of the medium that characterizes the columns of fluids involved in these circuits. Examples include cavitation, degassing (release/formation of air bubbles in the liquid), variation in the compressibility of the fluid, two-phase flow, vibrations in the pipelines, shocks in the supports, etc. Figure 2-20 of the SAFRAN circuit illustrates a simplified circuit of a PWR reactor, made on a scale model.

In this case, also after the severe phase of the transient, in which cavitation may occur, the fluid column will be placed in oscillatory movements, with a reduction in frequencies due to the degassing phenomenon, which alters the compressibility of the fluid (reduction of the speed of sound in the medium, Pedroso (1986)). Then, the final phase of the transient phenomenon is an analogy of what happens with the oscillating column of incompressible fluid in a TLCD caused by the oscillations of the structure (buildings, towers, etc.). The area marked by an ellipse in Figure 2-19 shows the damped oscillatory character of the fluid column, an effect also described in Pedroso et al. (1994). In the initial phase, it is possible to observe the severe response of the transient, which can reach tens of times the mean pressure value in the fluid before the transient, even causing cavitation of the fluid column.

The method used to answer this question usually consists of simply extrapolating conventional results obtained for stationary flows (steady and unidirectional), but it lacks precision and can lead to errors. Therefore, in TLCD studies, the adoption of head loss coefficients (localized and due to friction along the pipeline) for a fluid in a steady flow regime, which depends solely on the Reynolds number, has been a source of errors and inaccuracies, since these oscillatory flows are dependent on time, frequency and other factors besides the Reynolds number.

With the objective of solving this problem in a more satisfying way, the adoption of a parametric experimental approach using physical models/scale models/mockups becomes an irreplaceable resource for the correct treatment of the matter.

As seen previously, the tubular circuits traversed by fluids in these reactors present complex phenomena, whose theoretical and numerical simulation studies do not always provide satisfactory answers regarding the understanding of these phenomena. As a result, experimental models (in scale or simplified) are needed to clarify the understanding of the issue.

2.3.2 The different types of unsteady flow in pipelines

Real flows always present fluctuations in their fundamental quantities/variables. One can, however, distinguish two situations for them, in the case of a very little compressible fluid Pedroso (1986):

1) The case of established regimes, in which the fluctuations (essentially of the pressure) come from the instability of the flow due to the singularities and the existing turbulence. In these flows, very small flow fluctuations are observed only due to the compressibility of the fluid ("acoustic" effects).

2) The case of interest, in which the flow rate varies significantly:

a) The flow varies around a mean value with a low enough amplitude that it does not reverse. This regime of stationary fluctuations is called "pulsating flow". For example, the case of a flow generated by a rotating machine; b) The pipe flow systematically reverses in a regular or irregular way. This is the case, for example, with the oscillation of a liquid column between two gas reservoirs (oscillatory flow), typical case of PTLCDs and TLCDs; c) The flow changes during a fast transient. This is, for example, the case of the depressurization of a hydraulic circuit due to a sudden brutal rupture.

The flows of interest here are types b) and c). For reasons of simplicity of experimental analysis, considering the facilities available, flows of type b) will be analyzed next. More particularly, the alternating periodic flow generated by the movement of a piston in a tube (RIO test rig), which can very similarly simulate the oscillatory flow of the fluid column of a TLCD.

2.3.3 Experimental devices for the study of unsteady flow in pipelines at CEA France

Gascogne air/water circuit (CEN Saclay)

The Gascogne circuit was used for fundamental studies of pressure fluctuations, created by accidents (curves, elbows, branches) or by obstacles located within the flows, as well as for experimental studies on the vibratory behavior of different structures (fuel elements of water reactors) under the influence of fluid flows.

The test section below (Figure 2-17) is placed in the Gascogne circuit (loop), Gibert (1988, 1989). Rubber gaskets reduce as much as possible the mechanical coupling between the part of the circuit whose movement is studied and the rest of the circuit. Likewise, two pressurized tanks (attenuators), located upstream and downstream, ensure acoustic decoupling and, in particular, isolate the test section from pump noise.

The circuit studied is shown schematically in Figure 2-17. The piping is made of stainless steel and has a diameter of about 18 cm and a thickness of 2 mm. It has four 90° bends with a bending radius of 27.5 mm ($R/D = 1.54$). The circuit also has very rigid connection flanges and is supported vertically by elastic bands. The mass of the pipe is 250 kg and the fluid mass is less than 300 kg. The gate valve is located between the downstream pipe flexible joint at the right end of the duct and the pressurized cavity. Pipe movements are

measured by accelerometers and fluctuating pressure is measured by wall sensors. The locations of these measurement points are also shown in Figure 2-17.

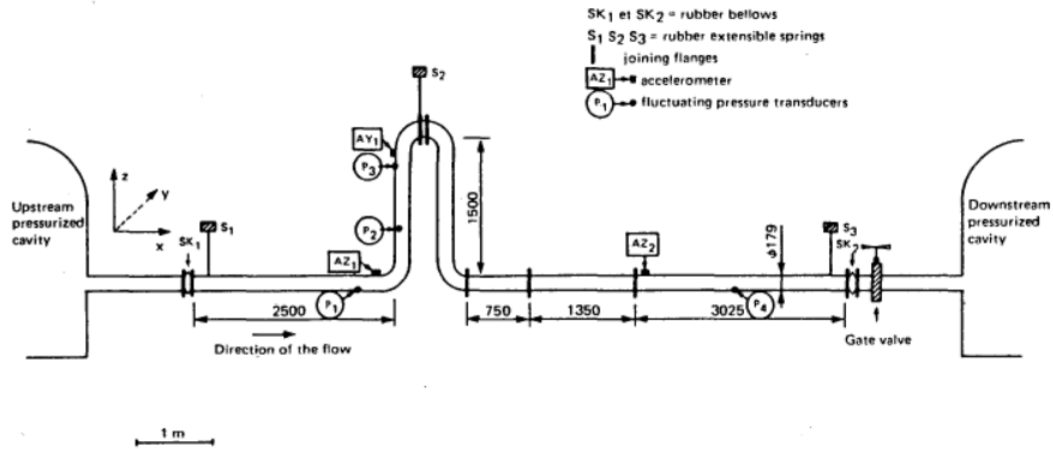


Figure 2-17 - Test section of the Gascogne experimental test rig (Gibert, 1988, 1989)

Gibert (1989) describes the main source of excitation present in the system under study, which is characterized by a semi-closed gate valve. Various flow velocities and valve opening parameter values were tested.

In general, the main sources of excitation in a pipeline transporting a fluid are located in singular areas, such as sudden widening, curves, pipe junctions, valves, pumps, obstacles, etc., as shown in the circuit in Figure 2-17. If we exclude the pumps that can generate excitations in the medium frequency domain, all of these singularities are sources of low frequency excitation.

The dimensions of the disturbed fluid volume zones around these accidents are small compared to the characteristic acoustic and structural wavelengths of the system. Therefore, the source associated with the flow in a singularity can be considered as a point source. Furthermore, there are natural modes of the structure (duct) that are virtually without deformation throughout the fluid domain (liquid column). Thus, we can explicitly specify this source, which can be simplified, for weakly compressible fluids only, to a discontinuity $\Delta p(t)$ of the mean fluctuating pressure over a cross section at the bends of the duct and at said valve. In this case, the pressure sources originating from the curves are secondary, in relation to the main source (valve). Or, in other words, using the local turbulent pressure fluctuation field on the wall of the structure, at the location of the singularity, as a “forced function” (force), pointwise on the structure.

This assumption is valid if the fluid is weakly compressible (as in our case) and if the characteristic length associated with the modal shape is of the order of magnitude equal to or less than the dimensions of the disturbed zone.

The valve becomes the largely preponderant source of excitation in relation to sources originating from elbows and other circuit accidents.

Thus, the problem is associated with a single source of excitation that excites the system at low frequency (the studies were carried out in the range of 0-10 Hz, therefore within the frequency ranges of liquid column oscillations of TLCDS).

It is observed, in these experiments, in the deformations of the structure, that the flexibility of the piping comes mainly from the elbows of the piping line and also from

the areas where the pressure profile (pressure diagram) is straight and the fluid can be considered incompressible. The characteristic of the straight pressure profile in the straight sections of the piping is typical of the inertia effect of the fluid column, Pedrosa and Gibert (1987). It is also noted that the change in the slope of the pressure profile at the level of the elbows is an indicative factor of the fluid-structure interaction.

Therefore, it can be concluded that singularities in TLCD experiments, in addition to inducing localized losses, can create non-negligible point sources of pressure under certain conditions. In addition to altering the properties of the fluid, the point sources of pressure act as forces on the pipe walls, which can even cause measurement errors on sensors located along the duct. These tests highlight the reciprocal influence of the flow and the response of the structure (duct), an aspect practically not considered in TLCD studies.

Claudia experimental test rig (CEN Cadarache)

This Claudia test rig reproduces a simplified circuit of a PWR reactor, described in the literature by Huet and Garcia (1985) and Pedrosa (1994), which was designed at CEN Cadarache, France.

It is basically a pipe, with a length of about 22 m and a diameter of 0.146 m, connected to a cylindrical cavity at one end, which maintains a constant high pressure (about 30 Bars), and, at the other end, there is a membrane and a valve set to close automatically (closing time of 68 ms) after membrane rupture. Figure 2-18 shows a representation of a view of the analyzed hydraulic system.

The transient generated by the rupture of the membrane will create a suppression wave, which will travel through the piping, producing cavitation and generating air bubbles in the system. Pressure sensors, strain gauges, flow meters, among others, were distributed along the pipeline. In the experimental test, all valves were kept open with the exception of the A-R valve, which closed during the test. Localized load losses (singular losses) were also computed.

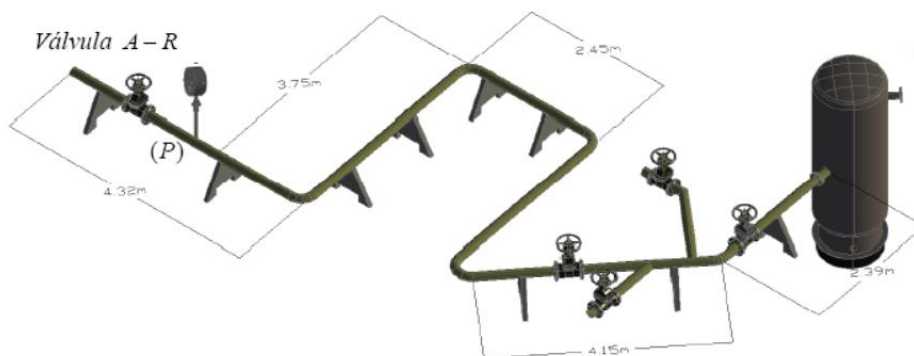


Figure 2-18 - Isometric representation of the hydraulic system of the Claudia test rig (Velez et al., 2015)

Figure 2-19 shows the experimental and numerical pressure transient waves, respectively. Results that were obtained for the Claudia test rig, Barbosa and Pedrosa (2005), are compared with the TRANSPETRO-1D program for point (P), Velez et al. (2015). Similar results were also obtained by the TRANS Program, Pedrosa et al. (1994).

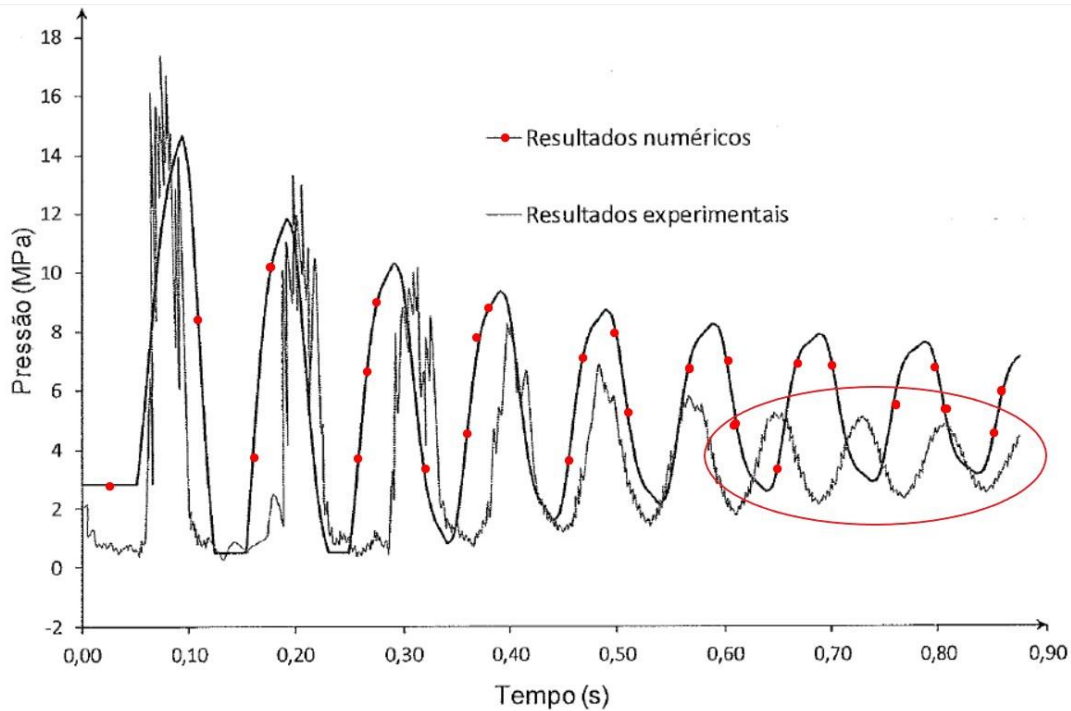


Figure 2-19 - Numerical (TRANSPECTRO-1D) and experimental evolution of pressure in the pressure transducer (P)

Comparing the pressure waves presented in Figure 2-19, the following findings can be made:

- The curves show a certain similarity in the amplitudes, widths and number of peaks.
- The greatest similarity between wave shapes is observed from the fourth peak onwards.
- The differences observed in the results, such as in the amplitudes, period and graphic form of the curves, are consequences of the lack of implementation of the more complex mechanisms in the system, such as cavitation, degassing, two-phase flow, etc., factors that attenuate the waves and change their celerity.
- The computational implementation incorporating cavitation, Barbosa and Pedroso (2005), carried out in the first two cycles to present the results with the cavitation effect, can better represent the phenomenon.

To obtain more information about the results acquired at the Claudia test rig, the reader can refer to the texts by Pedroso (1994) and Barbosa and Pedroso (2005).

SAFRAN Circuit (CEN Saclay)

The SAFRAN Circuit, Epstein and Assedo (1976), represents a scale model, fully instrumented, of a PWR reactor. It was designed for vibratory studies of the internal structures of this reactor through direct measurements of the structures' responses to excitations caused by steady and transient flows.

The vibrational behavior of the PWR reactor internals is governed by complex phenomena, whose understanding requires detailed analysis. The SAFRAN circuit allows studies that simultaneously include mechanical tests on reduced models (mockups) of the reactor internals and, on prototypes, hydro elastic tests (Fluid-Structure Interaction - FSI)

and calculations using the TRISTANA program. These studies, tests and calculations allowed the prediction of vibration levels in the Fessenheim Nuclear complex (France) and can also be transposed to other reactors.

Figure 2-20 illustrates this type of circuit. It shows the reactor core, other components, the pipes that reach the core and, on the left of the image, a prismatic metal box connected to the end of the pipe, where the rupture of the membranes occurs. Their ruptures allow the study of sources (generation) and propagation of waves in a section of the pipeline and their effects on the reactor internals. In experimental tests with membrane ruptures carried out in this more complete circuit, intricate phenomena (difficult to interpret and correlate) were observed. Because of this, it became necessary to create a simplified section of the circuit, characterized by the “DIPLODOCUS” mockup, shown in Figure 6(a), which was designed to address the issue through a simpler system. Figure 6(b) shows a schematic of the mockup.



Figure 2-20 - SAFRAN circuit, representing a simplified scale model of a PWR reactor

The next section introduces the different installations, equipment and measuring devices used for the experimental studies that were made especially for these researches: a preliminary device (DIPLODOCUS), using rupture and vibration of membranes as a variable pressure source, and a definitive device (RIO), allowing the determination of the main quantities associated with an oscillatory flow and whose results are directly transportable to TLC-D-related flows. Analytical models designed to understand these experimental devices are extensively discussed in Pedrosa (1992a, 1992c).

Preliminary test device - DIPLODOCUS model (CEN Saclay)

This is a preliminary device that initially used membrane rupture as a pressure source to generate transients. As these results were not repetitive and involved complex phenomena, the variable pressure source was replaced by the vibration of membranes in contact with the fluid column (FSI). The test rig consists of a straight, 3.0 m long, stainless steel tube, with an internal diameter of 0.035 m, 8.0 mm thick and fixed in a concrete block.

The membranes are placed at one end of the tubing and are excited by a vibrating exciter (shaker). Devices that allow measurements of pressure, sound speed and acceleration are distributed along the duct, among other measurement sensors.

Figure 2-21a and Figure 2-21b show, respectively, a photograph of this preliminary testing device and a schematic of the test rig, which is also presented by Barbosa (1998).

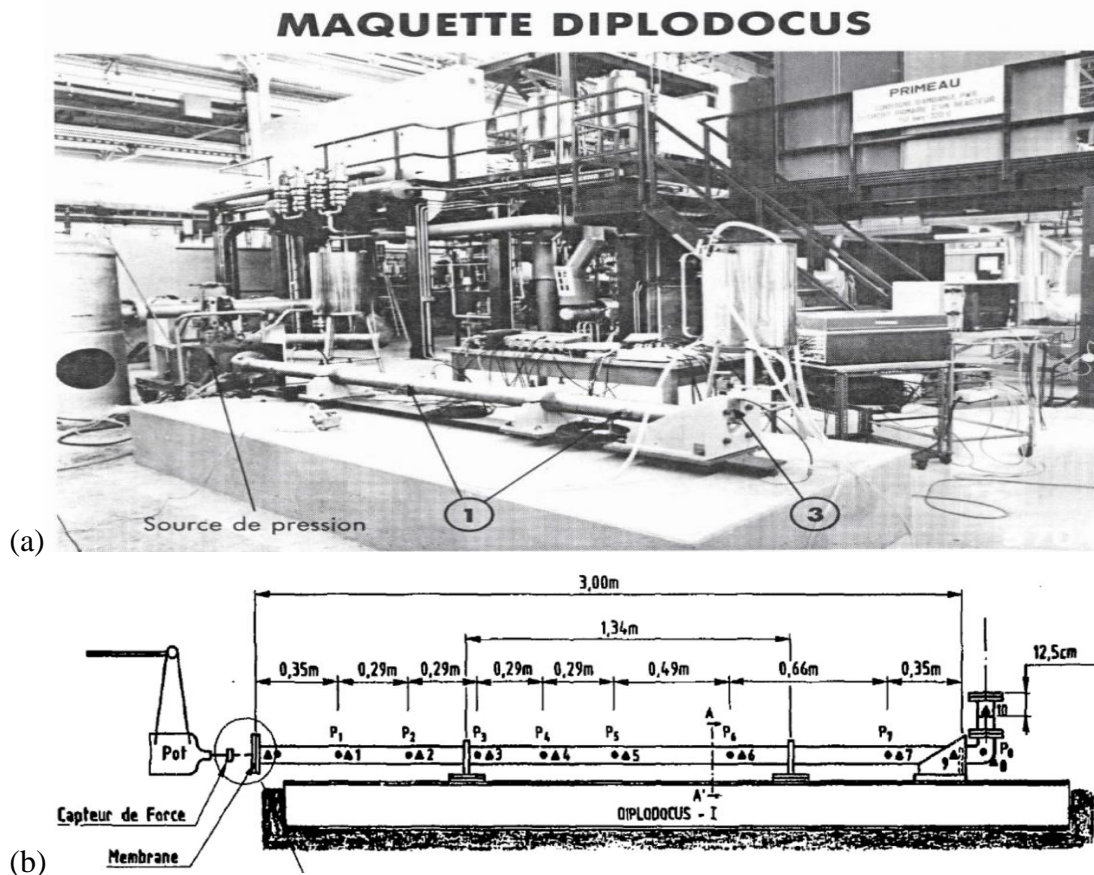


Figure 2-21 - DIPLODOCUS model: (a) preliminary test device using vibrating membranes as a variable pressure source and (b) simplified schematic of the device

RIO test rig (CEN Saclay)

The Rio test rig is characterized by a definitive and well-planned device that allows determining the main quantities associated with a flow, oscillatory or not. Its results are directly transportable to flows associated with TLCDS.

The difficulties encountered and the experience gained in the experimental tests on the DIPLODOCUS test rig provided important elements for the design of the RIO test rig, in which the unsuccessful aspects of the previous tests were corrected, Pedroso (1986).

This test rig was designed to study the propagation and damping of pressure waves in localized singularities and along tubular circuits of nuclear reactors due to transients, Pedroso et al. (1990). The test rig consists of a long steel tube (6.0 m long, 8.5 cm in diameter and 8.0 mm thick). This tube was adapted to the hydraulic system of a seismic table. At the left end of the tube, a piston coupled to the hydraulic system moves the fluid column. At the other end, a free surface pressurization tank was installed to eliminate cavitation problems and minimize the effects of degassing (this part of the device would

also simulate the case of a PTLCD). Piezoelectric pressure sensors are placed all along the tube at regular intervals. Accelerometers and static pressure sensors are also installed at important points. The test section is located approximately halfway through the tube, where the singularities under study are placed. The description and analysis of this device are also presented by Barbosa (1998). Figure 2-22a and Figure 2-22b illustrate said test rig, while Figure 2-22c shows a simplified schematic of the device. Each test consists of a frequency sweep for different piston displacements (X_m), where a computer at the measurement center controls the characteristics of the wave introduced into the system or the movement of the fluid column. The tests, which are carried out completely automatically, allow the results to be presented in the most diverse forms of representation.

Due to the viscosity and specific mass of liquid sodium being close to water's, which allows the study of the former in a mockup using the latter, it was possible to make considerable simplifications in the experimental studies and to extend its applications.

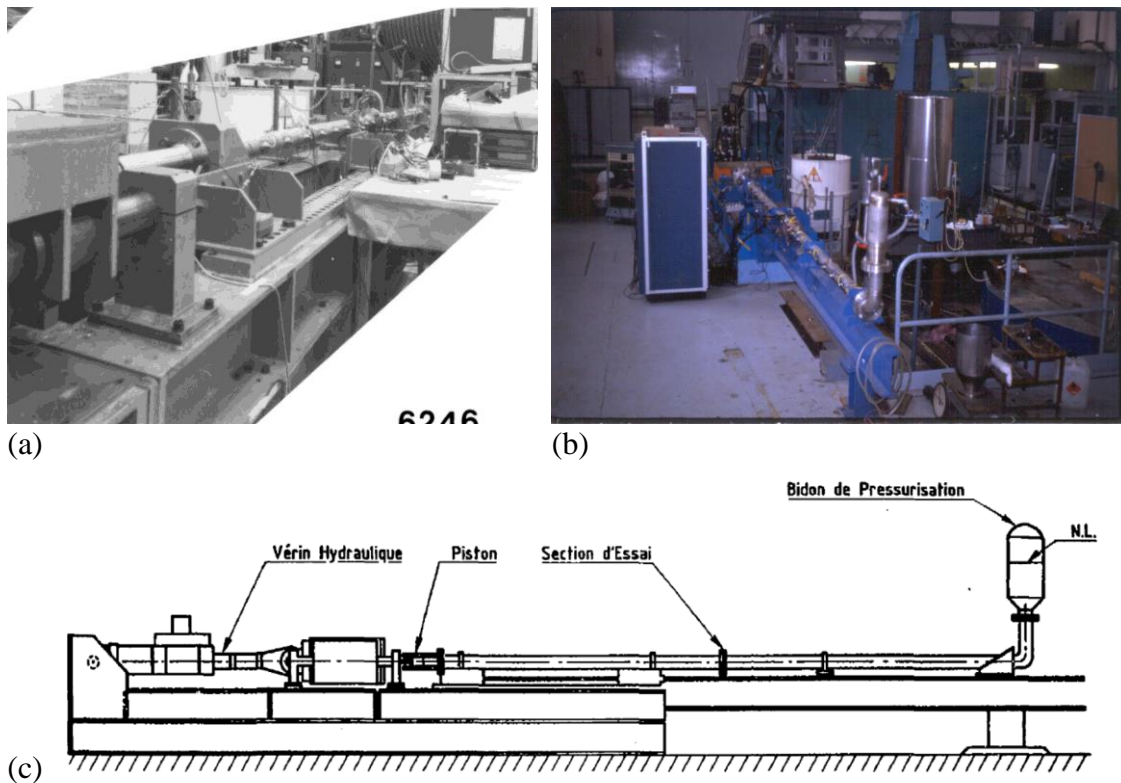


Figure 2-22 - Illustration of the Rio test rig: (a) piston-pressurizer view, (b) pressurizer-piston view and (c) simplified schematic of the device

Even though this device was not designed for studying TLCDS, it is capable of faithfully reproducing the conditions of the liquid column movement in the case of a TLCDS. Therefore, these results are useful and transportable to TLCDS studies.

2.3.4 Some conclusions obtained through the experimental results reported above and which are directly transportable to TLCDS studies

Considering that these tests were carried out for a certain type of singularity and were limited to a range of characteristic parameters, it is difficult to draw very general conclusions for TLCDS. In any case, within the range of values, and for the conditions studied, some important conclusions can be drawn.

When analyzing the test results, it was discovered that the correlation between the singular pressure loss coefficient in the oscillatory flow and the Reynolds number ($U_m d/\nu$) is not trivial. On the other hand, when this coefficient is analyzed as a function of the $U_m T/d$ parameter, a better defined and more regular correspondence is observed. That is, in unsteady (oscillatory) flows, the dissipation phenomena depend on the frequency of the oscillatory flow and are more intense for higher frequencies, Pedroso and Gibert (1988).

The parameter $U_m T/d$ represents the ratio between the distance that fluid particles travel in one direction in a period (T) of flow oscillation, in the absence of singularities (obstacles in the flow), and the diameter (d) of the orifice/duct, which constitutes the source singularity of the obstruction or not, that is: $U_m T/d = 2\pi U_m/\omega d$, where U_m is the maximum velocity (amplitude) of the flow.

The parameter $U_m T/d$ is the so-called period parameter (PP), a kind of inverse of the Strouhal number, which for free surface oscillatory flow (water waves) is called the Keulegan-Carpenter number.

For large values of $U_m T/d$, the total dimensionless pressure drop approaches the values of the pressure loss coefficient given for steady flows. This corresponds to the case of large fluid movements with predominance of localized loss effects, Pedroso et al. (1990). The phase angle tends towards the asymptote ($\theta \rightarrow \pi/2$).

For low values of ($U_m T/d$) the fluid movements become increasingly weaker (small displacements). The pressure drops are relevant, the fluid inertia effects (fluid column between the two measurement sections, plus the inertia due to the singularity) become significant and the phase angle tends to zero ($\theta \rightarrow 0$).

In fact, for low values of this parameter, the pressure loss coefficients show a large dispersion, but remain higher than the values for steady flows.

As an immediate consequence of this work, experimenters' attention is drawn to the following two aspects:

- 1) Flow measurements for unsteady flow rates, such as the ones through diaphragms, can be affected by errors related to the constants associated with the orifices, which occur during calibrations in stationary (steady) flows.
- 2) During intense transients, such as water hammer (small $U_m T/d$) or mass transfer phenomena (movement of the incompressible liquid column), the attenuations due to singularities are greater than those calculated adopting coefficients obtained for steady flows. However, these findings are partial and said with reservations, as specific tests for TLCDs were not carried out in these studies.

This suggests an experimental analysis for wider ranges of values of $U_m T/d$ (associated with higher frequencies), which can provide complementary information to these studies. It would still be desirable to carry out other tests to study the influence of different parameters, other types of singularities, geometries, etc., in order to produce universal type abacuses that are easy to use in calculations and engineering applications.

Furthermore, within the same scope of these investigations, specific tests relating to singular losses (attenuations) during intense transients (water hammer and depressurization) and then in the oscillatory phase of the phenomenon are really necessary.

From a practical point of view, the experience gained allows future experimenters to be informed about the precautions to be taken, such as:

- Strictly control the quality of the water and absolutely avoid the presence of air in the circuit.
- Avoid contact of the air from the pressurizer with the free surface through a membrane or balloon (avoid air diffusion).
- Make the model in transparent material so that the evolution of the phenomenon can be observed, helping to understand and model the problem under study.
- Calibrate the singularities for steady flows first and only then test them in oscillatory flow. In fact, the use of a piston can be effective for this type of test, as long as it is possible to extend the ranges of displacements and frequencies over a reasonably wide range of values.

Another device that one could think of to create the desired conditions and avoid the disadvantages of the piston (intense mechanical vibrations during high-level pressure tests) would consist of a fluid column between two gas reservoirs at variable pressure (U-shape tube type of a TLCD with a very long vertical branch). This is a system that has the advantage of simulating conditions found in fast neutron reactors and that allows other types of studies, such as the ones for TLCDs. Finally, parallel studies can be carried out for quantitative assessments of phenomena such as cavitation, degassing and two-phase flows. Under certain conditions, these phenomena may occur but are practically disregarded in TLCD studies.

Some not sufficiently addressed/studied problems in the TLCD area of knowledge influence more or less this matter, depending on each case, and have been extensively studied in nuclear technology, Pedroso (2015), namely:

- Fluid compressibility and variation in the speed of sound.
- Effect of degassing (caused by the oscillation of the fluid column and by the presence of a variable pressure field in the fluid).
- Deformation of the duct wall (fluid-structure interaction).
- Sloshing effects on the free surfaces of the ascending branches of the TLCDs.
- Nonlinear models associated with the rigidity of the fluid column and the fluid of the pressurizer (PTLCDs).
- Inertia effects in singularities (diaphragms, orifices, plates, grids, etc.).
- Assessment of the multiple origins of damping in the TLCD, such as fluid viscosity, wall roughness, structure interaction with the flow, imperfect mechanical assemblies, singularities in the duct (curves, plates, grids), bubble ratio in singularity zones, etc.
- Dependence of the localized head losses and the oscillation frequency of the TLCD.
- Study of flow models with other fluid types, such as mercury, liquid sodium and ferromagnetic fluids (magnetic induction would allow influence over the fluid flow with important effects on its behavior).

3. Theoretical Foundation

The mathematical aspects range from each individual system, such as the structure and the TLC, up to a system that combines the structure and one or more of them. For each system, it is explained how it is modelled, how its parameters are obtained, and how the equation of motion can be formulated from those parameters.

3.1 Mathematical formulation of the Shear Building

Of all the individual systems treated in this section, the structure is the most important of them since this study aims to reduce its response when subjected to dynamic loads. When the analyzed structure is a building, the simplest way to model it is by treating it as a shear building. In this model, shown below in Figure 3-1, the mass is concentrated in each story, represented by a rigid body. Each story is supported by columns that have no mass and cannot deform axially. Because of those conditions, the only degree of freedom in the shear building model is the horizontal displacement of each story.

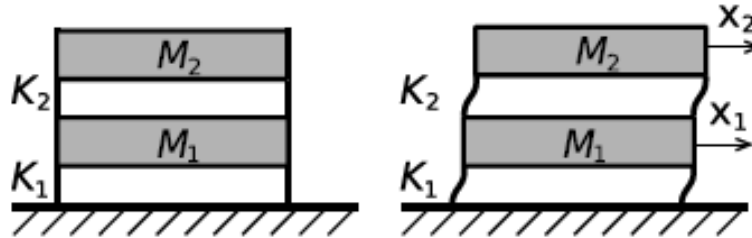


Figure 3-1 - Two-story building in the shear building model (Mendes, 2018)

For the two-story building under free vibration in Figure 3-1, the equation of motion, assuming no damping, is

$$\begin{bmatrix} M_1 & 0 \\ 0 & M_2 \end{bmatrix} \begin{Bmatrix} \ddot{x}_1(t) \\ \ddot{x}_2(t) \end{Bmatrix} + \begin{bmatrix} K_1 + K_2 & -K_2 \\ -K_2 & K_2 \end{bmatrix} \begin{Bmatrix} x_1(t) \\ x_2(t) \end{Bmatrix} = \begin{Bmatrix} 0 \\ 0 \end{Bmatrix} \quad (1)$$

where $\ddot{x}_1(t)$, $\ddot{x}_2(t)$, $x_1(t)$, $x_2(t)$ are, respectively, the accelerations and displacements of the first and second story, M_i is the mass of each story, K_i is the total stiffness for each story. This stiffness is obtained by adding the translational stiffness of each column in a story. Considering columns that are fixed on both ends, with Young's Modulus E , height h , and moment of inertia I , the translational stiffness for one particular column is

$$K_{fixed-fixed} = \frac{12EI}{h^3} \quad (2)$$

A simplified way to write Equation 1 is

$$[M_S]\{\ddot{x}(t)\} + [K_S]\{x(t)\} = \{0\} \quad (3)$$

which can be used as a generalized form to represent a structure with multiple stories, such as the one in Figure 3-2.

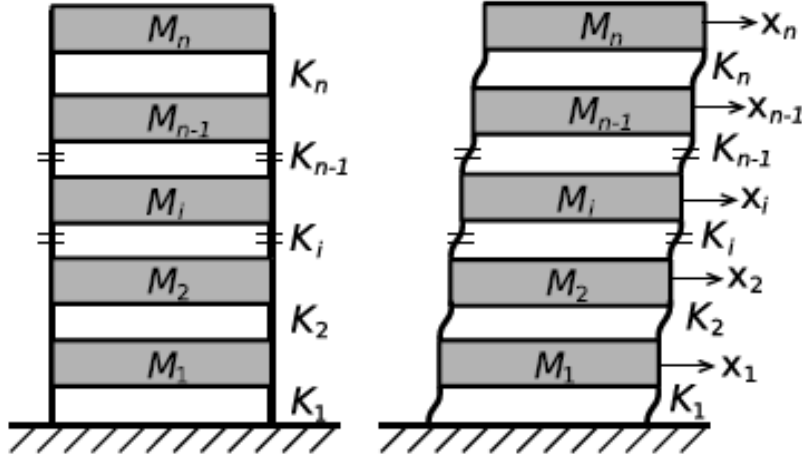


Figure 3-2 - Shear building model for a multiple-story structure (Mendes, 2018)

In this case, the coefficient matrices in Equation 3 are

$$[M_S] = \begin{bmatrix} M_1 & 0 & \dots & 0 \\ 0 & M_2 & \dots & 0 \\ \vdots & \vdots & \ddots & \vdots \\ 0 & 0 & 0 & M_n \end{bmatrix} \quad (4)$$

$$[K_S] = \begin{bmatrix} K_1 + K_2 & -K_2 & 0 & \dots & 0 \\ -K_2 & K_2 + K_3 & -K_3 & \dots & \vdots \\ 0 & -K_3 & \ddots & -K_{n-1} & 0 \\ \vdots & \vdots & -K_{n-1} & K_{n-1} + K_n & -K_n \\ 0 & \dots & 0 & -K_n & K_n \end{bmatrix} \quad (5)$$

Considering now the presence of a damping effect and the action of an external dynamic force on the structure, the equation of motion becomes

$$[M_S]\{\ddot{x}(t)\} + [C_S]\{\dot{x}(t)\} + [K_S]\{x(t)\} = \{P(t)\} \quad (6)$$

The vector $P(t)$ represents the dynamic loading, which in case of a ground acceleration caused by a seismic excitation becomes

$$\{P(t)\} = -[M_S]\{1\}\ddot{x}_g(t) \quad (7)$$

where $\{1\}$ is a unit column vector and $\ddot{x}_g(t)$ is the ground acceleration obtained from the seismic data recorded during an earthquake.

The damping matrix $[C_S]$ can be evaluated using the proportional damping model proposed by Rayleigh

$$[C_S] = A_0[M_S] + A_1[K_S] \quad (8)$$

Assuming that a same damping ratio ζ applies to all frequencies of vibration, then

$$A_0 = \frac{2\zeta\omega_1\omega_n}{\omega_1 + \omega_n} \quad (9)$$

$$A_1 = \frac{2\zeta}{\omega_1 + \omega_n} \quad (10)$$

where ω_1 and ω_n are the natural frequencies of vibration of the structure for the first and last vibration modes, respectively. These frequencies are determined from solution of the eigenvalue problem for Equation 3, that is

$$[[K_S] - \omega^2[M_S]]\{\phi\} = \{0\} \quad (11)$$

The nontrivial solution, $\{\phi\} \neq \{0\}$, is possible when

$$|[K_S] - \omega^2[M_S]| = 0 \quad (12)$$

3.2 TLCD model

In the modelling of the TLCD, represented in Figure 3-3, the same parameters calculated for the structure are also calculated for it.

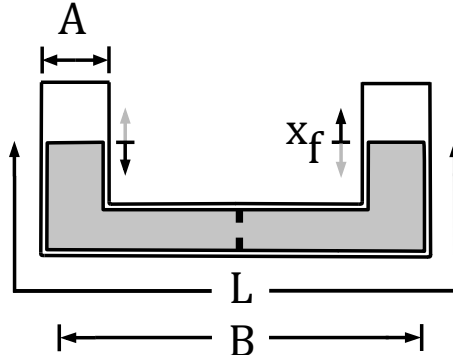


Figure 3-3 - Configuration of the tuned liquid column damper

The equilibrium equation for the TLCD is

$$m_f \ddot{x}_f + c_f \dot{x}_f + k_f x_f = F(t) \quad (13)$$

The TLCD mass m_f is easily obtained by multiplying the volume of fluid V_f by its density ρ_f

$$m_f = V_f \rho_f = \frac{\pi D^2}{4} L \rho_f \quad (14)$$

where D is the diameter and L is the total fluid length of the TLCD.

The stiffness coefficient cannot be obtained directly, since the fluid of the TLCD is considered incompressible. It can be obtained indirectly by using the expression for the natural frequency of the TLCD found in the literature - such as Blevins (1990) and Pestana (2012) apud Mendes (2018) - which is

$$\omega_f = \sqrt{\frac{k_f}{m_f}} = \sqrt{\frac{2g}{L}} \quad (15)$$

Substituting the expression for m_f and solving for k_f it is possible to obtain an equivalent stiffness for the TLCD, shown in Equation 16.

$$k_f = \frac{\pi D^2 \rho_f g}{2} \quad (16)$$

In the case of a pressurized TLCD, or PTLCD, the total stiffness is obtained by adding the gas stiffness to the equivalent fluid stiffness. The expression for the gas stiffness when air is used is (Pedroso, 1992a)

$$k_{air} = 2 \left(1.4 \frac{P \pi D^2}{Z \cdot 4} \right) = 0.7 \frac{\pi P D^2}{Z} \quad (17)$$

where P is the air pressure inside the gas chamber and Z is the height of the air column. The total stiffness for a PTLCD is

$$k_{ftot} = \frac{\pi D^2 \rho_f g}{2} + 0.7 \frac{\pi P D^2}{Z} \quad (18)$$

The damping coefficient can be obtained from the damping force, since the damping of a moving fluid is related to its pressure loss due to friction. Writing the damping force acting on a cross-section of the fluid in terms of its pressure drop gives

$$F_D = \Delta P_f A \quad (19)$$

Using the Darcy-Weisbach equation, the pressure drop can be written as

$$\Delta P_f = f \frac{\rho_f L \dot{x}_f^2}{2 D} \quad (20)$$

where the friction coefficient f is obtained using the Sousa-Cunha-Marques equation

$$\frac{1}{\sqrt{f}} = -2 \log_{10} \left(\left(\frac{\varepsilon}{3.7D} \right)^{1.11} - \frac{5.16}{Re} \log_{10} \left(\frac{\varepsilon}{3.7D} + \frac{5.09}{Re^{0.87}} \right) \right) \quad (21)$$

In Equation 21, ε is the roughness of the surface and Re is the Reynold's number. Using the kinematic viscosity of the fluid, ν_f , the Reynold's number can be calculated by Equation 22.

$$Re = \frac{\dot{x}_f D}{\nu_f} \quad (22)$$

After substitution, the damping force can then be written as

$$F_D = \left(f \frac{\rho_f L \dot{x}_f^2}{2 D} \right) \left(\frac{\pi D^2}{4} \right) = \left(\frac{\pi L D \rho_f}{8} \right) (f |\dot{x}_f|) \dot{x}_f \quad (23)$$

$$F_D = c_k c_x \dot{x}_f \quad (24)$$

where c_k is a constant and $c_{\dot{x}}$ is a correction factor that depends on the velocity of the fluid.

$$c_k = \frac{\pi L D \rho_f}{8} \quad (25)$$

$$c_{\dot{x}} = f |\dot{x}_f| \quad (26)$$

Comparing Equation 24 with Equation 13, it can be seen that the damping coefficient is

$$c_f = c_k c_{\dot{x}} \quad (27)$$

One way to increase the damping coefficient of the fluid is to insert a diaphragm through which the fluid must pass. Typically, this mechanism is inserted in the middle of the horizontal section of the TLCD. The localized head loss caused by the diaphragm is a function of its area A_c and can be calculated with the following expression:

$$\Delta h = \frac{\dot{x}_f^2}{2g} \left(\frac{A}{A_c} - 1 \right)^2 \quad (28)$$

Therefore, the damping force generated by this diaphragm is given by

$$F_D = \frac{\dot{x}_f^2}{2g} \left(\frac{A}{A_c} - 1 \right)^2 \gamma A \quad (29)$$

Rewriting this expression, we can define the constant c_{dk} and the variable $c_{d\dot{x}}$ so that:

$$c_{dk} = \frac{\rho_f A}{2} \left(\frac{A}{A_c} - 1 \right)^2 \quad (30)$$

$$c_{d\dot{x}} = |\dot{x}_f| \quad (31)$$

$$F_D = c_{dk} c_{d\dot{x}} \dot{x}_f \quad (32)$$

Therefore, a more general expression is obtained by adding the damping coefficient of the fluid due to the distributed head loss and the damping coefficient of the fluid due to the localized head loss c_d to obtain

$$c_f = c_k c_{\dot{x}} + c_{dk} c_{d\dot{x}} \quad (33)$$

Substituting all the above TLCD parameters into Equation 13, yields

$$\left(\frac{\pi D^4}{4} L \rho_f \right) \ddot{x}_f + (c_k c_{\dot{x}} + c_{dk} c_{d\dot{x}}) \dot{x}_f + \left(\frac{\pi D^2 \rho_f g}{2} + 0.7 \frac{\pi P D^2}{Z} \right) x_f = F(t) \quad (34)$$

which is the equation of motion of the fluid for a PTLCD. The equation of motion for the TLCD is obtained by removing the second term in the stiffness portion, which corresponds to the air stiffness from Equation 17.

3.3 Structure-TLCD model

Once the mass, damping, and stiffness parameters for both the structure and the fluid have been determined, it is possible to assemble the equation of motion of the system. This equation is actually a matrix equation that represents a system of equations. The number of equations of the system is related to the number of degrees of freedom of the problem and the number of elements in each subsystem. These elements can be either the number of stories in the structure subsystem or the number of TLCDS in the damping subsystem. The number of degrees of freedom depends on how the system is analyzed. In the case of a shear building, there is only one degree of freedom per story. Each TLD also has only one degree of freedom, associated with the primary direction of movement of the fluid it contains. If the structure moves along a given direction, then a TLD installed along a perpendicular direction of that movement has no degree of freedom associated with that motion.

When assembling the matrices for a certain parameter, it is important to know if what happens in one subsystem influences the other one. This will determine if the matrix for that parameter is going to be diagonal or not. For example, in a structure-TLD system, the displacement and the velocity do not generate forces on another degree of freedom. Because of that, both the damping matrix and the stiffness matrix are diagonal. That is not the case for the mass matrix. An acceleration of the structure to the right, for example, causes the fluid to move to the left, creating an inertial force on the fluid. Consequentially, the mass matrix is not diagonal, since forces appear on the degree of freedom of the fluid when the structure accelerates, and vice versa (Freitas, 2017). This is shown in Equation 35, which is the equation of motion for the simplest structure-TLCD system, consisting of a structure with a single story and only one TLCDS, as shown in Figure 3-4.

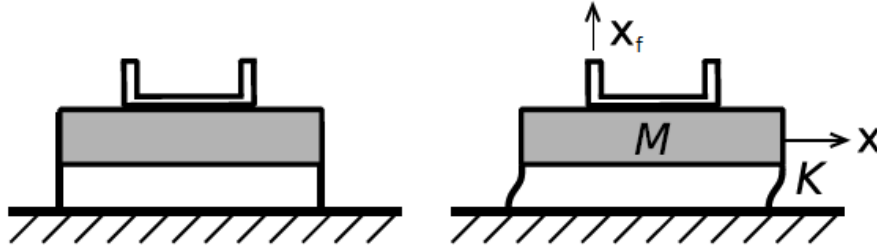


Figure 3-4 - Single degree of freedom structure with a TLCDS (Mendes, 2018a, adapted)

$$\begin{bmatrix} M + m_f & \frac{B}{L}m_f \\ \frac{B}{L}m_f & m_f \end{bmatrix} \begin{Bmatrix} \ddot{x}(t) \\ \ddot{x}_f(t) \end{Bmatrix} + \begin{bmatrix} C & 0 \\ 0 & c_f \end{bmatrix} \begin{Bmatrix} \dot{x}(t) \\ \dot{x}_f(t) \end{Bmatrix} + \begin{bmatrix} K & 0 \\ 0 & k_f \end{bmatrix} \begin{Bmatrix} x(t) \\ x_f(t) \end{Bmatrix} = \begin{Bmatrix} P_{Seq}(t) \\ P_{feq}(t) \end{Bmatrix} \quad (35)$$

Most of the variables in Equation 35 have been explained previously in the structure and TLCDS sections. The new ones are P_{Seq} and P_{feq} , which are the equivalent dynamic loads applied on the structure and on the TLCDS, respectively. In case of a ground acceleration of magnitude \ddot{x}_g , they become

$$P_{Seq}(t) = -(M + m_f)\ddot{x}_g \quad (36)$$

$$P_{feq}(t) = -\frac{B}{L} m_f \ddot{x}_g \quad (37)$$

As the number of stories and TLCDs increases, represented in Figure 3-5 and Figure 3-6, so does the size of the coefficient matrices and the vectors. This case can be generalized in an equation of motion containing submatrices and subvectors that correspond to the structure and the TLCDs, shown in Equation 38.

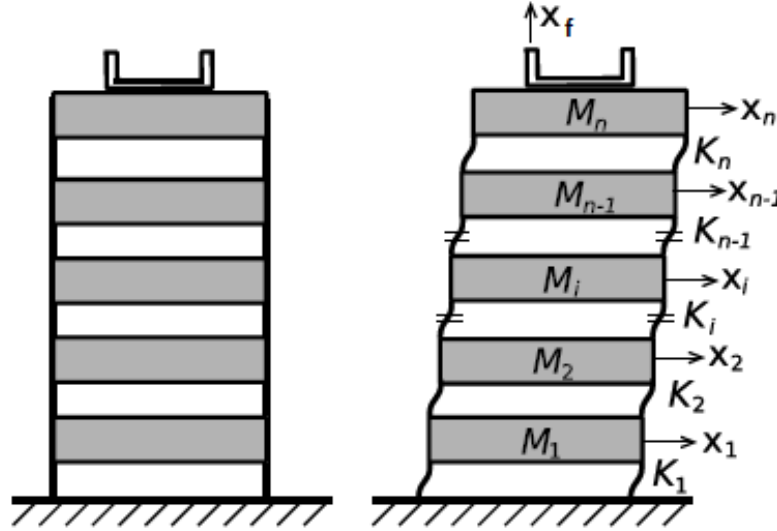


Figure 3-5 - Structure-TLCD system with multiple stories (Mendes, 2018a, adapted)

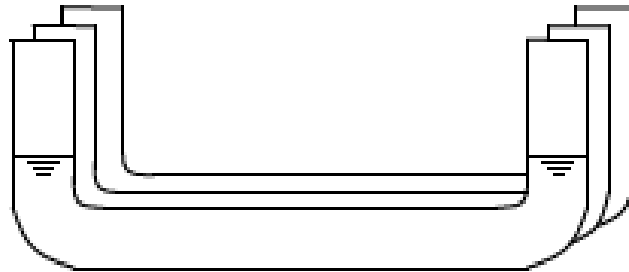


Figure 3-6 - Multiple parallel TLCDs (Mendes, 2018)

$$\begin{bmatrix} [M_S] & [M_{Sf}] \\ [M_{fS}] & [M_f] \end{bmatrix} \begin{Bmatrix} \{\ddot{X}_S\} \\ \{\ddot{X}_f\} \end{Bmatrix} + \begin{bmatrix} [C_S] & [0] \\ [0] & [C_f] \end{bmatrix} \begin{Bmatrix} \{\dot{X}_S\} \\ \{\dot{X}_f\} \end{Bmatrix} + \begin{bmatrix} [K_S] & [0] \\ [0] & [K_f] \end{bmatrix} \begin{Bmatrix} \{X_S\} \\ \{X_f\} \end{Bmatrix} = \begin{Bmatrix} \{P_S\} \\ \{P_f\} \end{Bmatrix} \quad (38)$$

Some submatrices in Equation 38 have already been defined, such as the structure's stiffness and damping matrices, $[K_S]$ and $[C_S]$, as shown by Equations 5 and 8. Other submatrices, such as the ones of the TLCDs, are just larger versions due to the multiple degrees of freedom. The $[0]$ submatrices represent matrices whose elements are all null. The remaining submatrices and subvectors are defined below, considering n stories and m TLCDs.

$$[M_S] = \begin{bmatrix} M_1 & 0 & \cdots & & 0 \\ 0 & M_2 & & & \vdots \\ \vdots & & \ddots & & \\ & & & M_{n-1} & 0 \\ 0 & \cdots & & 0 & M_n + \sum_{i=1}^m m_{fi} \end{bmatrix} \quad (39)$$

$$[M_{Sf}] = \begin{bmatrix} 0 & 0 & \cdots & 0 & 0 \\ \vdots & \vdots & & \vdots & \vdots \\ 0 & 0 & \cdots & 0 & 0 \\ \frac{B_1}{L_1} m_{f1} & \frac{B_2}{L_2} m_{f2} & \cdots & \frac{B_{n-1}}{L_{n-1}} m_{f_{m-1}} & \frac{B_n}{L_n} m_{fm} \end{bmatrix} \quad (40)$$

$$[M_{fS}] = [M_{Sf}]^T \quad (41)$$

$$\{X_S\}^T = \{X_S(t)\}^T = \{x_1(t) \quad x_2(t) \quad \cdots \quad x_{n-1}(t) \quad x_n(t)\} \quad (42)$$

$$\{X_f\}^T = \{X_f(t)\}^T = \{x_{f1}(t) \quad x_{f2}(t) \quad \cdots \quad x_{fm-1}(t) \quad x_{fm}(t)\} \quad (43)$$

$$[M_f] = \begin{bmatrix} m_{f1} & 0 & \cdots & & 0 \\ 0 & m_{f2} & & & \vdots \\ \vdots & & \ddots & & \\ & & & m_{fm-1} & 0 \\ 0 & \cdots & & 0 & m_{fm} \end{bmatrix} \quad (44)$$

$$[C_f] = \begin{bmatrix} c_{f1} & 0 & \cdots & & 0 \\ 0 & c_{f2} & & & \vdots \\ \vdots & & \ddots & & \\ & & & c_{fm-1} & 0 \\ 0 & \cdots & & 0 & c_{fm} \end{bmatrix} \quad (45)$$

$$[K_f] = \begin{bmatrix} k_{f1} & 0 & \cdots & & 0 \\ 0 & k_{f2} & & & \vdots \\ \vdots & & \ddots & & \\ & & & k_{fm-1} & 0 \\ 0 & \cdots & & 0 & k_{fm} \end{bmatrix} \quad (46)$$

Considering the system subjected to a base acceleration, the equivalent dynamic load vectors are

$$\{P_S\}^T = \{P_{Seq}(t)\}^T = - \left\{ M_1 \quad M_2 \quad \cdots \quad M_{n-1} \quad M_n + \sum_{i=1}^m m_{fi} \right\} \ddot{x}_g(t) \quad (47)$$

$$\{P_f\}^T = \{P_{feq}(t)\}^T = - \left\{ \frac{B_1}{L_1} m_{f1} \quad \frac{B_2}{L_2} m_{f2} \quad \cdots \quad \frac{B_m}{L_m} m_{fm} \right\} \ddot{x}_g(t) \quad (48)$$

3.4 Equivalent and parametric mathematical formulation for an SDOF structure with a TLCD

The equations presented above are considered here for the case of structure with a single degree of freedom with a TLCD attached. They are presented in a simpler and more compact version, which will be used to study the behavior of the structure-TLCD coupled system. The formulation in this section is from Mendes et al. (2023), a paper in which the author of this work is one of the authors.

3.4.1 Tuned liquid column damper

A simplified way to write the equation of motion of the U-shaped liquid column is

$$\rho_f AL\ddot{x}_f + \frac{1}{2}\rho_f A\xi|\dot{x}_f|\dot{x}_f + 2\rho_f Agx_f = 0 \quad (49)$$

where ρ_f is the liquid specific mass (in this case, water), A is the column cross section, L is the total length of the liquid column, x_f represents the liquid column response, ξ is the head loss coefficient and g is the gravity acceleration. As can be seen from Equation 49, the TLCD damping is nonlinear, but Yalla and Kareem (2000) propose to estimate an equivalent linear damping c_{feq} using statistical linearization methods such as

$$c_{feq} = 2\zeta_f m_f \omega_f \approx \frac{1}{2}\rho_f A\xi|\dot{x}_f| \quad (50)$$

where ζ_f , $m_f (= \rho_f AL)$ and ω_f are, respectively, the damping ratio, the mass and the natural frequency of the TLCD. The approximation error e between the nonlinear function and the equivalent linear function is expressed as

$$e = \frac{1}{2}\rho_f A\xi|\dot{x}_f|\dot{x}_f - c_f \dot{x}_f \quad (51)$$

where the value of the equivalent linear damping c_f can be obtained by minimizing the value of the standard deviation of the error. Yalla and Kareem (2000) present the equivalent linear damping c_f for specific cases, such as harmonic excitation and random excitation.

3.4.2 TLCD coupled to the structure

The equation of motion of the structure coupled with a TLCD (Figure 3-7) is given by

$$(m_s + m_f)\ddot{x}_s + c_s \dot{x}_s + k_s x_s = -\alpha m_f \ddot{x}_f + f(t) \quad (52)$$

where m_s , c_s e k_s are, respectively, the mass, the damping and the stiffness of the structure. α is the aspect ratio and represents the ratio of the horizontal length to the total length of the liquid column ($\alpha = B/L$). Finally, $f(t)$ is a force acting over the time. Thus, the response of the primary system and of the TLCD are determined by the solution of the following equation

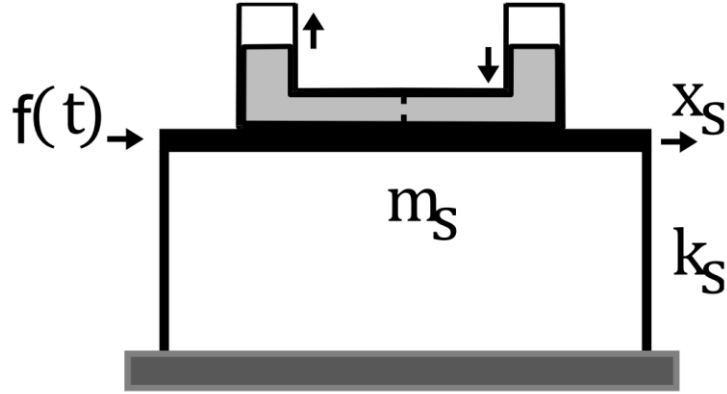


Figure 3-7 - Structure with TLCD attached

$$\begin{bmatrix} (m_s + m_f) & \alpha m_f \\ \alpha m_f & m_f \end{bmatrix} \begin{bmatrix} \ddot{x}_s \\ \ddot{x}_f \end{bmatrix} + \begin{bmatrix} c_s & 0 \\ 0 & c_f \end{bmatrix} \begin{bmatrix} \dot{x}_s \\ \dot{x}_f \end{bmatrix} + \begin{bmatrix} k_s & 0 \\ 0 & k_f \end{bmatrix} \begin{bmatrix} x_s \\ x_f \end{bmatrix} = \begin{bmatrix} f(t) \\ 0 \end{bmatrix} \quad (53)$$

with $k_f = 2\rho_f Ag$.

3.4.3 Parametric equations

To study the behavior of the structure with the TLCD, Equation 53 of the system can be reduced to:

$$\begin{bmatrix} (1 + \mu) & \alpha\mu \\ \alpha & 1 \end{bmatrix} \begin{bmatrix} \ddot{x}_s \\ \ddot{x}_f \end{bmatrix} + \begin{bmatrix} 2\zeta_s\omega_s & 0 \\ 0 & 2\zeta_f\omega_f \end{bmatrix} \begin{bmatrix} \dot{x}_s \\ \dot{x}_f \end{bmatrix} + \begin{bmatrix} \omega_s^2 & 0 \\ 0 & \omega_f^2 \end{bmatrix} \begin{bmatrix} x_s \\ x_f \end{bmatrix} = \begin{bmatrix} f(t)/m_s \\ 0 \end{bmatrix} \quad (54)$$

where $\mu = m_f/m_s$ represents the mass ratio, ζ_s represents the structure damping ratio and ω_s represents the natural frequency of the structure. Adopting $\gamma = \omega_f/\omega_s$ as the frequency ratio or tuning ratio, one has:

$$\begin{bmatrix} (1 + \mu) & \alpha\mu \\ \alpha & 1 \end{bmatrix} \begin{bmatrix} \ddot{x}_s \\ \ddot{x}_f \end{bmatrix} + \begin{bmatrix} 2\zeta_s\omega_s & 0 \\ 0 & 2\zeta_f\gamma\omega_s \end{bmatrix} \begin{bmatrix} \dot{x}_s \\ \dot{x}_f \end{bmatrix} + \begin{bmatrix} \omega_s^2 & 0 \\ 0 & (\gamma\omega_s)^2 \end{bmatrix} \begin{bmatrix} x_s \\ x_f \end{bmatrix} = \begin{bmatrix} f(t)/m_s \\ 0 \end{bmatrix} \quad (55)$$

4. Solution Methods

The solution to the equation of motion, which is a differential equation, can be obtained numerically by utilizing well-known direct integration methods available in the literature, such as the Central Difference, the Average Acceleration and the Runge-Kutta methods. The source is from Tedesco et al. (1999), but contributions to this work in this topic also appear in Freitas and Pedroso (2017a, 2017b, 2018) and Pedroso (2016).

4.1 Central Difference Method

The equation of motion is solved step by step using the central difference method, as shown in Equation 56.

$$X_{i+1} = \left(\frac{M}{\Delta t^2} + \frac{C}{2\Delta t} \right)^{-1} \left[F_i - \left(K - \frac{2M}{\Delta t^2} \right) X_i - \left(\frac{M}{\Delta t^2} - \frac{C}{2\Delta t} \right) X_{i-1} \right] \quad (56)$$

Using this method, it is possible to calculate the displacement X_{i+1} one step ahead given that the current external force F_i and the displacement on the current and previous iterations are known (X_i and X_{i-1} respectively). The distance between two steps is the time Δt . To evaluate X_{i-1} at time $t = 0$, Equation 57 and Equation 58 are used together with the known initial conditions X_0 and \dot{X}_0 .

$$\ddot{X}_0 = \frac{1}{m} [F_0 - C\dot{X}_0 - KX_0] \quad (57)$$

$$X_{-1} = X_0 - \dot{X}_0\Delta t + \frac{\ddot{X}_0(\Delta t)^2}{2} \quad (58)$$

With the displacements at various time steps, the central difference method can be used to approximate the velocity and the acceleration, given by Equation 59 and Equation 60. After solving for them, the dynamic response of the structure is determined and can be visualized by plotting the results.

$$\dot{X}_i = \frac{X_{i+1} - X_{i-1}}{2\Delta t} \quad (59)$$

$$\ddot{X}_i = \frac{X_{i+1} - 2X_i + X_{i-1}}{\Delta t^2} \quad (60)$$

An important consideration in the case of the central difference method is that the integration method is conditionally stable and requires the time step Δt to be smaller than a critical value Δt_{cr} or

$$\Delta t \leq \Delta t_{cr} \quad (61)$$

where

$$\Delta t_{cr} = \frac{T}{\pi} \quad (62)$$

and T is the natural period of the system. However, for SDOF systems, the accuracy criteria of $\Delta t < T/10$ will control maximum time step size.

4.2 Newmark Method

Another time integration method is a special form of the Newmark method and is equivalent to the trapezoidal rule. It is presented below in the form of the average linear acceleration method (or constant average acceleration method).

In the derivation of recurrence formulas for this method, the assumption made is that, within a small increment of time Δt , the acceleration is the average value of the acceleration at the beginning of the interval \ddot{X}_i and the acceleration at the end of the time interval \ddot{X}_{i+1} . Thus, the acceleration at some time τ between t_i and t_{i+1} is expressed as

$$\ddot{X}(\tau) = \frac{1}{2}(\ddot{X}_i + \ddot{X}_{i+1}) \quad (63)$$

Integrating Equation 63 twice yields

$$\dot{X}_{i+1} = \dot{X}_i + \frac{\Delta t}{2}(\ddot{X}_i + \ddot{X}_{i+1}) \quad (64)$$

and

$$X_{i+1} = X_i + \Delta t \dot{X}_i + \frac{(\Delta t)^2}{4}(\ddot{X}_i + \ddot{X}_{i+1}) \quad (65)$$

To solve for displacement, velocity and acceleration at time t_{i+1} , the equation of motion must also be considered at time t_{i+1} ; thus

$$M\ddot{X}_{i+1} + C\dot{X}_{i+1} + KX_{i+1} = F_{i+1} \quad (66)$$

After some substitutions, the recurrence formula for the displacement is given as

$$X_{i+1} = \left[\frac{1}{k + \frac{4m}{(\Delta t)^2} + \frac{2c}{\Delta t}} \right] \left[m \left(\frac{4X_i}{(\Delta t)^2} + \frac{4\dot{X}_i}{\Delta t} + \ddot{X}_i \right) + c \left(\frac{4X_i}{\Delta t} + \dot{X}_i \right) + F_{i+1} \right] \quad (67)$$

After X_{i+1} is determined above, \ddot{X}_{i+1} can be obtained from

$$\ddot{X}_{i+1} = \frac{4}{(\Delta t)^2}(X_{i+1} - X_i) - \frac{4\dot{X}_i}{\Delta t} - \ddot{X}_i \quad (68)$$

and then \dot{X}_{i+1} can be calculated from Equation 64.

4.3 Runge-Kutta Method

The Runge-Kutta methods are classified as single-step, since they require knowledge of only X_i to determine X_{i+1} . Therefore, the methods are self-starting and require no special starting procedure as did the central difference method. The most popular of the Runge-Kutta methods is the fourth-order, or classic form. In application of this method, the second-order differential equation of motion is expressed as two first-order equations. Considering the system of differential equations of motion of a viscously damped MDOF system gives

$$M\ddot{X} + C\dot{X} + KX = F(t) \quad (69)$$

which represents a system of second-order ordinary differential equations in x . However, by setting $\dot{X} = Y$, Equation 69 can be expressed as two systems of first-order differential equations. Thus

$$\dot{X} = Y \quad (70)$$

and

$$\dot{Y} = \ddot{X} = \frac{1}{M} [F(t) - C\dot{X} - KX] \quad (71)$$

The Runge-Kutta recurrence formulas for X_{i+1} and Y_{i+1} are given by

$$X_{i+1} = X_i + \frac{\Delta t}{6} (Y_1 + 2Y_2 + 2Y_3 + Y_4) \quad (72)$$

and

$$Y_{i+1} = Y_i + \frac{\Delta t}{6} (\dot{Y}_1 + 2\dot{Y}_2 + 2\dot{Y}_3 + \dot{Y}_4) \quad (73)$$

4.4 Nonlinearity Treatment

As seen in the previous sections, the PTLCD damping coefficient is dependent on the fluid velocity. This causes the damping matrix C to be nonlinear and, consequentially, the equation of motion is also nonlinear. In order to be able to use the algorithms described by solution methods directly, the damping matrix must be linearized. One way to achieve this is by approximating the instant velocity \dot{x}_f on the iteration i by its value on the iteration $i - 2$, which can be calculated numerically at each step using the central difference method. As long as the discretization is very big, meaning that the time step used between iterations is small enough, this linearization method is valid and tends to converge to the exact solution as discretization increases (Freitas, 2017).

5. Computational Aspects

The text in this section is based on Ghedini and Pedroso (2019), on Ghedini et al. (2019) and on the work of Freitas (2017), containing extractions of it.

5.1 An Overview of DynaPy

One of the programs used in this work is called DynaPy, a structural dynamics modelling and simulation software that can be used to study simple two-dimensional structures. It allows its users to run many simulations in a short amount of time and gather all sorts of results, according to their need. In the current version, this software supports shear building structures, TLCDs, PTLCDs, harmonic excitations and generic excitations.

DynaPy is based on the Python programming language, which is free, open source and widely disseminated, having a large and active community. This enables the creation of many libraries and packages for all kinds of uses and situations. The two most important and fundamental to DynaPy are called Numpy (Walt et al., 2011) and Matplotlib (Hunter, 2007). The first is a numeric library containing all kinds of programming functions responsible for handling equations, linear systems, matrices, vectors and many more. The second is a graphical library for 2D and 3D plotting. By utilizing both of them, it is possible to perform numerical analyzes and do the post-processing with ease.

The program is composed of three main parts - pre-processing, processing and post-processing. In the first one, the user inputs the data by interacting with a graphical interface. This involves geometric parameters of the structure and the TLCD, as well as physical parameters, such as the structure mass and the modulus of elasticity. Other input parameters include the duration and time step of the analysis, boundary conditions and seismic characteristics. Two of DynaPy's pre-processing windows are shown in Figure 5-1 and Figure 5-2.

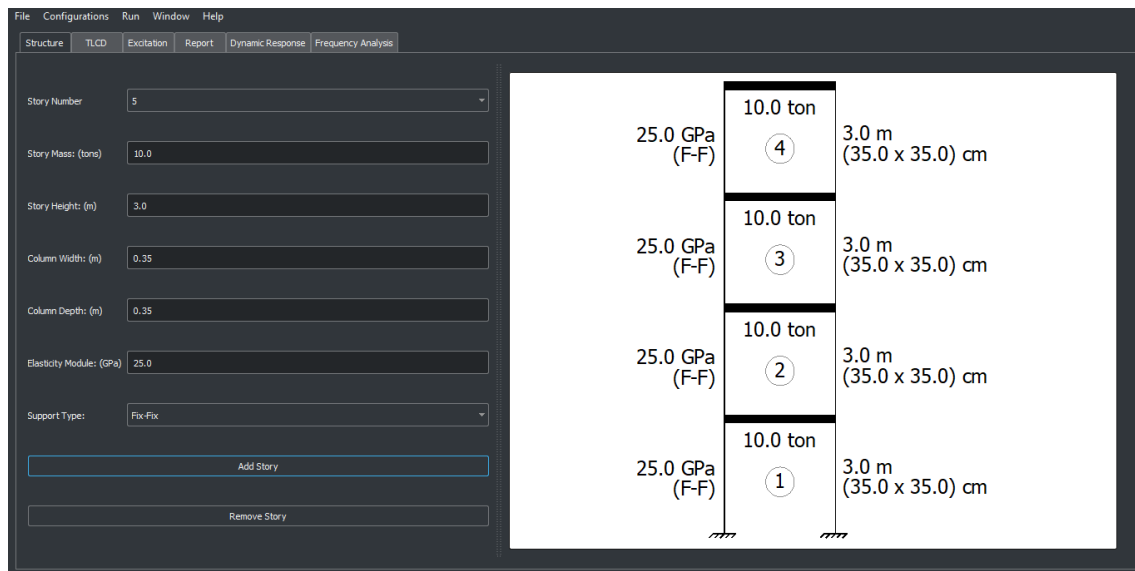


Figure 5-1 - Structure tab of the DynaPy software

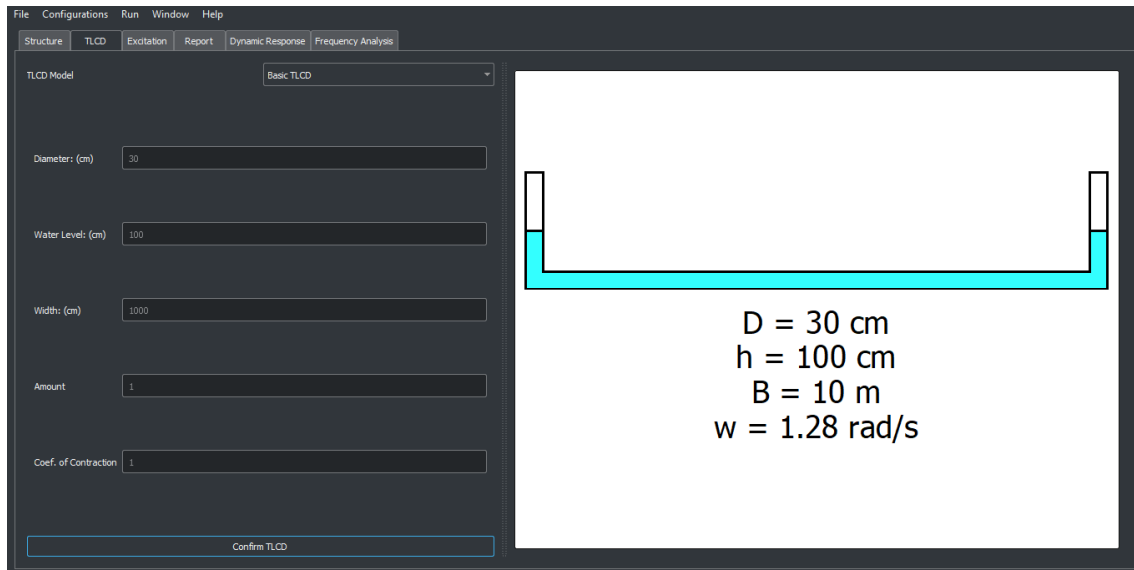


Figure 5-2 - TLCD tab of the DynaPy software

Next, at the beginning of the processing step, the software calculates every other property necessary for solving the problem. Then, it assembles the system mass, damping and stiffness matrices, as well as the time-dependent vectors of force, displacement, velocity and acceleration. With the assembled elements, it utilizes one of the direct integration methods, such as the Central Difference Method, combined with Numpy to solve the equations of motion and obtain the dynamic response of the structure.

Finally, the post-processing step generates graphs that are used to analyze the efficiency of the studied damper. Figure 5-3 shows the dynamic response plots screen with the “Displacement Vs. Time” plot option selected. It is possible to plot different graphs, such as such as displacement versus time, velocity versus time, acceleration versus time, displacement versus velocity, dynamic amplification factor versus frequency ratio and maximum displacement versus frequency ratio. It is also possible to export the data to a CSV file and then use it to plot graphs comparing responses from different cases, such as with and without a PTLCD, shown in Figure 5-4, and due to seismic excitations, as can be seen in Figure 5-5.

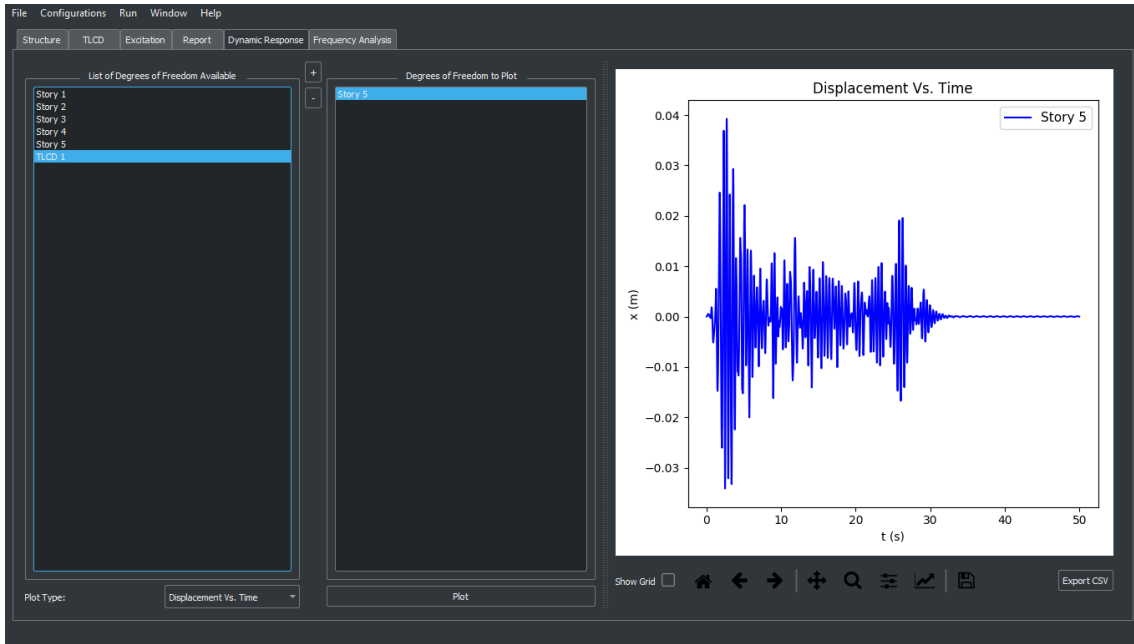


Figure 5-3 - DynaPy's dynamic response screen

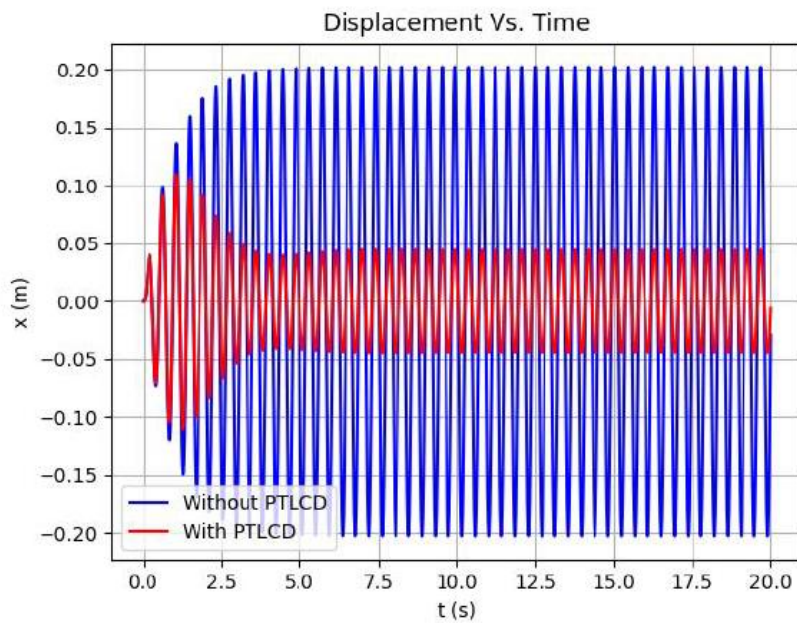


Figure 5-4 - Comparison of the dynamic responses with and without a PTLCD for a five-story shear building in resonance (Freitas, 2017)

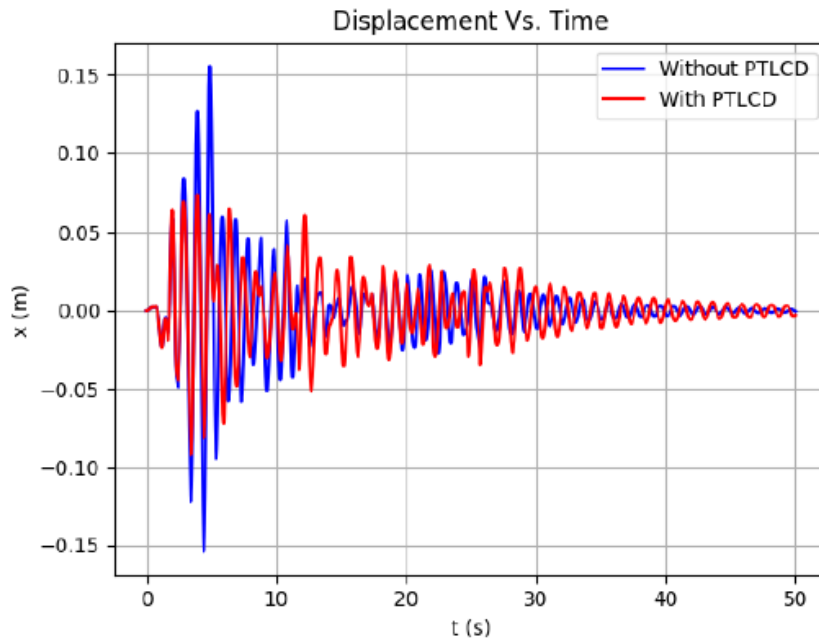


Figure 5-5 - Comparison of the dynamic responses with and without a PTLCD for a one-story shear building submitted to the El Centro earthquake (Freitas, 2017)

5.2 DynaPy Architecture and Methodology

DynaPy is meant to be used with its graphical user interface, but it is not tied to it. Figure 5-6 shows the software's flowchart when it is used with the GUI, as intended. First, using the GUI, the user inputs all the data about the structure, the external damper, the excitation and the software configurations. It is stored in an object called `InputData`. Then, the user has the option to run two types of analysis - a time history analysis and a frequency analysis. By choosing the first one, the software assembles the system mass, damping and stiffness matrices, as well as the force vectors for each time step simulated. Then, the matrices and vectors are used to solve the equation of motion for each time step using one of the methods available in the `DynaSolver` algorithm. This algorithm outputs the dynamic response of the system in terms of displacement, velocity, and acceleration. If the user chooses the frequency analysis, instead, the software will perform a loop in which the system will be excited at the base by a sine-shaped acceleration. At each iteration, the matrices will be assembled, the equation of motion will be solved and the maximum values of displacement, velocity and acceleration will be stored. In both cases, the outputs are stored in an object called `OutputData`, which will handle the data for post-processing in the DynaPy GUI.

Since DynaPy was designed to be expandable and tweakable, the entire software is designed in a modular way. As a result, the functions to assemble the matrices and to solve the equations of motion, for example, are completely independent of the rest of the software, meaning that if one desires, they can code another solution method or another way to assemble the matrices in order to adapt the program to different mechanical systems.

DynaPy also has a save file system, which saves the contents of `InputData` to a human-readable text file that can later be used to load the data back to the program. Since the save file is human-readable, it is possible to make changes directly to the file or even to write it from scratch if the user understands the file structure. This makes it possible to

completely bypass the pre-processing phase in the GUI and run DynaPy more like a script-based software.

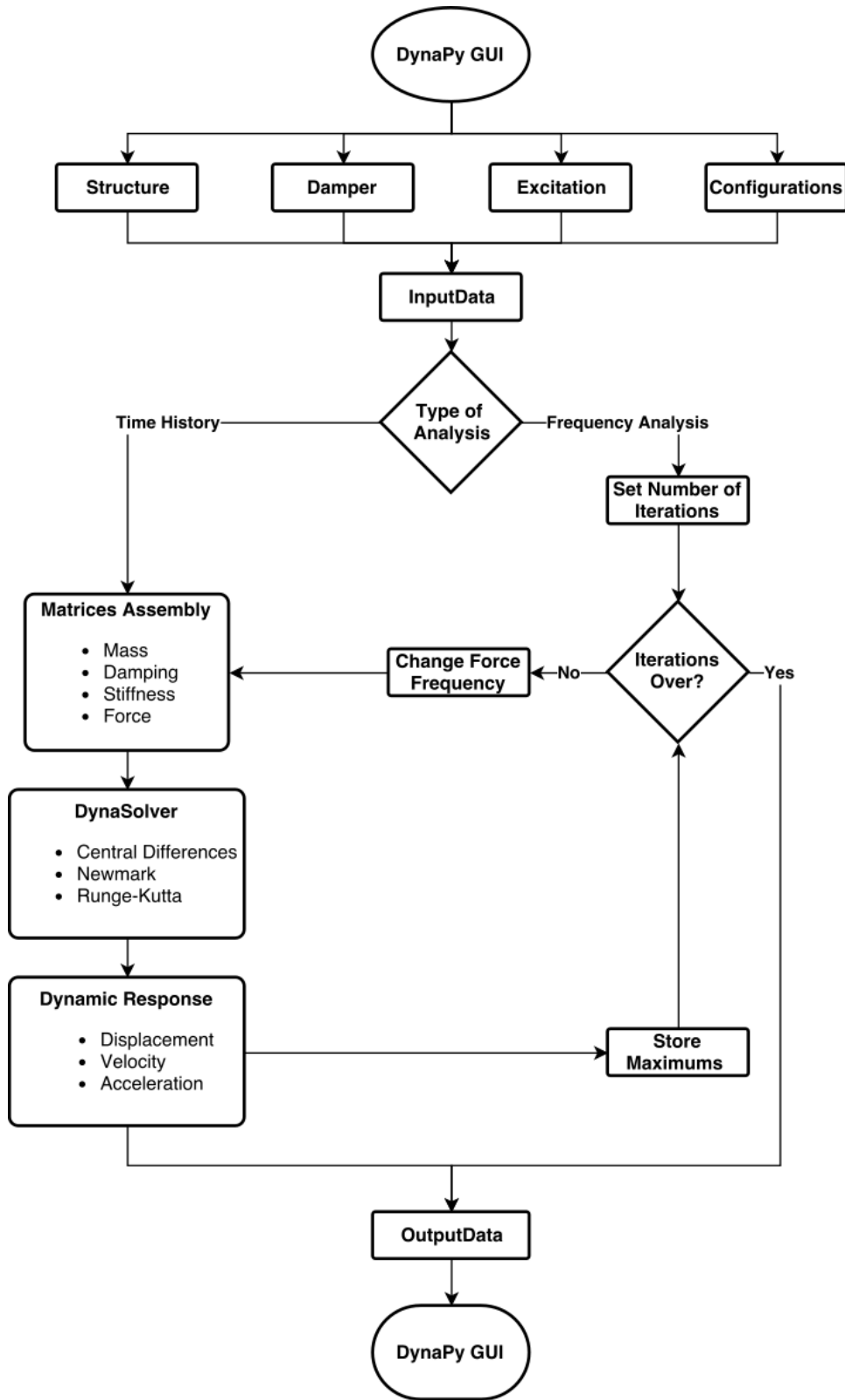


Figure 5-6 - DynaPy's flowchart

5.3 Step-by-Step Mode

A feature added to DynaPy (Ghedini et al., 2019) is a run option called Step-by-Step Mode that is only available after the studied case is run and the dynamic response is generated. The following figures show the tabs of the Step-by-Step Mode, which represent and summarize all the work done by DynaPy in order to run the case study presented herein. With them, the user has a full grasp of what is happening and has freedom to plot and analyze every scenario.

Figure 5-7 shows the Inputs Summary tab, which contains the input data entered by the user for the structure, the damper and the excitation. This tab will first appear blank, requiring the user to load the data from the case that was run by pressing the Load Results button. Additional information can be seen in the form of a pop-up window by pressing the Details button below each figure in this tab. This tab contains all the information necessary to assemble the matrices that appear in the equation of motion and is an excellent way to view all the input parameters of the system in a single screen.

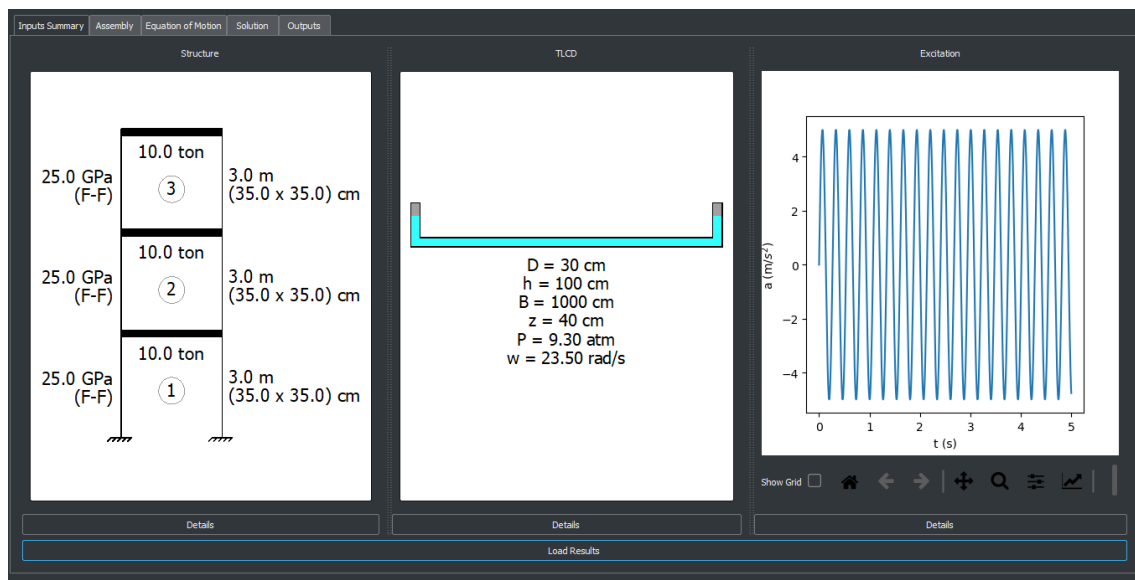


Figure 5-7 - Inputs Summary tab

Figure 5-8 shows the Assembly tab, which displays the mass, damping and stiffness matrices in their symbolic or numeric values. Each one of these matrices starts with null terms when the tab is first accessed. By pressing the Previous and Next buttons, the correct terms are added or removed from the matrix, respectively. Due to this, the assembly of the matrices can be visualized in an interactive way. The figure in this tab also changes accordingly when the buttons are pressed, so that the size of the matrix corresponds to the structure-TLCD system being displayed. Because of that, this tab highlights the contribution that each story and the damper have on each one of the matrices, as well as how they are coupled or not. It is also one of the most valuable tabs of the Step-by-Step Mode for teaching.

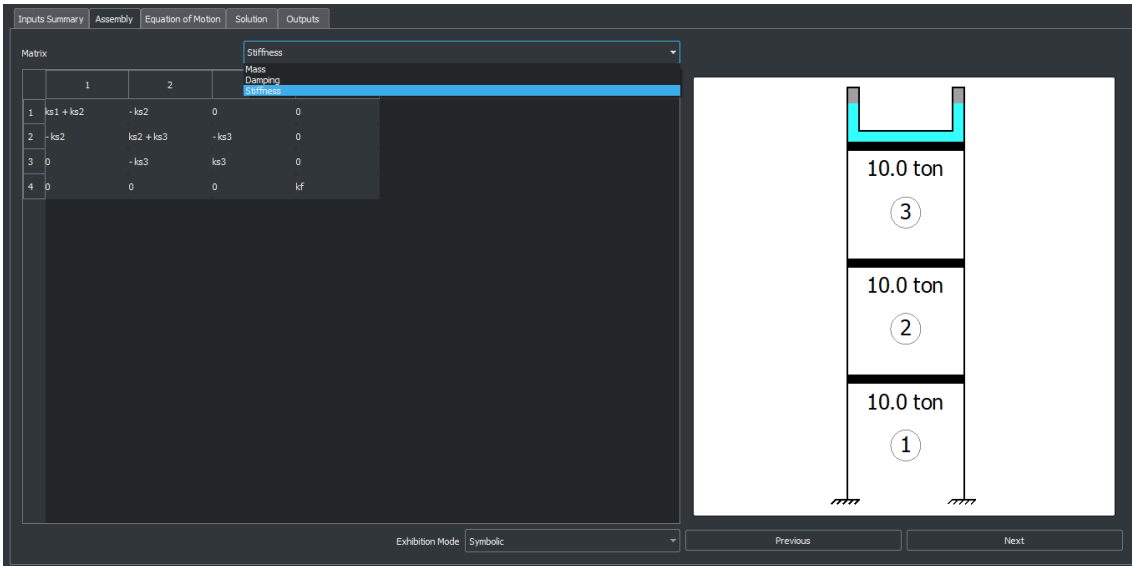


Figure 5-8 - Assembly tab

Figure 5-9 shows the Equation of Motion tab, where the previously assembled matrices are used in the dynamic equation of motion. This tab contains a figure of this system of equations in its matrix form, as well as the definition of some submatrices. Below it, the user chooses a line from the system of equations to be displayed. Each equation that composes this system can be visualized separately in their symbolic or numeric form. This tab allows the user to better see all the parameters that influence the dynamic response of a given story or the damper.

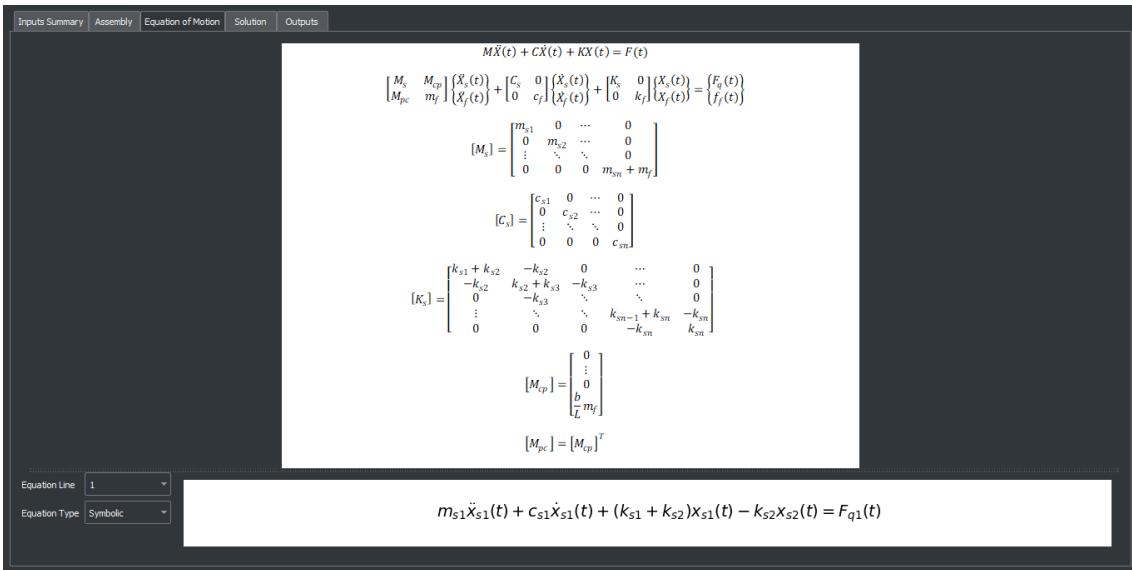


Figure 5-9 - Equation of Motion tab

A screenshot of the Solution tab is shown in Figure 5-10. This tab explains the solution steps taken by DynaPy to obtain the dynamic response of the system. This is done explaining the central difference method to the user with images containing text and equations. The Solution tab also contains additional information, such as why a nonlinearity occurs and how the modal frequencies are obtained. It is a path that connects the system parameters and its dynamic response.

The derivatives in the equation of motion can be estimated by the Central Finite Difference Method (FDM) as

$$\dot{X}_i = \frac{X_{i+1} - X_{i-1}}{2\Delta t}$$

$$\ddot{X}_i = \frac{X_{i+1} - 2X_i + X_{i-1}}{\Delta t^2}$$

Substituting the derivatives in the equation of motion, yields

$$M\left(\frac{X_{i+1} - 2X_i + X_{i-1}}{\Delta t^2}\right) + C\left(\frac{X_{i+1} - X_{i-1}}{2\Delta t}\right) + KX_i = F_i$$

Which can be rearranged as

$$X_{i+1} = \left(\frac{M}{\Delta t^2} + \frac{C}{2\Delta t}\right)^{-1} \left(F_i - \left(K - \frac{2M}{\Delta t^2}\right)X_i - \left(\frac{M}{\Delta t^2} - \frac{C}{2\Delta t}\right)X_{i-1}\right)$$

To solve the first iteration ($i=0$), the following initial condition equations are needed

$$\ddot{X}_0 = \frac{1}{M}[F_0 - C\dot{X}_0 - KX_0]$$

$$X_{-1} = X_0 - \dot{X}_0\Delta t + \frac{\ddot{X}_0\Delta t^2}{2}$$

Figure 5-10 - Explanation of the central difference method in the Solution tab

The final tab is shown in Figure 5-11 and is called Outputs. It contains a canvas where it is possible to plot up to three different graphs for the response of the structure-TLCD system. To plot a graph, the user selects which degree of freedom (DOF) they want to be displayed, followed by what will be displayed on each axis. The options include the displacement x , the velocity v , the acceleration a , the force f_q and the excitation acceleration \ddot{x}_q . By default, the x axis is the same for all three graphs. This tab is a collection of all the output data stored by DynaPy and that can be promptly plotted by the user at will. The capability of manipulating and visualizing up to three different graphs at once makes this tab a valuable educational tool in the Step-by-Step Mode.

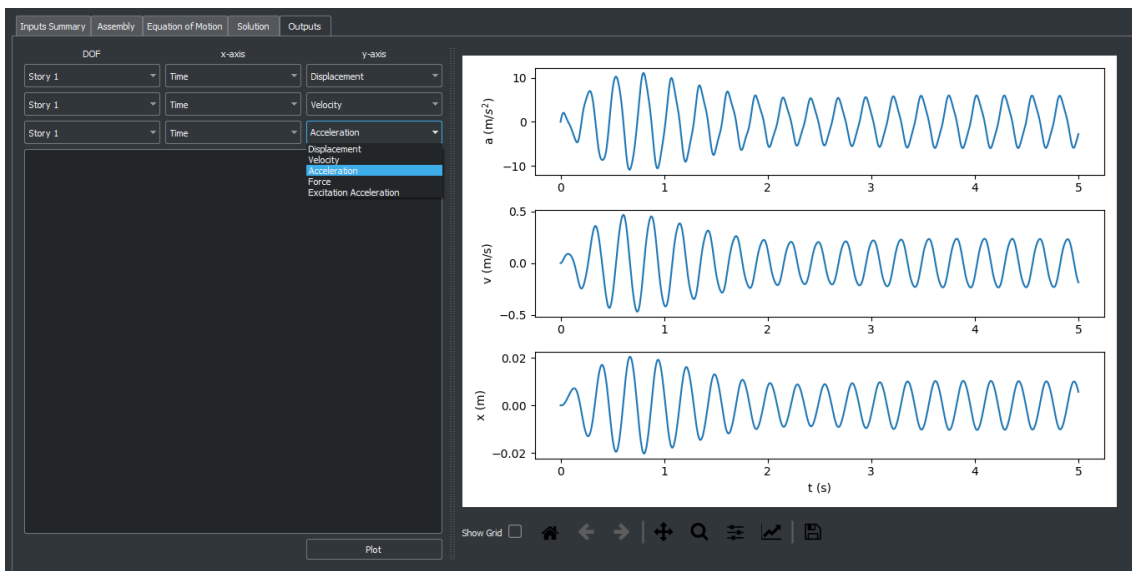


Figure 5-11 - Outputs tab containing many plot options

6. Results

The results presented in this work were obtained by different software packages: both DynaPy and a MATLAB[®] routine containing one of the numerical methods were used to generate and to plot results, while Excel was used to both plot and compare results from the first two. The captions below each graph contain information on which software was used to generate the results presented on each of them. Many results presented in this section are from Mendes et al. (2023), a paper in which the author of this work is one of the authors.

6.1 Validations

To ensure that the results utilized in this section and generated by the software were accurate, two validations were performed: one in the time domain and another in the frequency domain. The first validation ensures that the numerical solution method employed is a valid approximation of the analytical solution. The second validation depends on the first one and is important to the analysis of the coupled structure-TLCD system.

6.1.1 Analytical and numerical solution in the time domain

To validate the numerical solutions obtained from the computational routines, many cases for an SDOF system were analyzed. Those include the system with or without damping and subjected or not to a harmonic excitation.

Free vibration without damping

The analytical solution for the response of an undamped SDOF system with no force acting on it can be given by

$$x(t) = x(0) \cos \omega_n t + \frac{\dot{x}(0)}{\omega_n} \sin \omega_n t \quad (74)$$

in which $x(0)$ and $\dot{x}(0)$ are, respectively, the initial conditions of displacement and velocity of the system and ω_n is the natural frequency of the system. The system analyzed has $\omega_n = 68.8530$ rad/s, $x(0) = 0.50$ m and $\dot{x}(0) = 0$. Figure 6-1 shows the comparison between the analytical and numerical solutions.

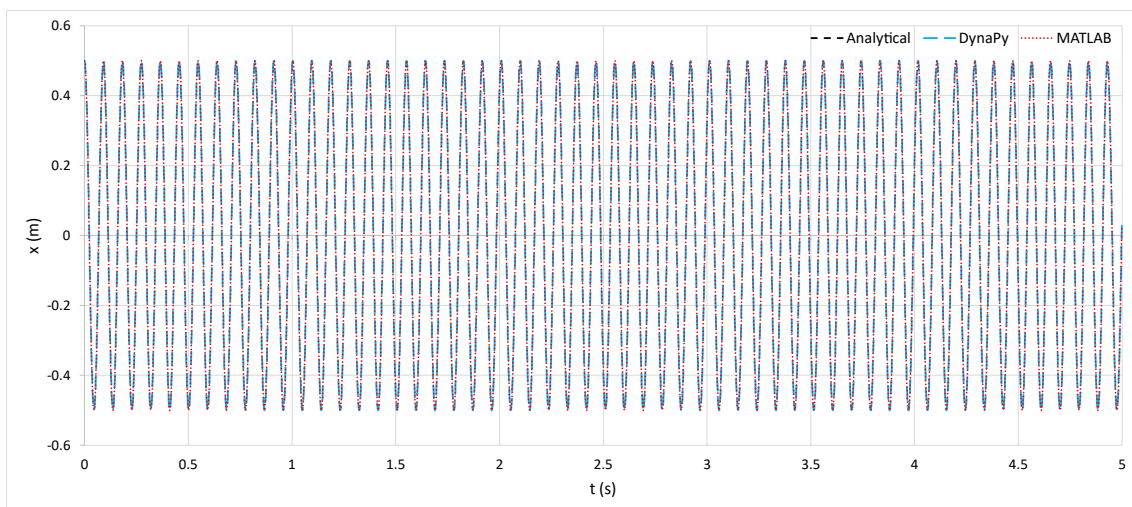


Figure 6-1 - Free vibration and no damping (plotted in Excel)

Free vibration with damping

The analytical solution for the response of a damped SDOF system with no force acting on it can be given by

$$x(t) = e^{-\zeta\omega_n t} \left[x(0) \cos \omega_d t + \left(\frac{\dot{x}(0) + x(0)\zeta\omega_n}{\omega_d} \right) \sin \omega_d t \right] \quad (75)$$

where ζ is the damping ratio and $\omega_d = \omega_n \sqrt{1 - \zeta^2}$ is the damped frequency. The system analyzed has $\omega_n = 68.8530$ rad/s, $\zeta = 0.01$ and $\omega_d = 68.8496$ rad/s. The initial conditions for displacement and velocity are $x(0) = 0.50$ m and $\dot{x}(0) = 0$. Figure 6-2 shows the comparison between the analytical and numerical solutions.

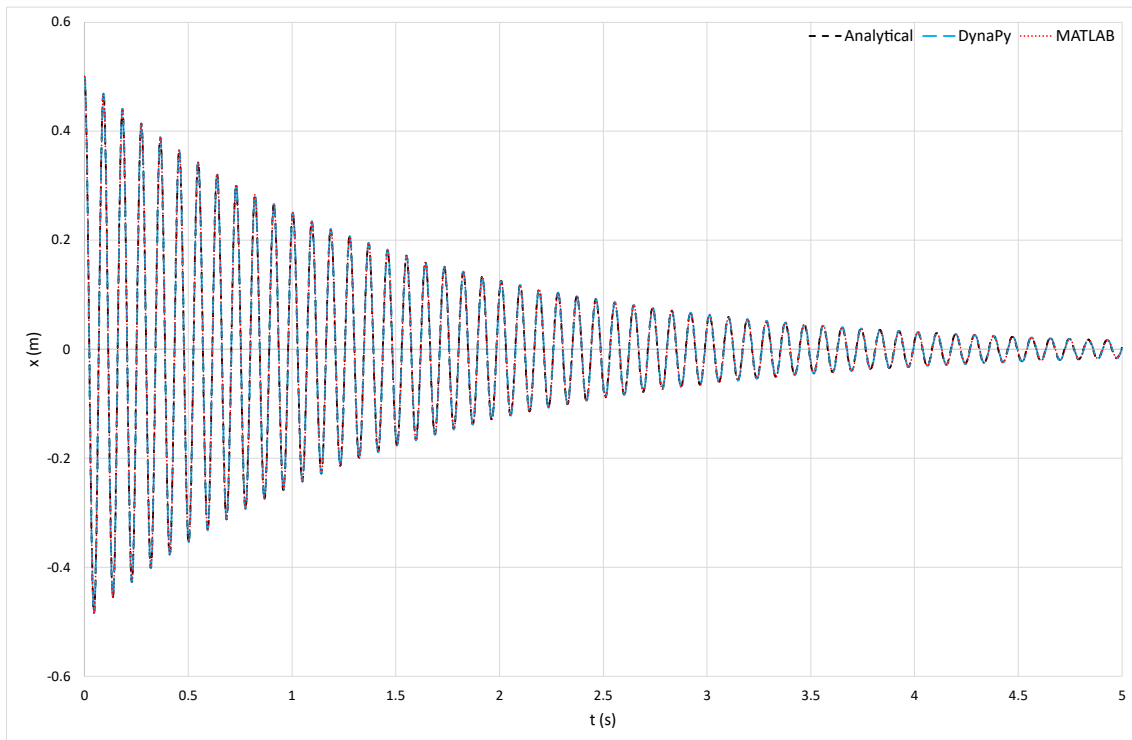


Figure 6-2 - Free vibration with damping (plotted in Excel)

Forced vibration without damping

The analytical solution for the response of an undamped SDOF system with a harmonic force of frequency ω_e acting on it can be given by

$$x(t) = \frac{f_0}{k} \left[\frac{1}{1 - \beta^2} \right] (\sin \omega_e t - \beta \sin \omega_n t) \quad (76)$$

in which f_0/k is the equivalent static deflection that would result from applying a force of magnitude f_0 to the system and $\beta = \omega_e/\omega_n$ is the frequency ratio and represents the ratio of the excitation frequency to the natural frequency of the system. The SDOF system analyzed has $\omega_n = 68.8530$ rad/s, $\beta = 0.90$, $\omega_e = 61.9677$ rad/s and $f_0/k = 9.4922 \times 10^{-3}$ m. The initial conditions for displacement and velocity are $x(0) = \dot{x}(0) = 0$. Figure 6-3 shows the comparison between the analytical and numerical solutions.

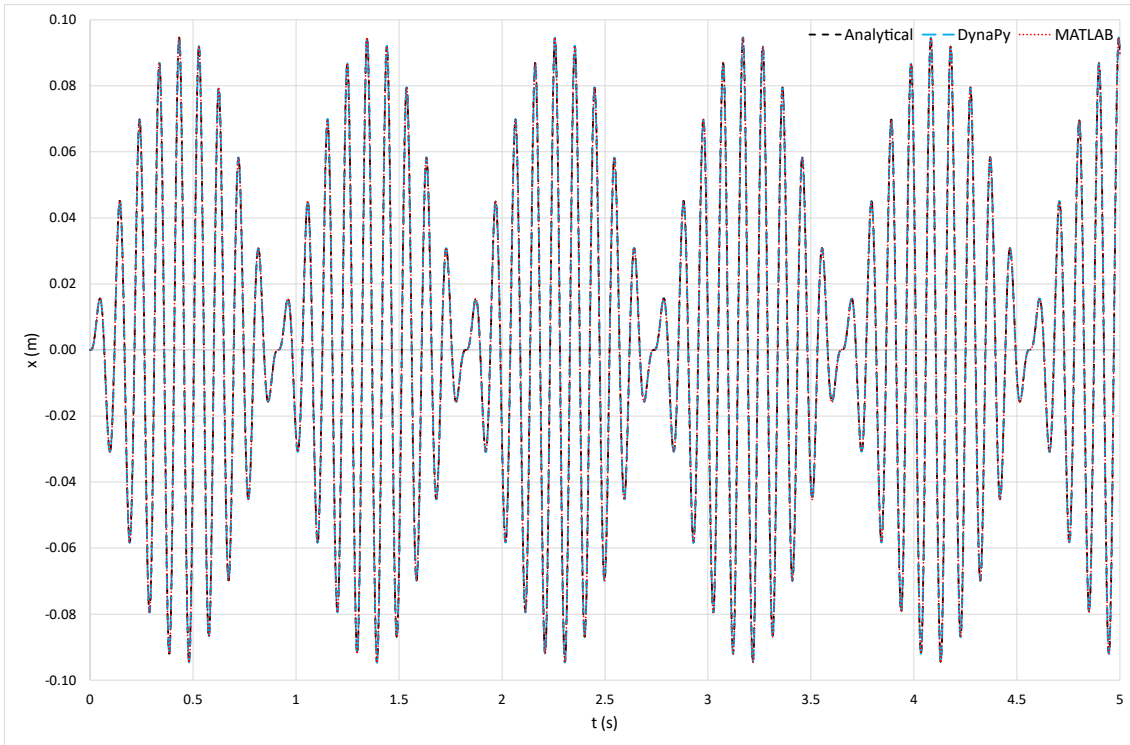


Figure 6-3 - Forced vibration and no damping (plotted in Excel)

Forced vibration with damping

The analytical solution for forced harmonic vibrations with viscous damping are available in the literature in many forms, such as

$$x(t) = e^{-\zeta\omega_n t} (A \cos \omega_d t + B \sin \omega_d t) + \frac{f_0}{k} \left[\frac{1}{(1 - \beta^2)^2 + (2\zeta\beta)^2} \right] [(1 - \beta^2) \sin \omega_e t - 2\zeta\beta \cos \omega_e t] \quad (77)$$

where A and B are constants evaluated from the initial conditions of displacement and velocity of the system. The system analyzed has $\omega_n = 68.8530$ rad/s, $\zeta = 0.01$, $\omega_d = 68.8496$ rad/s, $\beta = 0.90$, $\omega_e = 61.9677$ rad/s and $f_0/k = 9.4922 \times 10^{-3}$ m. The initial conditions for displacement and velocity are $x(0) = \dot{x}(0) = 0$. For those conditions, the evaluated constants are $A = 4.6911 \times 10^{-3}$ m and $B = -4.4521 \times 10^{-2}$ m. Figure 6-4 shows the comparison between the analytical and numerical solutions.

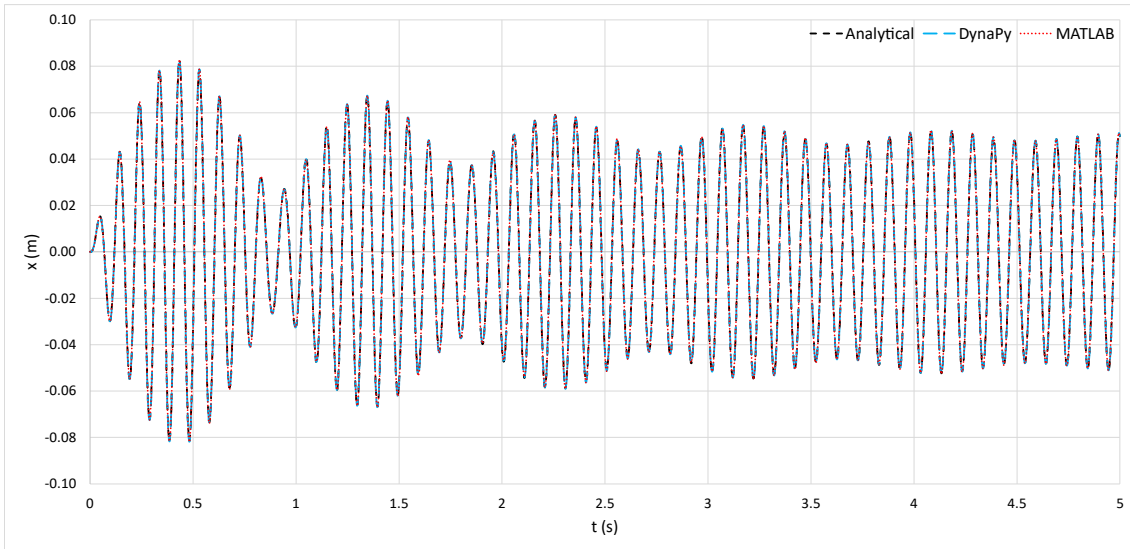


Figure 6-4 - Forced vibration with damping (plotted in Excel)

Another way to write the analytical solution for the response of a damped SDOF system with a harmonic force of frequency ω_e acting on it is

$$x(t) = e^{-\zeta\omega_n t}(A \sin \omega_d t + B \cos \omega_d t) + \frac{f_0/k}{\sqrt{(1-\beta^2)^2 + (2\zeta\beta)^2}} \sin(\omega_e t - \theta) \quad (78)$$

in which θ is the phase angle of the steady-state solution, given by

$$\theta = \tan^{-1}\left(\frac{2\zeta\beta}{1-\beta^2}\right) \quad (79)$$

The system analyzed has $\omega_n = 68.8530$ rad/s, $\zeta = 0.01$, $\omega_d = 68.8496$ rad/s, $\omega_e = 20$ rad/s, $\beta = 0.2905$, $\theta = 0.0063$ radian, and $f_0/k = 0.0211$ m. The initial conditions for displacement and velocity are $x(0) = \dot{x}(0) = 0$. For those conditions, the evaluated constants are $A = -6.6904 \times 10^{-3}$ m and $B = 1.4616 \times 10^{-4}$ m. Figure 6-5 shows the comparison between the analytical and numerical solutions.

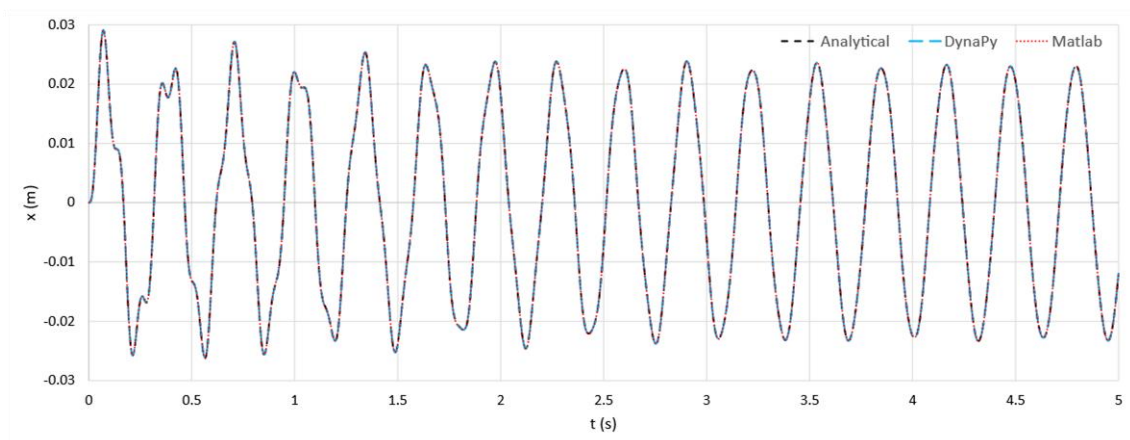


Figure 6-5 - Comparison between analytical and numerical solutions (plotted in Excel)

As can be seen by the superposition of the solutions in all the cases analyzed, the numerical results show good agreement with the analytical results.

6.1.2 Frequency analysis through a harmonic excitation

This validation can only be performed after the time domain response has been validated. This is because the frequency analysis is a compilation of the maximum time responses of a system under harmonic excitations of many frequencies. This analysis can be used to find the resonance frequency of a system by performing a frequency sweep. Figure 6-6 shows the results obtained in MATLAB® for an SDOF system of $\omega_n = 68.8530$ rad/s and for three different damping ratios.

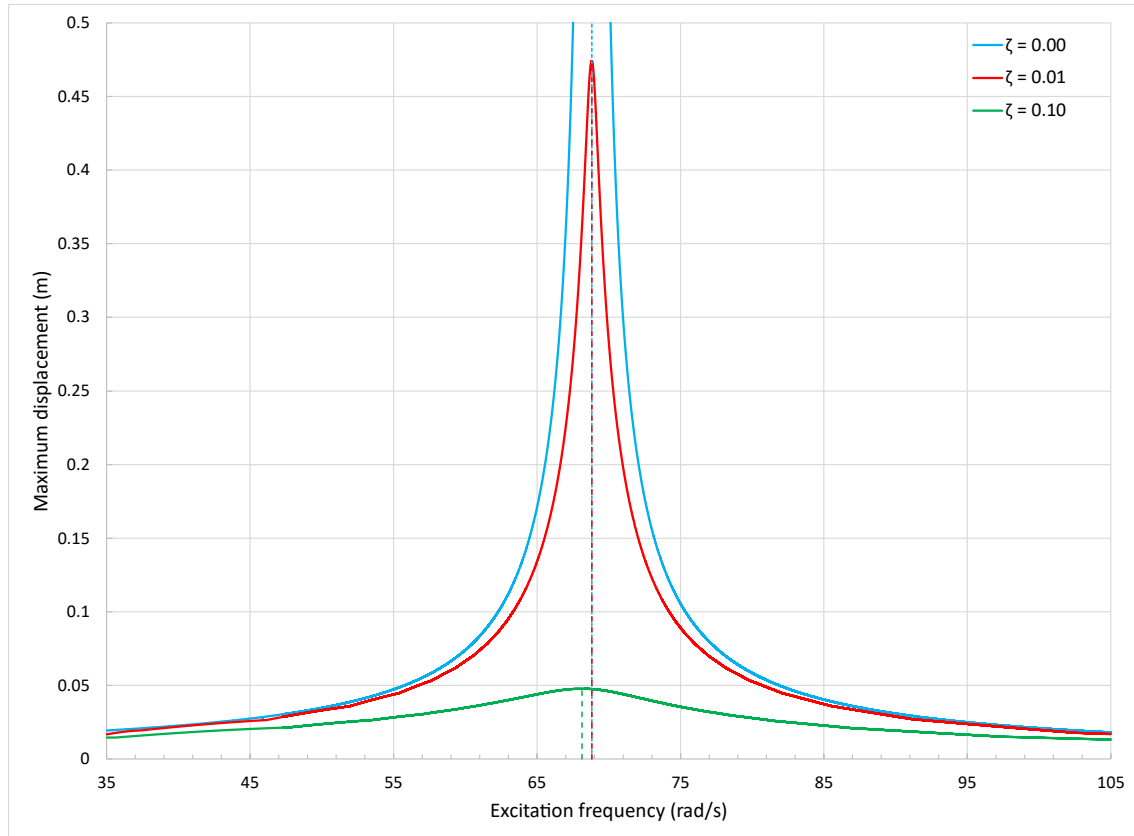


Figure 6-6 - Frequency analysis for an SDOF system for different values of damping (MATLAB®/Excel)

Table 6-1 presents the analytical damped frequencies $\omega_d = \omega_n \sqrt{1 - \zeta^2}$ for the different damping ratios, along with the numerical frequencies obtained from the sweep in Figure 6-6.

Table 6-1 - Comparison between the analytical and numerical frequencies of an SDOF

	$\zeta = 0.00$	$\zeta = 0.01$	$\zeta = 0.10$
Analytical Frequency (rad/s)	68.8530	68.8496	68.5079
Numerical Frequency (rad/s)	68.8230	68.8140	68.1270
Error	0.04%	0.05%	0.56%

The small errors show that the results obtained from MATLAB[®] are a valid approximation to the analytical solution.

In a single degree of freedom system, the natural frequency is determined in a straightforward manner and many formulations for several problems are available in the literature, such as the ones presented in chapter 3 for an SDOF structure and for a TLCD. For a multi-degree of freedom system, the natural frequencies are obtained from an eigenvalue problem. In the case of a coupled structure-TLCD system, they are determined from

$$\begin{bmatrix} (1 + \mu) & \alpha\mu \\ \alpha & 1 \end{bmatrix} \begin{bmatrix} \ddot{x}_s \\ \ddot{x}_f \end{bmatrix} + \begin{bmatrix} \omega_s^2 & 0 \\ 0 & (\gamma\omega_s)^2 \end{bmatrix} \begin{bmatrix} x_s \\ x_f \end{bmatrix} = \begin{bmatrix} 0 \\ 0 \end{bmatrix} \quad (80)$$

which nontrivial solution is an eigenvalue problem and can be obtained by

$$\det \left(\begin{bmatrix} \omega_s^2 & 0 \\ 0 & (\gamma\omega_s)^2 \end{bmatrix} - \Omega^2 \begin{bmatrix} (1 + \mu) & \alpha\mu \\ \alpha & 1 \end{bmatrix} \right) = 0 \quad (81)$$

where Ω represents the natural frequency of the coupled system. Expanding the determinant yields

$$(1 + \mu - \alpha^2\mu)\Omega^2 - [\omega_s^2 + \gamma\omega_s^2(1 + \mu)]\Omega + \gamma^2\omega_s^4 = 0 \quad (82)$$

from which the following natural frequencies of a coupled structure-TLCD system are evaluated

$$\Omega_{1,2} = \sqrt{\{\omega_s^2 + (\gamma\omega_s)^2(1 + \mu) \pm \Lambda\} / \{2(1 + \mu - \alpha^2\mu)\}} \quad (83)$$

where

$$\Lambda = \sqrt{[\omega_s^2 - \gamma^2\omega_s^2(1 + \mu)]^2 + 4\alpha^2\mu\gamma^2\omega_s^4} \quad (84)$$

Thus, the natural frequencies of the structure with the liquid column damper can be determined analytically.

In another validation test, a frequency sweep was conducted for an undamped coupled structure-TLCD system. The coupled system has the following parameters: structure natural frequency $\omega_s = 68.8530$ rad/s, structure damping ratio $\zeta_s = 0$, aspect ratio $\alpha = 0.95$, mass ratio $\mu = 0.03$, frequency ratio $\gamma = 0.95$, TLCD damping ratio $\zeta_f = 0$. The analytical frequencies obtained for this system are $\Omega_1 = 61.6689$ rad/s and $\Omega_2 = 72.9238$ rad/s. Using DynaPy, a frequency plot against amplitude consisting of 301 points ranging from 55 to 80 rad/s was done. Figure 6-7 shows the maximum displacement recorded for each excitation frequency.

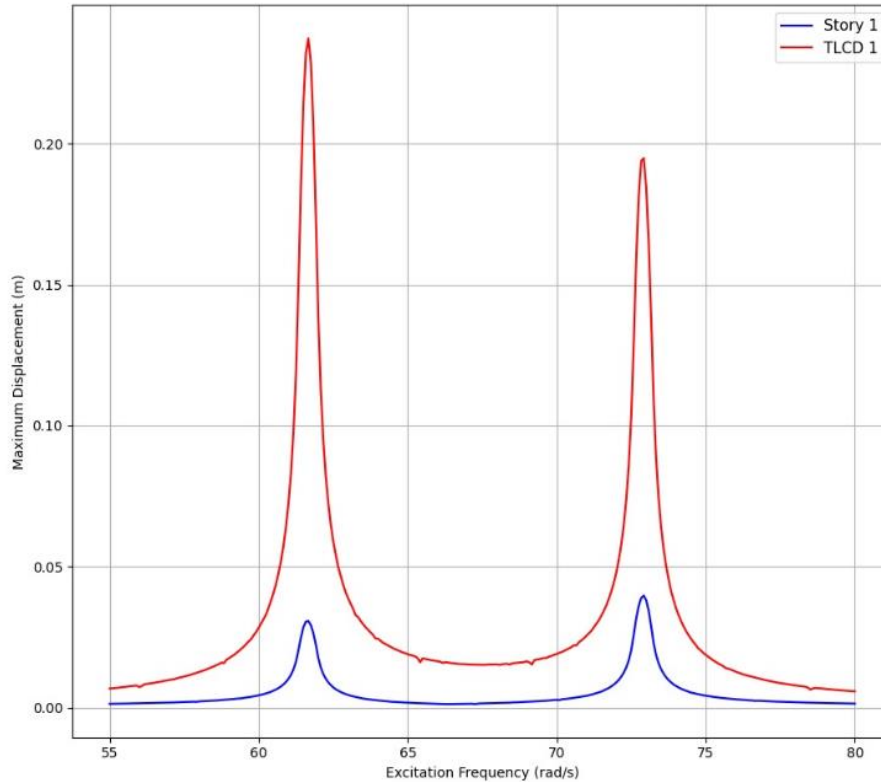


Figure 6-7 - Frequency analysis in DynaPy

Using the analytical natural frequencies as a starting point, two separate sweeps were performed in the 61-62 rad/s range and in the 72.5-73.5 rad/s range, consisting of 101 points each. The natural frequencies obtained this way were $\Omega_1 = 61.68$ rad/s and $\Omega_2 = 72.94$ rad/s, with respective errors of 0.0181 % and 0.0222 % when compared to the analytical frequencies. Once again, the numerical results obtained using DynaPy represent a valid approximation to the analytical solution.

In one last structure-TLCD frequency analysis, a frequency sweep was conducted in MATLAB[®] for an undamped system with the following parameters: structure natural frequency $\omega_s = 68.8530$ rad/s, structure damping ratio $\zeta_s = 0$, aspect ratio $\alpha = 0.80$, mass ratio $\mu = 0.07$, frequency ratio $\gamma = 0.90$, TLCD damping ratio $\zeta_f = 0$. The analytical frequencies obtained for this system are $\Omega_1 = 58.1411$ rad/s and $\Omega_2 = 72.4735$ rad/s. Figure 6-8 shows the uncoupled systems in addition to the coupled system to understand the effect that the coupling has on the natural frequencies of both systems. It can be seen that the addition of a TLCD with a slightly smaller frequency than the structure causes a frequency shift to the left and to the right.

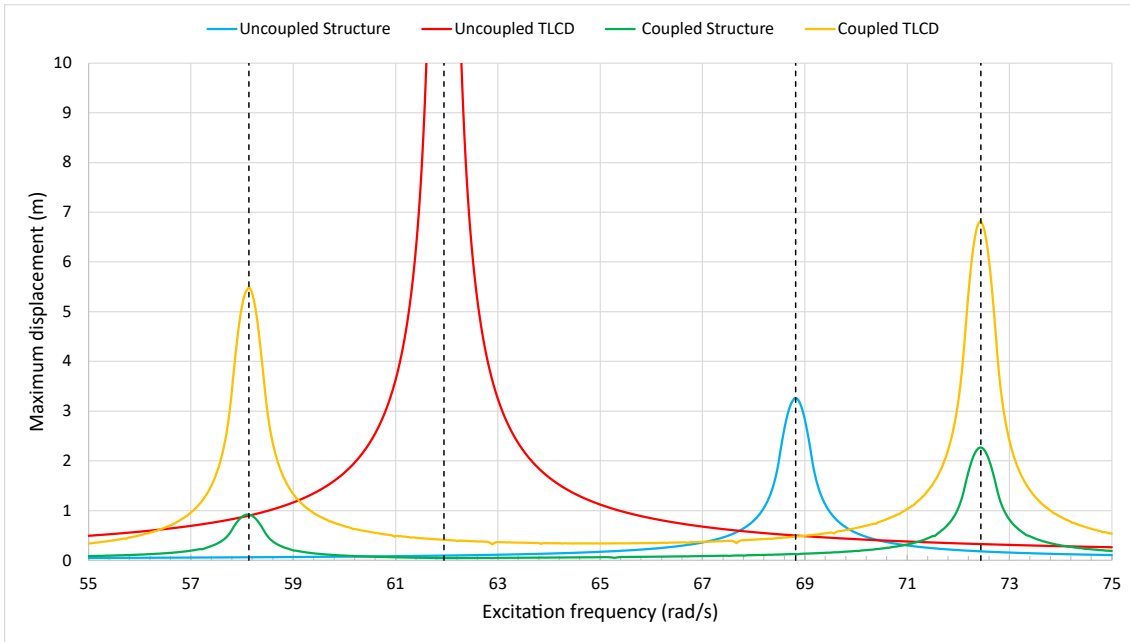


Figure 6-8 - Frequency analysis for the uncoupled and the coupled structure-TLCD systems (MATLAB[®]/Excel)

Table 6-2 presents the analytical frequencies calculated for the uncoupled and coupled systems, along with the numerical frequencies obtained from the sweep in Figure 6-8. Once more, the minor errors demonstrate that the numerical results are in good agreement with the analytical results.

Table 6-2 - Comparison between the analytical and numerical frequencies of an MDOF

	Uncoupled Structure	Uncoupled TLCD	Coupled Structure 1st freq.	Coupled Structure 2nd freq.	Coupled TLCD 1st freq.	Coupled TLCD 2nd freq.
Analytical Frequency (rad/s)	68.8530	61.9707	58.1411	72.4735	58.1411	72.4735
Numerical Frequency (rad/s)	68.8230	61.9450	58.1120	72.4400	58.1310	72.4270
Error	0.04%	0.04%	0.05%	0.05%	0.02%	0.06%

6.2 Parametric Analyses

In order to evaluate how the parameters presented in section 3 influence the behavior of a structure with a coupled TLCD, a series of analyses were conducted in the time domain through the solution of Equation 55 using the Newmark method, from which the maximum displacements of the structure in its steady state of vibration were obtained.

Initially, an uncoupled structure with a fundamental frequency of $\omega_s = 68.853$ rad/s was adopted as reference. Then, a variation of the parameters of aspect ratio α , mass ratio μ , tuning ratio γ and damping ratio of the TLCD ζ_f was performed. This variation produced the surfaces and graphics presented in the following sections.

For all cases, the force acting on the system was a harmonic excitation with unity amplitude and frequency equal to that of the uncoupled structure. The maximum

displacements of the coupled structure in each of the simulations were taken from the response after about forty-three system oscillation cycles. This was done to obtain values corresponding to the steady-state and to avoid isolated peaks that eventually appear in the transient state. The total analysis time was 10 seconds, in which the excitation force remained acting on the system.

6.2.1 Mass ratio (μ) and tuning ratio (γ)

To evaluate the influence of the μ and γ parameters, four possible values were initially defined for the parameter α (0.60, 0.70, 0.80 and 0.90). From these values of α , surfaces obtained through the variation of μ (0.01 to 0.05), γ (0.84 to 1.16) and ζ_f (0.03 to 0.12) were generated, shown in Figure 6-9 in isometric view and in Figure 6-10 as a colormap. The vertical axis represents the response ratio λ , which is the ratio of the maximum steady-state displacement of the structure coupled with the TLCD to the maximum displacement of the uncoupled structure, considering the ζ_f that guaranteed the best performance of the damper.

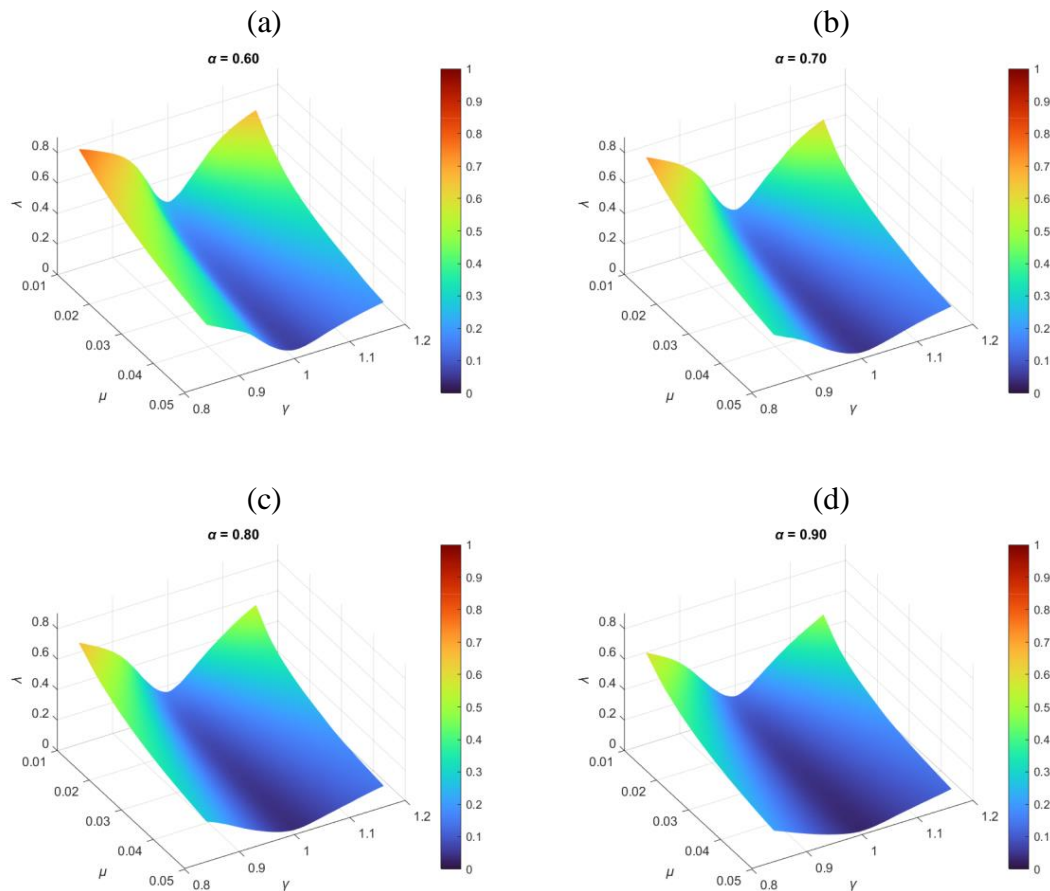


Figure 6-9 - Surfaces relating the response ratio (λ) to the parameters of mass ratio (μ) and tuning ratio (γ), considering different values of aspect ratio: (a) $\alpha = 0.60$ (b) $\alpha = 0.70$ (c) $\alpha = 0.80$ e (d) $\alpha = 0.90$

Both Figure 6-9 and Figure 6-10 demonstrate that greater values of α return smaller values of λ , that is, the TLCD acts more effectively in attenuating structure vibrations. The use of a value of α equal to 0.60 (Figure 6-9a) returned a value of 0.0628 for λ , while α equal to 0.90 (Figure 6-9d) allowed a value of λ equal to 0.0296. In addition to the reduction of

the minimum surface value, there was a general decrease in the values of the response ratio, even for tuning ratios far from the unit value. This is noticed by the smoothing of the surface slopes toward its lowest point.

Also, it can be verified the presence of a region with considerably smaller values for the response ratio (λ) when the tuning ratio (γ) is close to unity, indicating that the relationship between the structure and TLCD frequencies is a parameter of extreme importance in the attenuator design.

Figure 6-9 and Figure 6-10 allow the visualization of a smooth decreasing slope of the surface along the axis corresponding to the mass ratio parameter (μ) as this ratio is increased. This is due to the mass coupling between the structure and the TLCD and the reduction mechanism of the structure responses due to the inertial effect of the horizontal displacement of the fluid in the attenuator.

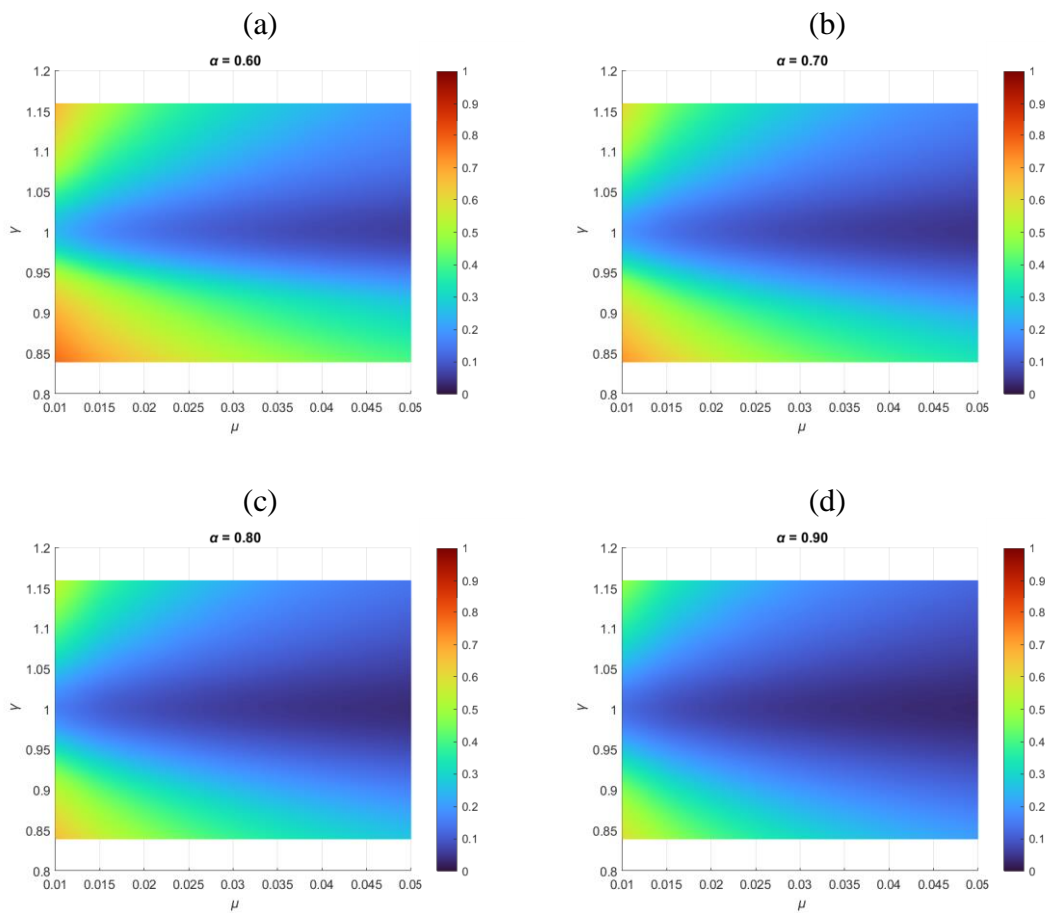


Figure 6-10 - Colormap relating the response ratio (λ) to the mass ratio (μ) and the tuning ratio (γ), considering different values of aspect ratio (α): (a) $\alpha = 0.60$ (b) $\alpha = 0.70$ (c) $\alpha = 0.80$ e (d) $\alpha = 0.90$

6.2.2 Damping ratio (ζ_f)

The results of the response ratio (λ) presented in the previous section, obtained from the variation of the parameters α , μ , γ and ζ_f , are related to the maximum displacements of the structure coupled with the TLCD, considering the ζ_f that guaranteed the best performance of the attenuator. Thus, for each combination of the other parameters a more adequate damping ratio was calculated for the TLCD. This was done within the range

determined for its variation, which was from 0.03 to 0.12. Figure 6-11 and Figure 6-12 present, respectively, the surface and its respective colormap in which the vertical axis corresponds to the parameter ζ_f . It is possible to verify that there is a wide range in which the ideal TLCD damping ratio is a minimum of the predefined interval (0.03). This range lies around the unity tuning ratio. These values change significantly as γ moves away from unity.

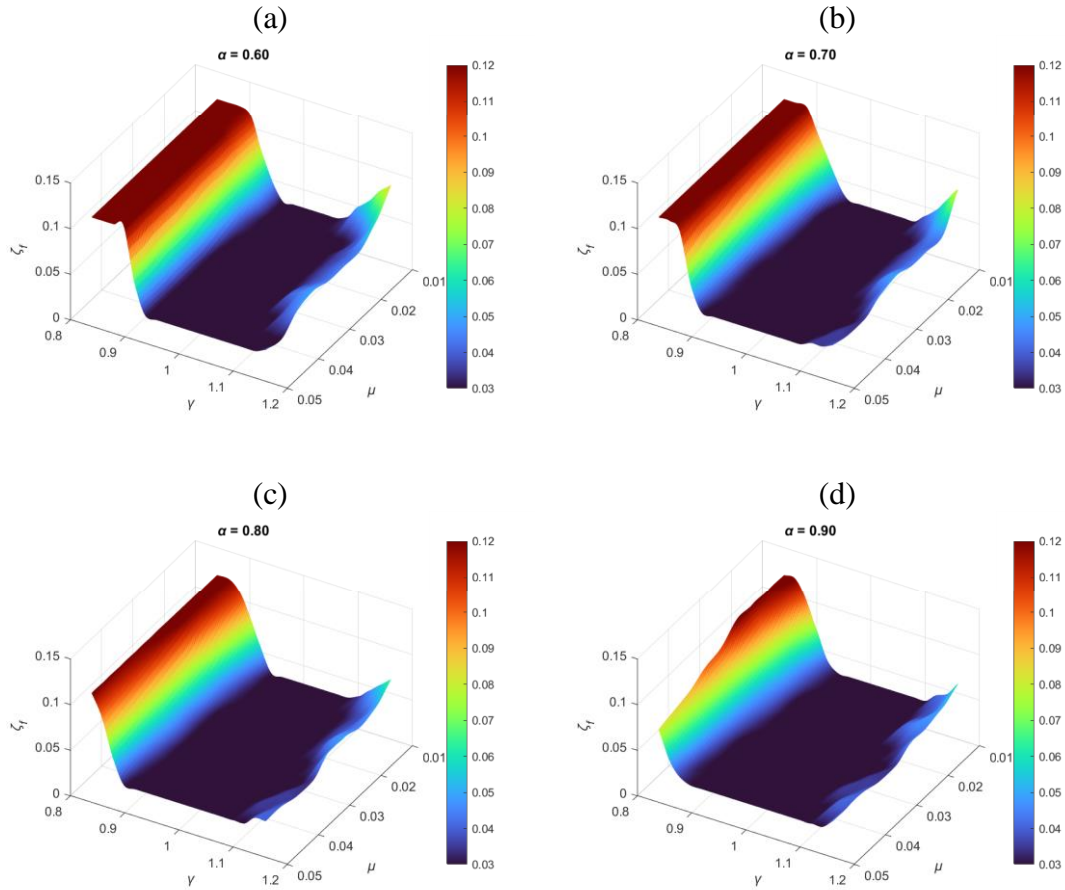


Figure 6-11 - Surfaces relating the TLCD damping ratio (ζ_f) to the mass ratio (μ) and tuning ratio (γ) parameters, considering different values of aspect ratio (α): (a) $\alpha = 0.60$ (b) $\alpha = 0.70$ (c) $\alpha = 0.80$ e (d) $\alpha = 0.90$

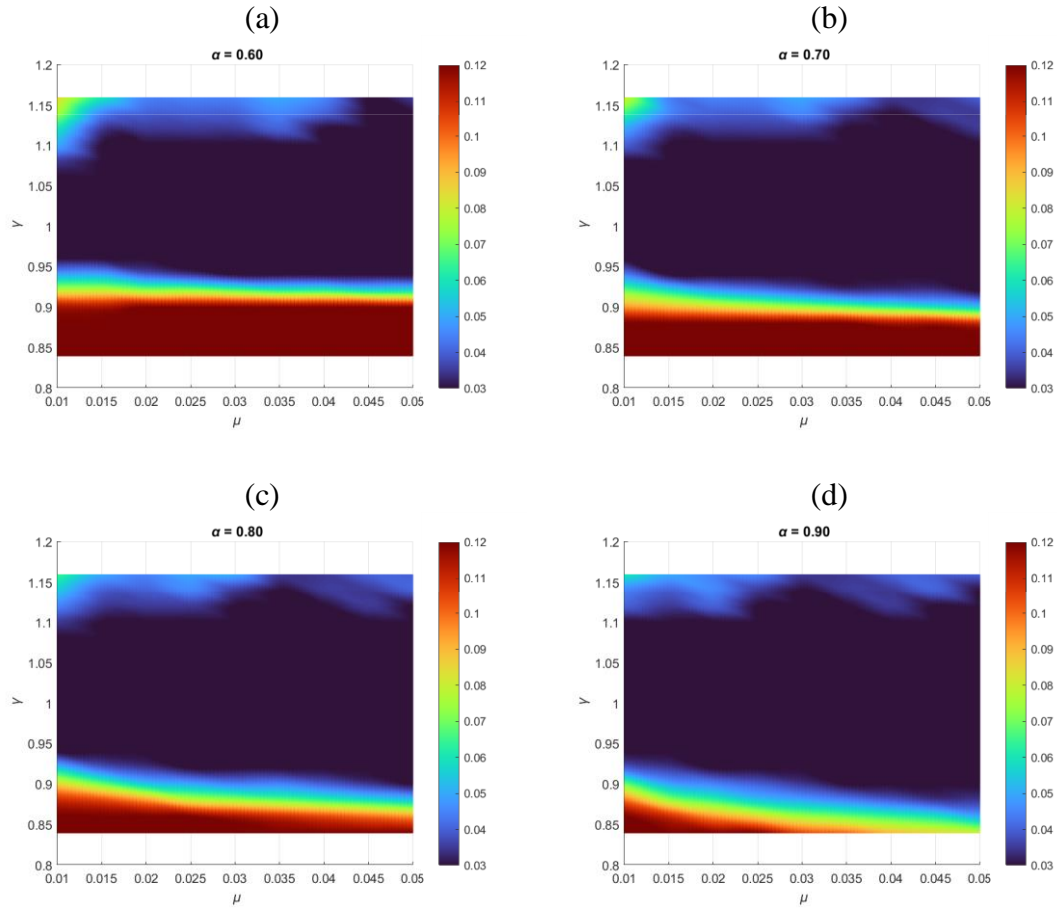


Figure 6-12 - Colormap relating the TLCD damping ratio (ζ_f) to the mass ratio (μ) and the tuning ratio (γ), considering different values of aspect ratio (α): (a) $\alpha = 0.60$ (b) $\alpha = 0.70$ (c) $\alpha = 0.80$ e (d) $\alpha = 0.90$

It is noticed that the mass ratio (μ) exerts little influence on the ideal damping ratio when the TLCD and structure are tuned, which corresponds to most cases in practice. Furthermore, an increase of the aspect ratio (α) promotes an enlargement of the range corresponding to the minimum value of ζ_f , as is easily verified by comparing Figure 6-12a and Figure 6-12d.

Therefore, for this studied case, in which a harmonic excitation force acts on the coupled system with a frequency equal to that of the uncoupled structure, small values of fluid damping ratio (ζ_f) already allow an optimal attenuation of the maximum displacements of the structure when the TLCD is properly tuned.

In this case, the reduction of vibrations is due to inertial forces arising from the fluid displacement in the horizontal section of the attenuator. Thus, the reduction little depends on the dissipation of energy by the movement of fluid.

6.2.3 Analysis of a surface point

The surfaces generated in the previous sections are the culmination of thousands of time domain results from the combination of the considered TLCD parameters. To demonstrate and validate that the results they contain match those obtained in the time domain and to also show how one would make use of them, consider the surfaces for an aspect ratio $\alpha = 0.70$ shown in Figure 6-13.

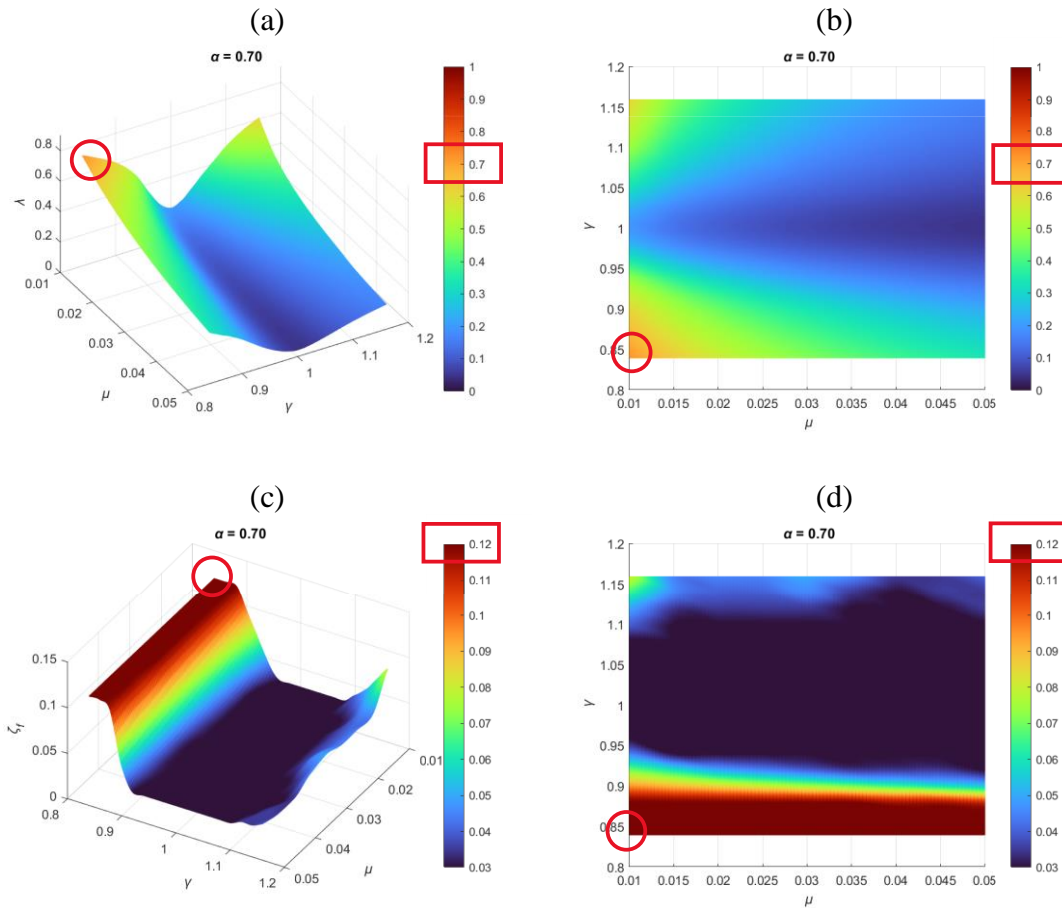


Figure 6-13 - Example of validation for a response ratio (λ) of 0.70, an aspect ratio of 0.70, a mass ratio of (μ) 0.01 and a tuning ratio of 0.85

The surface point analyzed is the one located at the top left corner of the surface in Figure 6-13a. It is also the one with a corresponding location at the bottom left corner of the colormap in Figure 6-13b. This point represents a TLCD with mass ratio $\mu = 0.01$, a tuning ratio $\gamma = 0.85$ and the intensity of the colormap suggests a response ratio of approximately $\lambda = 0.70$. To find out which value of TLCD damping ratio ζ_f generated this value of λ , look for the corresponding surface point in Figure 6-13c and in Figure 6-13d. These parameters point out to $\zeta_f = 0.12$, according to the intensity of the colormap.

Next, a simulation for an uncoupled structure is run, followed by a simulation for a structure coupled to a TLCD with the aforementioned parameters. The results are plotted in Figure 6-14.

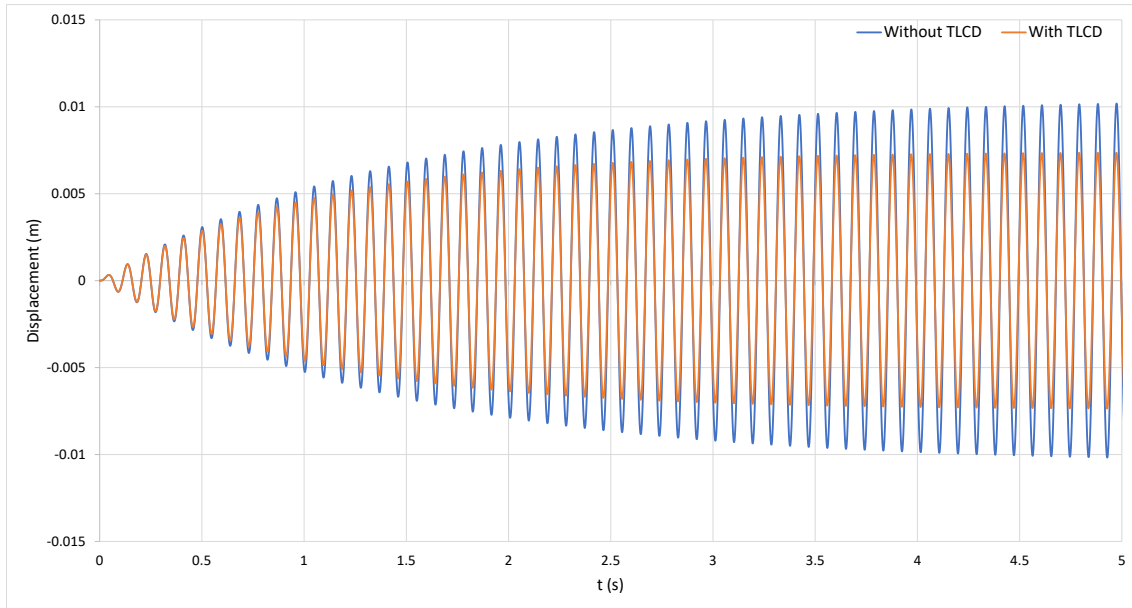


Figure 6-14 - Time responses for the structure with and without TLCD (MATLAB[®]/Excel)

Table 6-3 contains the maximum structure displacement for the cases with and without a TLCD. It also contains the value of the calculated response ratio considering these two scenarios.

Table 6-3 - Maximum structure responses with and without TLCD and the corresponding λ

Maximum structure displacement without TLCD (m):	0.0105181
Maximum structure displacement with TLCD (m):	0.0074218
Response ratio (λ):	0.7056

The result for the response ratio confirms the result obtained visually from the surfaces and the colormaps. It did not match exactly, but it provided a very good approximation considering it is a visual tool.

6.3 Case study, simulations, and practical applications

In the last part of the results section, the software packages are used to model and analyze situations that approximate practical examples and real life scenarios, such as coherent structure geometry and properties, the use of an earthquake's recorded ground acceleration history, finding the TLCD parameters that better attenuate a given structure subjected to seismic loads and then compare different structure responses coupled to different TLCDs, reducing the TLCD response for a real application and also the use of multiple TLCDs.

6.3.1 Case study 1

In order to visualize the effect of the TLCD on the building, a three-story building equipped with a PTLCD was modeled in DynaPy. Each story in the building was 3 m high, had 10000 kg of mass and columns made of reinforced concrete with a square cross section with 0.35 m sides. With these values, the first modal frequency of the structure is equal to 23.46 rad/s. The building damping ratio was set to 2%. The PTLCD had a

diameter of 0.30 m, water height of 1 m, width of 10 m, gas height of 0.40 m, gas pressure of 9.3 atm (942.23 kPa) and its valve opening was set to 25% of the cross-section area. With these values, the mass of the PTLCD is estimated to be 846.7 kg. A harmonic excitation with an amplitude of 5 m/s² and frequency of 23.50 rad/s, which is very close to the first modal frequency of the structure, was applied to the base. It is important to note that the addition of the PTLCD to the structure slightly changes the modal frequencies of the system. Figure 6-15 and Figure 6-16 show the input data on the interface of the program for the structure and the PTLCD, respectively.

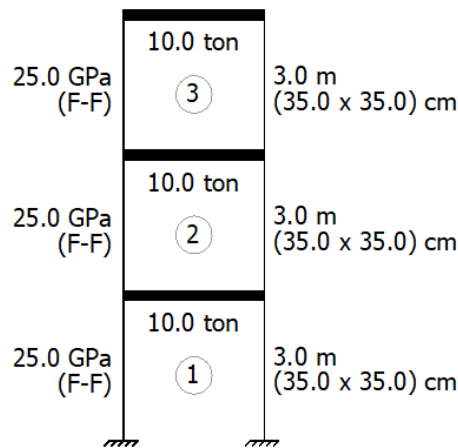


Figure 6-15 - Structure input data



D = 30 cm
h = 100 cm
B = 1000 cm
z = 40 cm
P = 9.30 atm
w = 23.50 rad/s

Figure 6-16 - PTLCD input data

Figure 6-17 and Figure 6-18 show the comparison between the dynamic response with and without the PTLCD. It was found that the use of the damping mechanism reduced the maximum displacement by about 60%, while the displacement in the steady state was reduced by about 80%. The shape of the response is also changed, reaching the maximum displacement much earlier and reducing the amplitude of displacements to a steady value afterward. The mass of the PTLCD represents only 2.8% of the total mass of the structure, but that is enough to provide a satisfactory damping.

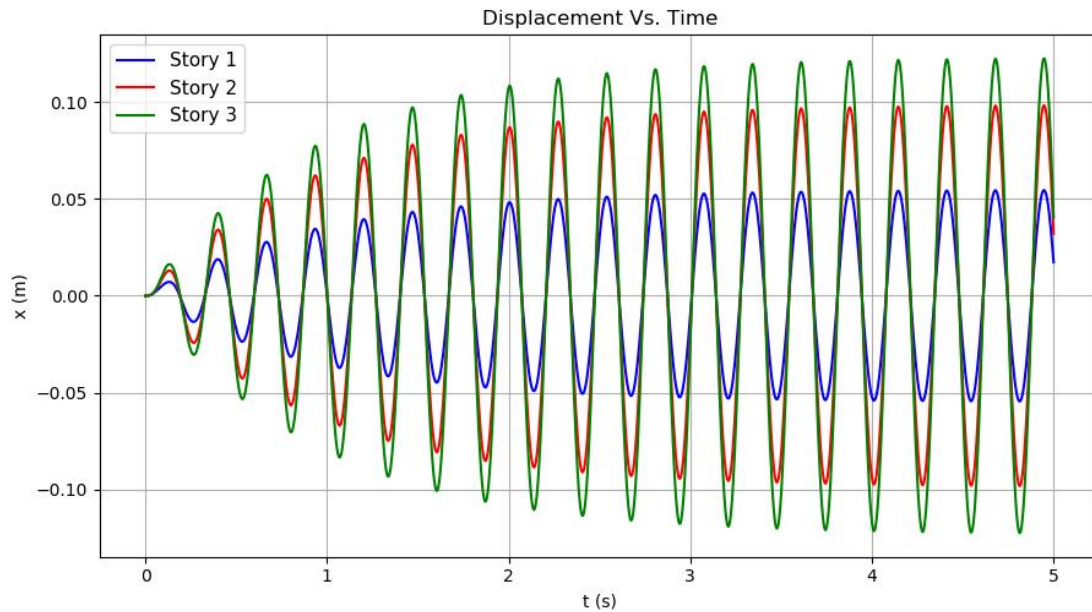


Figure 6-17 - Response of each story of the building without PTLCD (plotted in DynaPy)

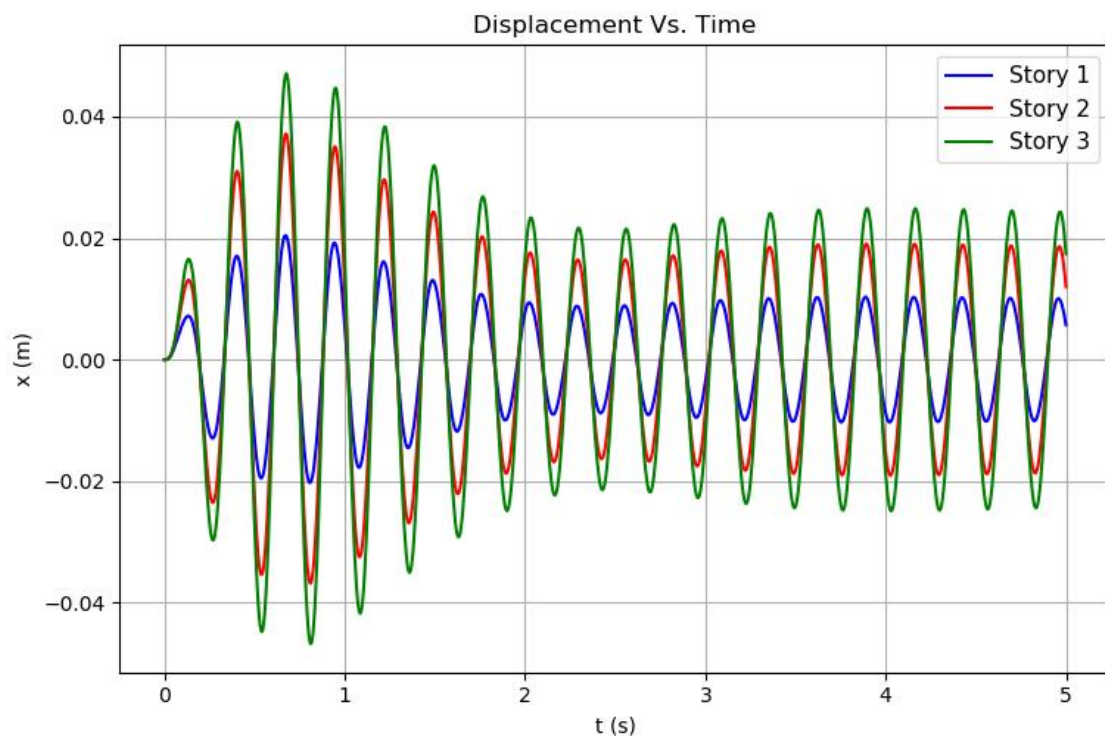


Figure 6-18 - Response of each story of the building with PTLCD (plotted in DynaPy)

A similar result can be found in a previous work that used DynaPy. Freitas and Pedrosa (2017a) analyzed the use of a PTLCD on a five-story building submitted to a base harmonic excitation with a frequency equal to the natural frequency of the building. The maximum displacement was reduced by 45%, while the displacement in the steady state was reduced by about 80%. The mass of the PTLCD represented only 1.7% of the total mass of the structure.

In the same study, a more realistic simulation was done by applying the El Centro earthquake to a ten-story building equipped with a PTLCD with a mass of about 2.0% of

the total mass of the structure. The use of the damping system greatly reduced the amplitude of vibration. The maximum displacement was reduced by 45% and, for most part of the analysis duration, the response with the PTLCD is significantly smaller than the one without the PTLCD.

6.3.2 Case study 2

The results obtained from the parametric analyses in section 6.2 were for an SDOF structure coupled with a TLCD. Despite being a simple model, the relations obtained can be used for the control of an MDOF structure's dominant vibration mode. To visualize the effect that the TLCD has in controlling an MDOF structure, DynaPy will be used in a case study (Figure 6-19).

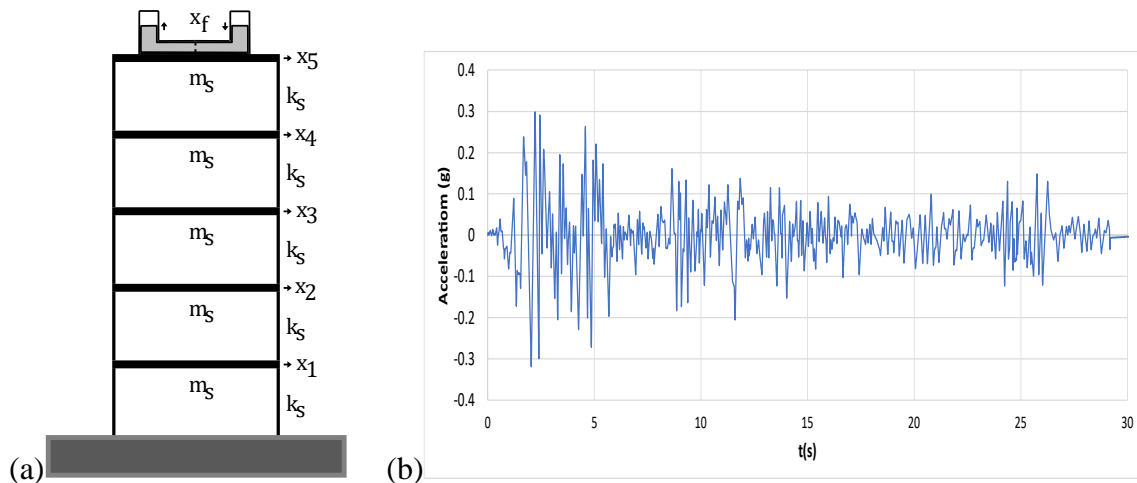


Figure 6-19 - (a) Five-story shear building with TLCD attached to the fifth story and (b) time history of ground acceleration for the El Centro earthquake

Each floor has the same lumped mass $m = 45357.6$ kg and the same stiffness $k = 5523.5$ kN/m. The natural frequencies of the 5DOF structure are, in rad/s: 3.1410, 9.1684, 14.4531, 18.5669, 21.1765. A TLCD is attached to the last floor of the structure.

To determine the ideal TLCD to be attached to the structure subjected to the random action of the El Centro earthquake, a parametric study of the liquid column is conducted using the response map of the last story of the structure (x_5). According to the previous study, the values (0.60, 0.70, 0.80 and 0.90) are considered for the aspect ratio α , while the values considered for the mass ratio μ , tuning ratio γ and damping ratio ζ_f are in the range (0.01 to 0.05), (0.75 to 1.15) and (0.00 to 0.15), respectively.

Given that the earthquake signal is random, the *rms* response is adopted for the structure response due to the seismic excitation and it is defined as

$$rms_i = \sqrt{\frac{1}{T_{tot}} \int_0^{T_{tot}} x_i^2 dt} \quad (85)$$

where the subscript i represents the i -eth story and T_{tot} is the total calculation time.

Thus, in the following pictures the vertical axis represents the *rms* response ratio (λ), defined by the ratio between the *rms* displacement of the top story of the structure coupled with the TLCD and the *rms* displacement of the top story of the uncoupled structure.

$$\lambda = \frac{\sqrt{\frac{1}{T_{tot}} \int_0^{T_{tot}} x_5^2 dt}}{\sqrt{\frac{1}{T_{tot}} \int_0^{T_{tot}} x_{5_{unc}}^2 dt}} \quad (86)$$

where $x_{5_{unc}}$ is the uncontrolled response of the top story in this case study.

Figure 6-20 and Figure 6-21 present the results in isometric view and as a colormap, respectively. Higher mass ratios represent a greater reduction in displacements. Also, the higher the TLCD aspect ratio, the greater the attenuator efficiency. The tuning frequency is more relevant for attenuators with lower B/L ratios, given that there is a significant performance loss with smaller reductions in the structure displacement outside of the central region.

The results of the response ratio λ presented in section 6.2, obtained from the variation of the parameters α , μ , γ and ζ_f , are related to the maximum displacements of the structure coupled to the TLCD considering the ζ_f that guaranteed the best performance of the attenuator.

Figure 6-22 and Figure 6-23 present the damping ratio values ζ_f of the liquid column, in which they are associated with the minimum values determined for the top story *rms* displacement of the structure coupled with the TLCD and with the variation of parameters α , μ , γ . Unlike the previous case, it is observed that there is a reduced range for the ideal damping ratio of the TLCD. Once again, however, the range for its ideal value is close to a unity tuning ratio.

In this case of the structure subjected to an earthquake, the aspect ratio, the mass ratio and the tuning ratio demonstrate a greater relationship with the ideal TLCD damping ratio. Increasing the attenuator mass requires a higher damping ratio, while increasing the aspect ratio (α) smoothes the surface behavior for different frequencies. And again, for a lower aspect ratio, the surface presents a narrow valley for the damping values. Thus, it is demonstrated that for the case of a force with different frequency amplitudes, such as an earthquake, the variation of the parameters of the liquid column is significant for its behavior and performance.

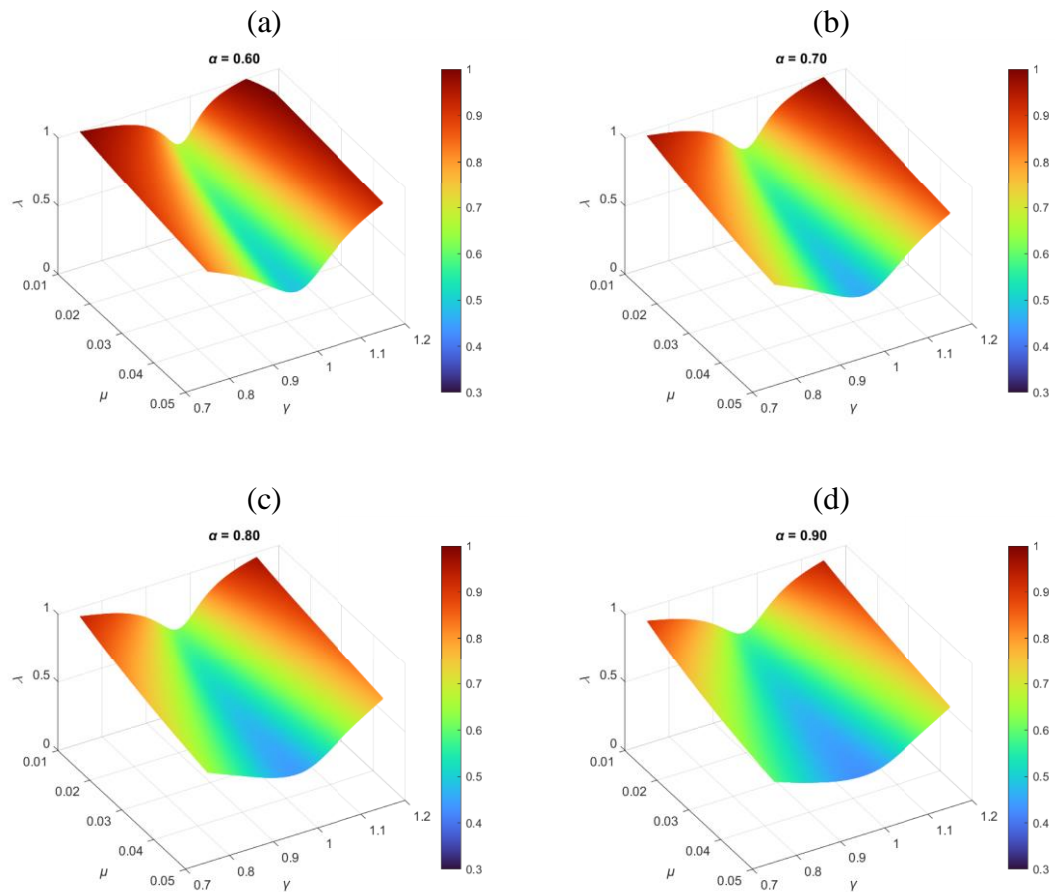


Figure 6-20 - Surfaces relating the structure displacement response ratio (λ) for the El Centro earthquake to the parameters of mass ratio (μ) and tuning ratio (γ), considering different values of aspect ratio (α): (a) $\alpha = 0.60$ (b) $\alpha = 0.70$ (c) $\alpha = 0.80$ e (d) $\alpha = 0.90$

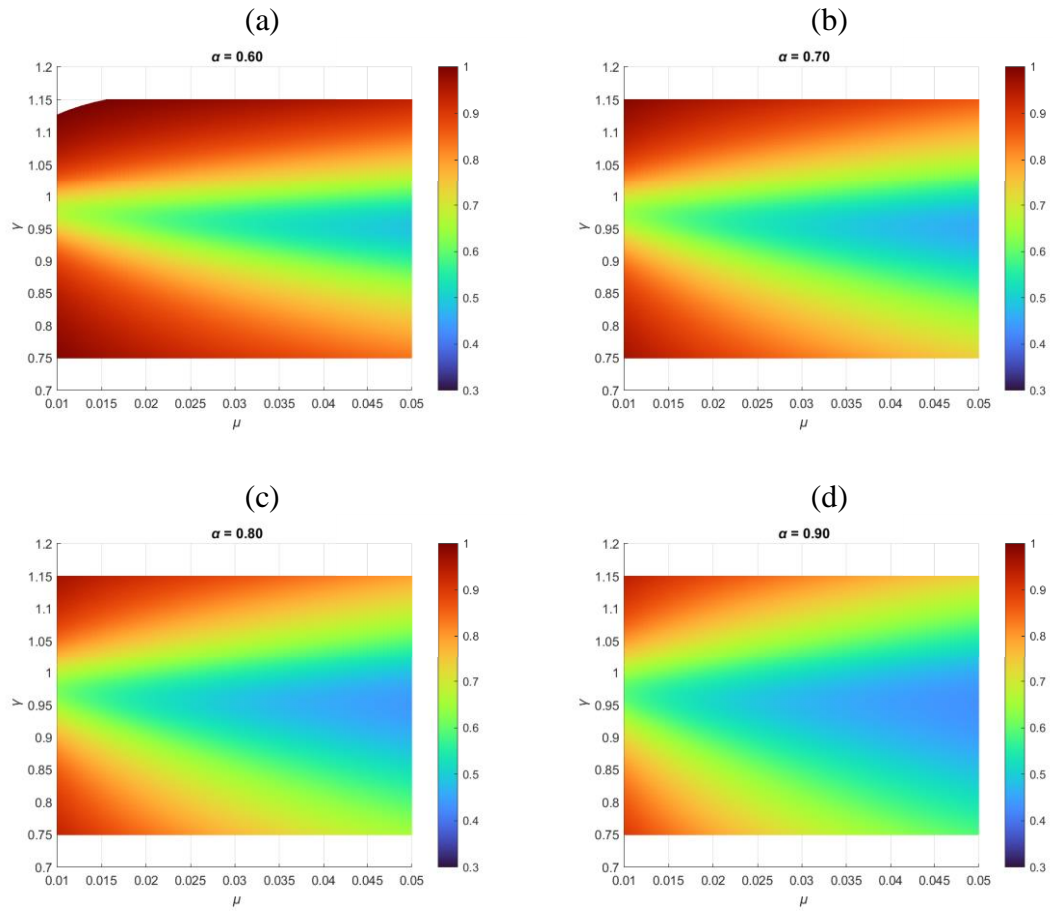


Figure 6-21 - Colormap relating the structure response ratio (λ) for the El Centro earthquake to the parameters of mass ratio (μ) and tuning ratio (γ), considering different values of aspect ratio (α): (a) $\alpha = 0.60$ (b) $\alpha = 0.70$ (c) $\alpha = 0.80$ e (d) $\alpha = 0.90$

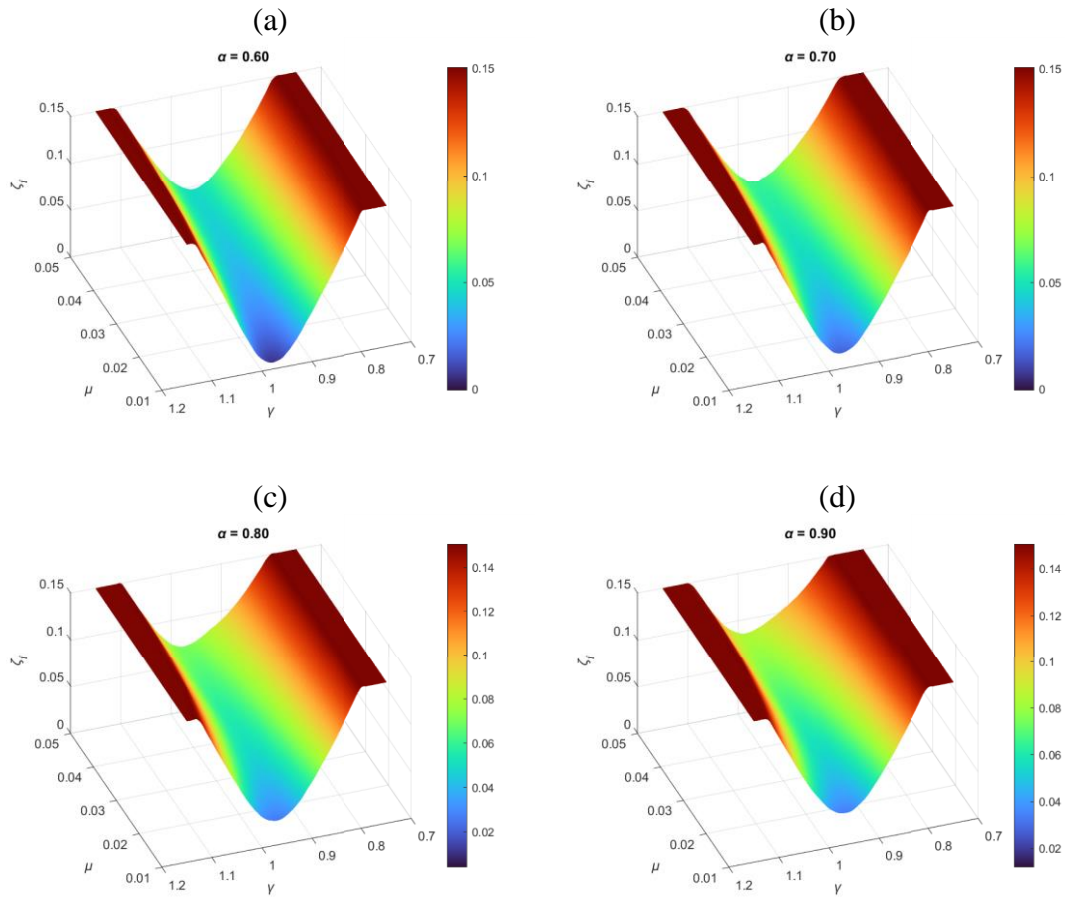


Figure 6-22 - Surfaces relating the TLCD damping ratio (ζ_f) to the mass ratio (μ) and tuning ratio (γ) parameters, considering different values of aspect ratio (α): (a) $\alpha = 0.60$ (b) $\alpha = 0.70$ (c) $\alpha = 0.80$ e (d) $\alpha = 0.90$

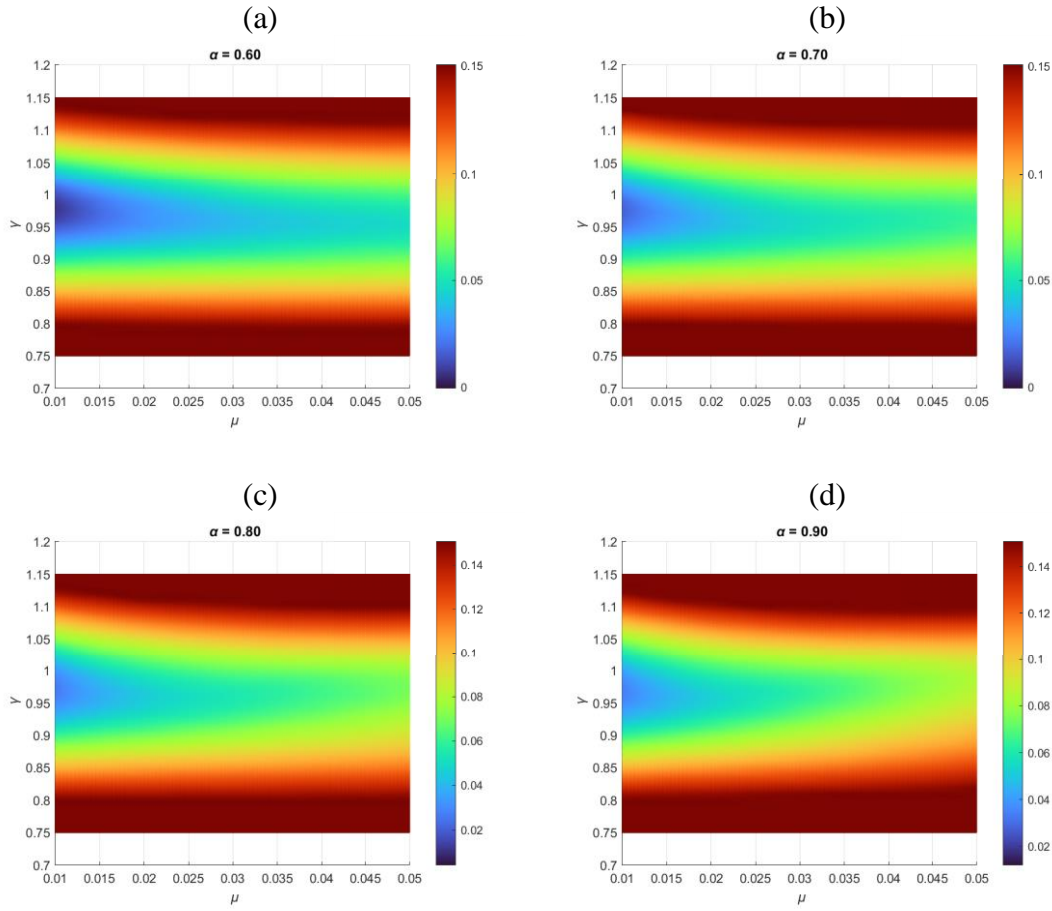


Figure 6-23 - Colormap relating the TLCD damping ratio (ζ_f) to the mass ratio (μ) and tuning ratio (γ) parameters, considering different values of aspect ratio (α): (a) $\alpha = 0.60$ (b) $\alpha = 0.70$ (c) $\alpha = 0.80$ e (d) $\alpha = 0.90$

As shown, the parameters adopted for the liquid column damper influence its performance. Figure 6-24 presents the time response of the top of the structure (x_5) with an ideal TLCD obtained from the response map and dimensioned with the parameters shown in Table 6-4. Increasing the mass ratio of the TLCD provides greater reductions in the *rms* displacement of the top of the structure. For $\mu = 1\%$ and $\mu = 5\%$, the response reduction is approximately 40% and 58%, respectively.

Table 6-4 - Mass ratio variation of the ideal TLCD designed from the response map

α	μ	γ	ζ_f	λ
0.90	0.01	0.9681	0.0339	0.5928
0.90	0.02	0.9560	0.0521	0.5135
0.90	0.03	0.9520	0.0645	0.4713
0.90	0.04	0.9520	0.0765	0.4463
0.90	0.05	0.9480	0.0906	0.4293

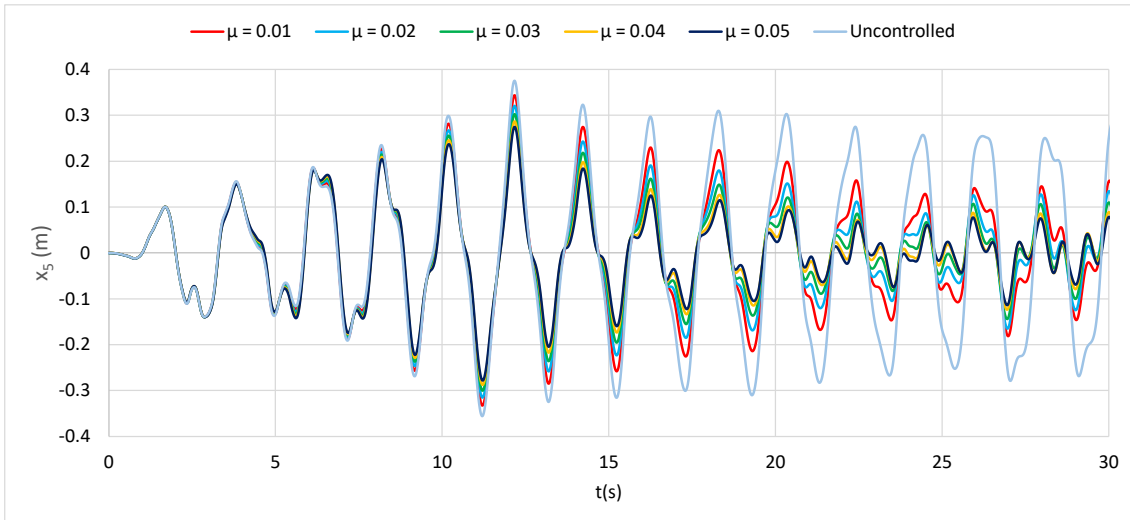


Figure 6-24 - Time response of the top of the structure (x_5) with the mass ratio variation of the ideal TLCD designed from the response map (plotted in Excel)

It is also observed that changing the aspect ratio causes a significant change in the damping ratio of the liquid column (Table 2), while the tuning frequency is slightly altered. The ideal TLCD determined from the parametric study and dimensioned with the parameters shown in Table 6-5 for the variation of α has the time response of the top of the structure (x_5) shown in Figure 6-25. The aspect ratio has influence on the response, but it is small when compared to the mass ratio. This is a relevant factor for structures with limited space to receive the TLCD.

Table 6-5 - Aspect ratio variation for the TLCD with a fixed mass ratio of 5% and designed from the response map

α	μ	γ	ζ_f	λ
0.60	0.05	0.9520	0.0469	0.4881
0.70	0.05	0.9480	0.0593	0.4585
0.80	0.05	0.9480	0.0735	0.4402
0.90	0.05	0.9480	0.0906	0.4293

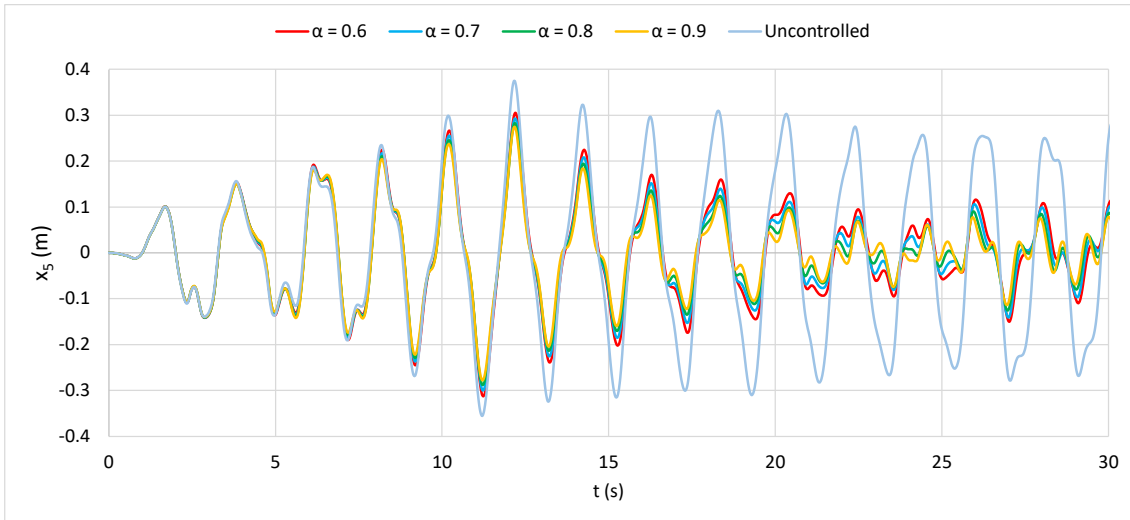


Figure 6-25 - Time response of the top of the structure (x_5) with the aspect ratio variation for the TLCD with a fixed mass ratio of 5% and designed from the response map (plotted in Excel)

6.3.3 Extra simulation for case study 2

In the previous section, the parameters found were those that minimized the structure response. This was possible, however, at the expense of the TLCD response, which wasn't considered if the objective was also avoiding fluid spill. The previous example was run in DynaPy and Figure 6-27 shows the superposition of the response of the structure and the response of the TLCD.

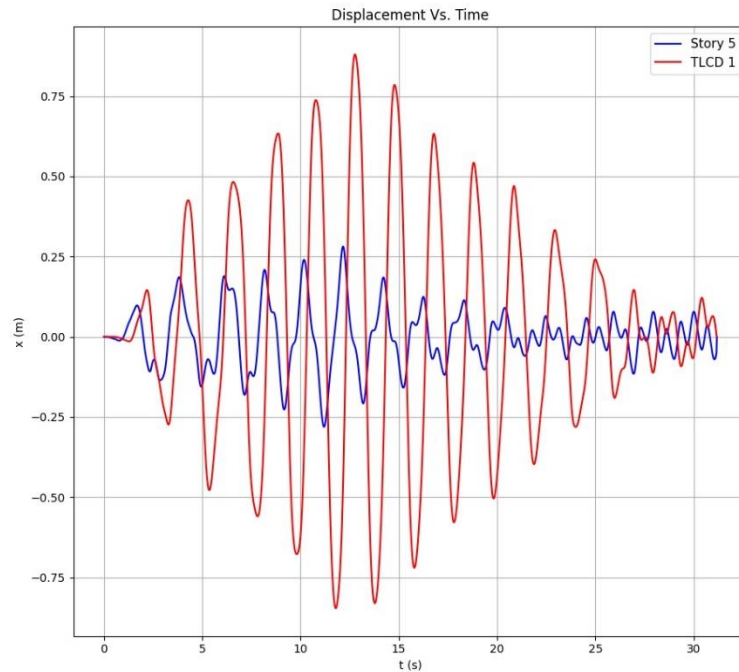


Figure 6-26 - Both responses superposed (plotted in DynaPy)

It can be seen that the response of the latter is much higher than the former. This scenario works in a purely theoretical model but could result in performance loss in practice due to fluid overflow. Thus, it is necessary to reduce the TLCD response in a real case scenario like that. To do this, it is necessary to increase its damping, which can be achieved by

using embossments, diaphragms, plates with orifices, valves, metal balls, among other damping mechanisms. The addition of those mechanisms, however, end up influencing the TLCD tuning ratio, which should stay at the designed value to maximize its performance. It is possible to change the TLCD stiffness without changing its geometry by means of a pressurized tank on both of its ends, for example. By doing this, the TLCD becomes a PTLCD and it allows for a better control of its stiffness and, consequentially, its tuning ratio. Figure 6-27 illustrates the same example from the previous case study modelled in DynaPy, but this time using a PTLCD instead of the classic TLCD.

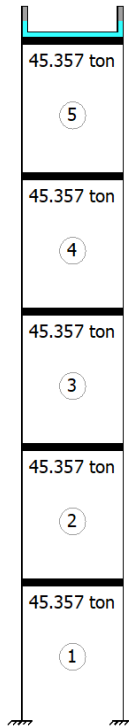


Figure 6-27 - Structure-PTLCD system analyzed and modelled in DynaPy

The simulation was run again but this time with a much higher (about 10 times) damping for the PTLCD, while maintaining the same tuning ratio. The result can be seen in Figure 6-26, and a very significant reduction in the TLCD response was achieved, from about 0.87 m to 0.10 m. This also caused an increase in the structure response, which went from a maximum of about 0.25 m to about 0.35 m. This is due to the attenuation effect from the TLCD being caused by the movement of the fluid mass in the opposite direction of the structure movement. The greater the dislocated mass, the greater the opposing force, with the opposite also being true. Hence, extra care should be considered when increasing the damping ratio.

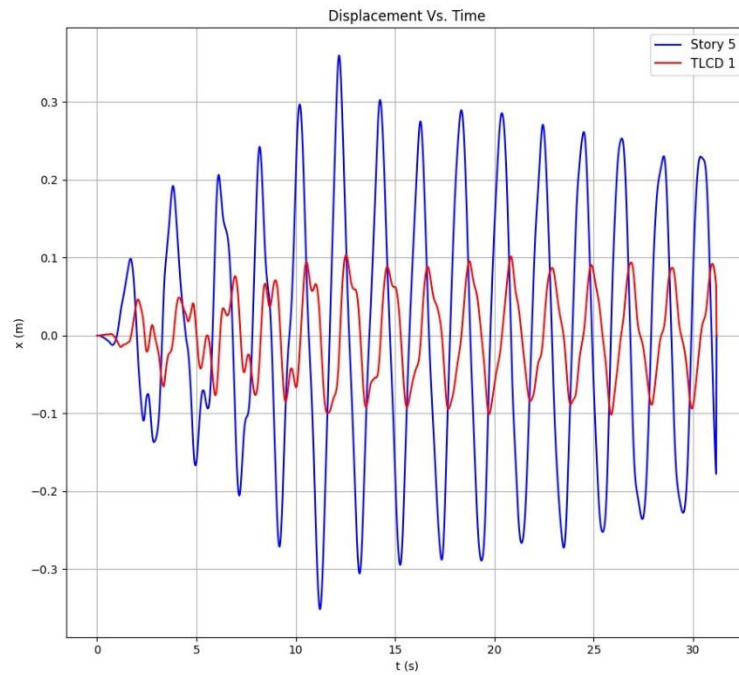


Figure 6-28 - Reduction achieved in the TLCD response (plotted in DynaPy)

6.3.4 Multiple PTLCD

This section is an adapted excerpt from the work of Oliveira (2021), who added a feature to DynaPy allowing the positioning of TLCDs in more than 1 story at the same time. It illustrates the different possibilities that DynaPy is capable of modelling and generating results from.

The dynamic response of a four-story building subjected to sinusoidal base excitation was analyzed. Each story of the building has a mass of 10 tons and pillars with a square section of 35 cm x 35 cm. Dampers will be added to the structure to analyze the influence on system displacements, as shown in Figure 6-29.

For this, four combinations of PTLCD type dampers were considered, and the total mass of dampers will always be 2% of the total mass of the structure. First, a damper was placed on the top floor. Then, two dampers, one on the top floor and the other on the third floor. Then, a damper was placed on each of the last three floors. Finally, a damper was placed on each of the four floors. All dampers, in all combinations, were tuned to the first vibration mode of the structure. The damper specifications are shown in Table 6-6.

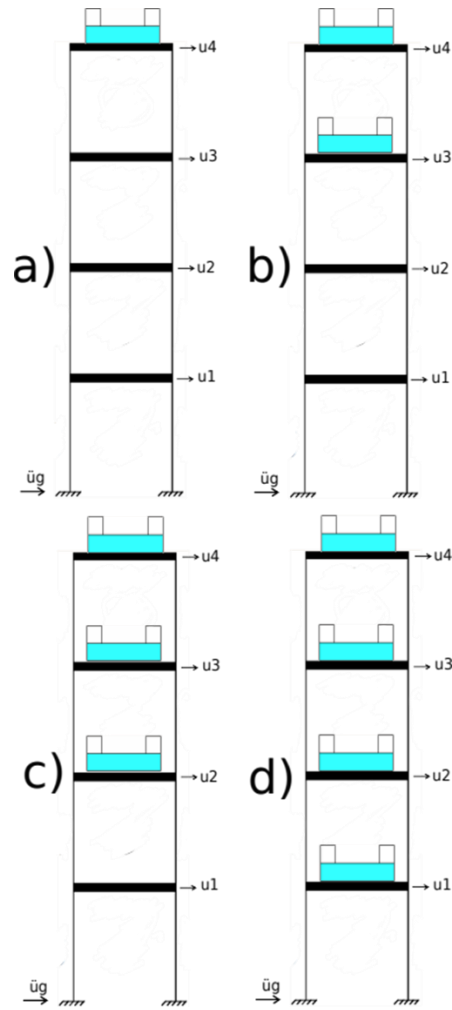


Figure 6-29 - Damper arrangements: a) only one damper, b) two dampers, c) three dampers and d) four dampers

Table 6-6 - Damper specifications

	1 PTLCD	2 PTLCDs	3 PTLCDs	4 PTLCDs
B (cm)	794	397	265	198
h (cm)	170	85	57	43
D (cm)	30	30	30	30
Z (cm)	40	40	40	40
P (atm)	5.32	2.65	1.76	1.31

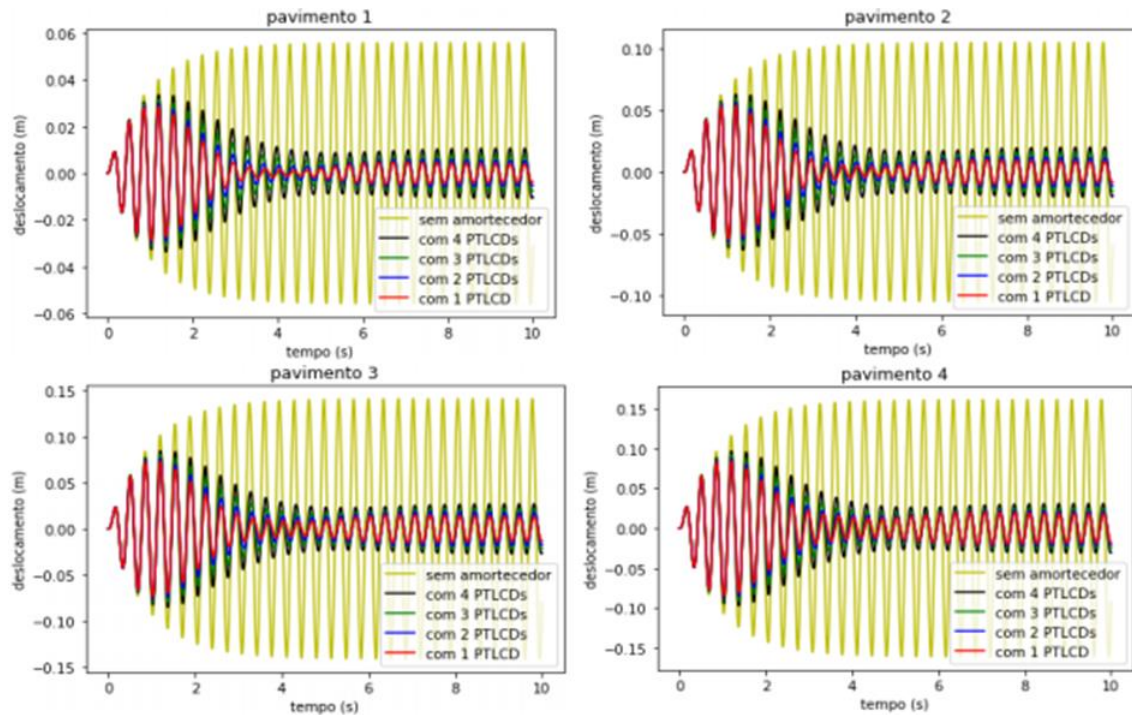


Figure 6-30 - Comparison between the response of a building with and without dampers subjected to a sinusoidal resonant load (plotted in DynaPy)

From Figure 6-30, it is clear that the arrangement of dampers along the building decreases the damping performance. In the steady state the difference is small, but the maximum displacements show a greater difference. Table 6-7 presents the percentage reduction of each of the configurations, for the maximum displacement and for the permanent regime of the last floor.

Table 6-7 - Percentage reductions in displacements

	1 PTLCD	2 PTLCDs	3 PTLCDs	4 PTLCDs
Maximum displacement	47.77 %	45.79 %	42.98 %	40.00 %
Steady state	88.60 %	86.82 %	84.27 %	80.82 %

Another problem arising from the use of multiple PTLCDs is the maximum displacement of the liquid being greater than the initial water level. Table 6-8 presents the maximum displacements and water column heights of the multiple PTLCD configurations. The cases in which multiple dampers were used presented invalid displacements. To combat this problem, diaphragms will be placed in the center of the tube to generate a localized head loss, thus reducing the displacements. The new displacements and contraction coefficients for each damper arrangement are also shown in Table 6-8.

Table 6-8 - Water column displacements with and without diaphragms

	1 PTLCD	2 PTLCDs	3 PTLCDs	4 PTLCDs
h (m)	1.70	0.85	0.57	0.43
Maximum fluid displacement without contraction (m)	0.85	0.93	1.05	1.22
Ac/A	1.00	0.70	0.45	0.37
Maximum fluid displacement with contraction (m)	0.85	0.84	0.56	0.41

The new responses with diaphragms are shown in Figure 6-31. It is evident that the presence of the diaphragms ends up reducing the impact that the dampers will have on the displacements of the structure. However, the case where two dampers are used does not present a very significant loss. Table 6-9 presents the percentage reductions of the new dampers.

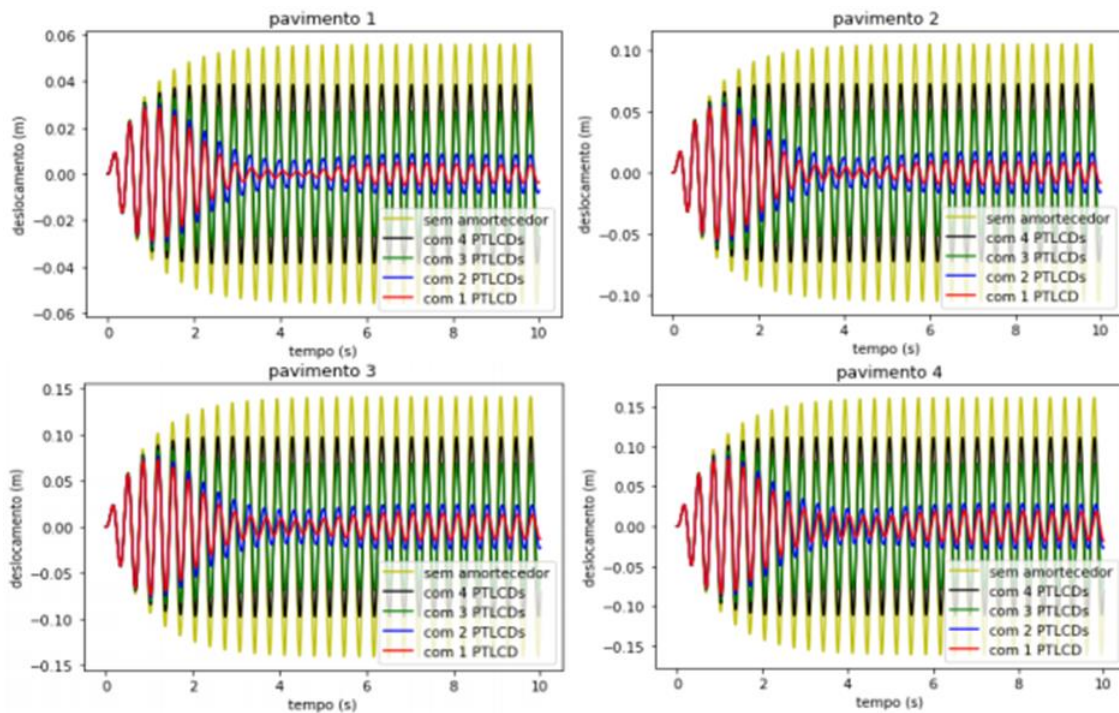


Figure 6-31 - System response with diaphragm additions (plotted in DynaPy)

Table 6-9 - Percentage reductions in displacements with diaphragm

	1 PTLCD	2 PTLCDs	3 PTLCDs	4 PTLCDs
Maximum displacement	47.77 %	45.61 %	41.09 %	30.75 %
Steady state	88.60 %	82.79 %	51.23 %	31.01 %

The dampers suffer little loss of efficiency with the diaphragms considering the maximum displacements. However, in the case of the steady state, the smaller the contraction ratio, the smaller the influence of the dampers. The presence of dampers on more than one floor reduces the possible damping, but it is a viable solution to avoid overloads in larger buildings.

7. Conclusions and future perspectives

7.1 Conclusions

The effectiveness of a TLCD in reducing structural vibration has been demonstrated for different types of force. A numerical analysis methodology was presented to determine the parameters of the liquid column damper by means of a structure response map. As shown by the response map, it appears that the TLCD tuning range, represented by the tuning ratio, has a great influence on the attenuator's performance. However, it is interesting to note that even if the TLCD is not perfectly tuned it is still possible to obtain satisfactory performance from the damper. This is an important factor, since real structures throughout their service life may present changes in their fundamental frequency generated by deterioration. Increasing the mass ratio, followed by decreasing the tuning frequency and then by increasing the liquid column damping ratio are the steps that generate greater reductions in structural displacement. However, the structure naturally imposes a limit on the configuration of the TLCD. Thus, it is important to emphasize that the reduction of the aspect ratio makes the TLCD more sensitive to parameter variations. Therefore, the value of the methodology applied in this work for the parametric analysis of the liquid column damper and its design needs to be considered.

DynaPy, one of the software packages used in this work, is a tool developed to assist researchers and students interested in the field of structural dynamics and vibration control. It provides a fast and interactive way to run simple simulations with 2D buildings, TLCDs and PTLCDs. Although being relatively simple, it is easy to use and provides a reliable way to test and measure the effectiveness of these damping mechanisms. A simple run shows that the maximum response of a three-story building under a base harmonic excitation can be reduced by about 60%, while the steady state response was reduced by about 80%. For this case, even though the mass of the PTLCD represents only 2.8% of the total mass of the structure, it was enough to provide a satisfactory reduction in the response. Previous studies with DynaPy have also shown similar results. For a five-story building, also submitted to a harmonic excitation, reductions of 45% in the maximum displacement and of about 80% in the steady state were observed. A more realistic simulation, done by applying the El Centro earthquake to a ten-story building equipped with a PTLCD, showed that the use of the damping system greatly reduced the amplitude of vibration.

In this work, a new feature was added to DynaPy in the form of the Step-by-Step Mode. Containing many interactive objects on its interface, the Step-by-Step Mode guides the user through all the steps taken by the program in order to obtain the dynamic response of the studied system. Ideally, this mode should be used by professors as an interactive tool to facilitate teaching of Structural Dynamics. Not only can this tool be used to teach about the attenuation effects of TLCDs and PTLCDs on the structure vibration, but it can also be used to teach more basic topics like single degree of freedom vibrations, multiple degrees of freedom vibrations, modal analysis and numerical integration. The Assembly tab is particularly important to show the contribution of each element of the structure in the mass, damping and stiffness matrices, as well as to show how the structure-TLCD coupling is done. The Outputs tab is also very useful to show many important results in structure dynamics such as the relation between the input excitation and the resulting structural response, and the beating and resonance phenomena. With this new feature added to DynaPy, the attenuation of vibrations using TLCDs and PTLCDs as well as other structural dynamics topics certainly becomes easier to understand.

7.2 Perspectives and recommendations for future works

Recommendations for future works in regard to DynaPy:

- i. Implement a structure model that considers the rotational degrees of freedom.
- ii. Implement a structure model that considers the interaction of the structure with the soil.
- iii. Implement a general structure model that can be analyzed as a tower, frame, or shear building.
- iv. Add new damping mechanisms to the TLCD.
- v. Add multiple TLCDs of different dimensions and/or orientations.
- vi. Design the program to be as versatile and easy to use as possible.
- vii. Design the program to be able to receive useful information from other sources and works, for example, a damping coefficient obtained by a colleague for a specific damping mechanism by using a Computational Fluid Dynamics software.

Recommendations for future works in regard to TLCDs:

- i. Study, combine and create new mechanisms to increase the damping and the stiffness of the TLCD and model them in a CFD software.
- ii. Create a small-scale model and perform experimental tests on it with different damping devices.
- iii. Do parametric and optimization studies considering new TLCD configurations.

References

- Altay, O. and Klinkel, S. (2018). A semi-active tuned liquid column damper for lateral vibration control of high-rise structures: Theory and experimental verification.
- Aono, H., Hosozawa, O., Kimura, Y. and Yoshimura, C. (2011). Seismic retrofit of high-rise building with deformation-dependent oil dampers. In CTBUH Conference, Seoul (pp. 255–265).
- Au, S.-K., Zhang, F.-L. and To, P. (2012). Field observations on modal properties of two tall buildings under strong wind. *Journal of Wind Engineering and Industrial Aerodynamics*, 101, 12–23. DOI: 10.1016/j.jweia.2011.12.002
- Balendra, T., Wang, C. M. and Cheong, H. (1995). Effectiveness of Tuned Liquid Column Dampers for Vibration Control of Towers. *Engineering Structures*, v. 17, n. 9, p. 668-675.
- Balendra, T., Wang, C. M. and Rakesh, G. (1999). Effectiveness of TLCD on Various Structural Systems. *Engineering Structures*, v. 21, pp. 291-305.
- Banavalkar, P. V. (1990). Structural systems to improve wind induced dynamic performance of high rise buildings. *Journal of Wind Engineering and Industrial Aerodynamics*, 36, 213–224. DOI: 10.1016/0167-6105(90)90306-W
- Banerji, P. and Samanta, A. (2011). Earthquake vibration control of structures using hybrid mass liquid damper. *Engineering Structures*, Volume 33, Issue 4, Pages 1291-1301, ISSN 0141-0296. <https://doi.org/10.1016/j.engstruct.2011.01.006>
- Barbosa, A.N. (1998). A Symmetric Potential Formulation for the Calculus Static and Dynamic in Problems of Fluid-Structure Interaction. Master's dissertation in Structures and Civil Construction, Publication E.DM-008A/98, Department of Civil and Environmental Engineering, University of Brasilia.
- Barbosa, A. N. and Pedroso, L. J. (2005). Pressure Waves Induced by Transients in a Pipe Flowing Fluid. 18th International Conference on Structural Mechanics in Reactor Technology (SMiRT 18). Beijing, China, August 7-12, 2005. SMiRT18 - B05-5; PP.338-344. Available at: https://repository.lib.ncsu.edu/bitstream/handle/1840.20/31447/B05_5.pdf?sequence=1&isAllowed=y
- Bashor, R., Bobby, S., Kijewski-Correa, T. and Kareem, A. (2012). Full-scale Performance Evaluation of Tall Buildings under Wind. *Journal of Wind Engineering and Industrial Aerodynamics*, 104-106, 88–97. DOI: 10.1016/j.jweia.2012.04.007
- Batista, R. N. and Pedroso, L.J. (2022). Proposta para Estudo Analítico-Numérico da Atenuação de Vibrações em Aerogeradores Provocadas por Ações Dinâmicas com uso de Absorvedores de Coluna Líquida Sintonizada. Technical Research Report - RTP-RNB3-10/2022. University of Brasilia-UnB, Faculty of Technology-FT, Department of Civil and Environmental Engineering-ENC, Postgraduate in Structures and Civil Construction-PECC, Structural Engineering, Dynamics and Fluid Structure Group-GDFE.

Bergman, L. A., Mc Farland, D. M., Hall, J. K., Johnson, E. A. and Kareem, A. (1989). Optimal Distribution of Tuned Mass Dampers in Wind Sensitive Structures. Proceedings of 5th ICOSSAR, New York.

Bhattacharyya, S., Ghosh, A. and Basu, B. (2017). Nonlinear modelling and validation of air springs effects in a sealed tuned liquid column damper for structural control. *Journal of Sound and Vibration* 410. Elsevier Ltd: 269-286. DOI: 10.1016/j.jsv.2017.07.046

Bigdeli, Y. and Kim, D. (2016). Damping Effects of the Passive Control Devices on Structural Vibration Control: TMD, TLD and TLCD for Varying Total Masses. *KSCE Journal of Civil Engineering*, v. 20, n. 1, pp. 301-308.

Bist (1978). La Centrale à Neutrons Rapides de CREYS-Malville Super Phénix, No. 227, CEA, France.

Blevins, R. (1990). *Flow-Induced Vibration*. Krieger Publishing Company.

Bomtempo, T. B. S. and Pedroso, L. J. (2017). Um Estudo Analítico-Numérico Da Influência Do Deck No Comportamento Dinâmico De Uma Plataforma Offshore Mono Leg Em Vibrações Livres. *Revista Interdisciplinar De Pesquisa Em Engenharia*, 2(24), 246–254. <https://doi.org/10.26512/ripe.v2i24.21025>

Buckley, T., Watson, P., Cahill, P., Jaksic, V. and Pakrashi, V. (2018). Mitigating the structural vibrations of wind turbines using tuned liquid column damper considering soil-structure interaction. *Renewable Energy* 120. Elsevier Ltd: 322–341. DOI: 10.1016/j.renene.2017.12.090

CEA - From research to industry - Science and Technology for Tomorrow's (2023). Available at: <https://www.cea.fr/english>. Accessed on January 15, 2023.

CEA PARIS-SACLAY - Le CEA Paris-Saclay, Centre de Recherche Scientifique et d'Innovation (2023). An Overview of the Center. Available at: <https://www.cea.fr/paris-saclay>. Accessed on January 15, 2023.

CEA PARIS-SACLAY - Les Plateformes de Simulation et Modélisation (2023). Available at: <https://www.cea.fr/paris-saclay/Pages/CEA-Paris-Saclay/environnement-scientifique/plateformes/simulation-et-modelisation.aspx> or <http://data-tamaris.fr/>. Accessed on January 15, 2023.

CEA360 - Centre Paris-Saclay - General Information Guide (2023). Available at: https://www.cea.fr/lists/staticFiles/cea360/cea360/index_CEA360.html?prefilter=234. Accessed on January 15, 2023.

Chakraborty, S., Debbarma, R. and Marano, G. C. (2012). Performance of tuned liquid column dampers considering maximum liquid motion in seismic vibration control of structures. *Journal of Sound and Vibration* 331. Elsevier Ltd: 1519-1531. DOI: 10.1016/j.jsv.2011.11.029

Chang, C. C. (1999). Mass dampers and their optimal designs for building vibration control. *Engineering Structures*, 21(5), 454–463. DOI: 10.1016/S0141-0296(97)00213-7

- Chang, C. C. and Hsu, C. T. (1999). Control performance of Liquid column vibration absorber. *Engineering Structures*, 20(7), 580-586.
- Chopra, A. (1995). *Dynamics of Structures Theory and Application to Earthquake Engineering*. Prentice Hall, New Jersey.
- Clough, R., Penzin, J. (2003). *Dynamics of Structures, Computers and Structures, Incorporated*, Berkeley.
- Colherinhas, G. B. (2020). Design of an optimal pendulum-tuned mass damper applied to offshore wind turbines. *Relatório de Doutorado, Publicação ENM.DM - Departamento de Engenharia Mecânica, Universidade de Brasília, Brasília, Distrito Federal*, xviii, 143p.
- Colwell, S. and Basu, B. (2009). Tuned liquid column dampers in offshore wind turbines for structural control. *Engineering Structures* 31(2). Elsevier Ltd: 358–368. DOI: 10.1016/j.engstruct.2008.09.001
- Costa, J. (1979). Study of the sodium boiling hazard in fast reactors, *La Houille Blanche*, 65:6-7, 413-417, DOI: 10.1051/lhb/1979039
- Coudurier, C., Lepreux, O. and Petit, N. (2018). Modelling of a tuned liquid multi-column damper. Application to floating wind turbine for improved robustness against wave incidence. *Ocean Engineering* 165. Elsevier Ltd: 277–292. DOI: 10.1016/j.oceaneng.2018.03.033
- Epstein, A. and Assedo, J. (1976). The SAFRAN Loop. *Bull Inf Sci Tech (Paris)*, (213), 25-28. Available at https://inis.iaea.org/search/search.aspx?orig_q=RN:7269088
- Espinoza, G., Carrillo, C. and Suazo, A. (2018). Analysis of a tuned liquid column damper in non-linear structures subjected to seismic excitations. *Latin American Journal of Solids and Structures* 15(7). Brazilian Association of Computational Mechanics: 1–19. DOI: 10.1590/1679-78254845
- Freitas, M. R. (2017). *Análise Dinâmica de Edifícios Equipados com Amortecedores de Líquido Sintonizado Assistida pelo Software DynaPy*. Monografia de Projeto Final em Engenharia Civil, Departamento de Engenharia Civil e Ambiental, Universidade de Brasília, Brasília, DF.
- Freitas, M. R. and Pedroso, J. L. (2017a). A Comparative Analysis of TLCD Equipped Shear Buildings Under Dynamic Loads. <http://dx.doi.org/10.20906/CPS/CILAMCE2017-0164>
- Freitas, M. R. and Pedroso, L. J. (2017b). Rotinas Computacionais em Python Para o Estudo do Comportamento de Amortecedores de Líquido Sintonizado na Atenuação de Vibrações em Estruturas. *Revista Interdisciplinar de Pesquisa em Engenharia*, 2(26): 128-135. Available at: <http://periodicos.unb.br/index.php/ripe/article/view/20830>
- Freitas, M. R., and Pedroso, L. J. (2018). A Comparative Analysis of TLCD Equipped Shear Buildings Under Dynamic Loads. *Journal of Applied and Computational Mechanics*, 5(1): 40-45. DOI: 10.22055/JACM.2018.24779.1212. Available at: https://jacm.scu.ac.ir/article_13520.html

Gao, H., Kwok, K. C. S. and Samali, B. (1997). Optimization of Tuned Liquid Column Dampers. *Engineering Structures*, 19(6), pp. 476-486.

Gazeta do Povo (2020). Prédio mais alto do Brasil recebe prêmio internacional de arquitetura. Available at: <https://www.gazetadopovo.com.br/haus/arquitetura/predio-mais-alto-brasil-premio-internacional-arquitetura-balneario-camboriu>. Accessed on January 3, 2023.

Ghedini, L. B. and Pedroso, L. J. (2019). Proposal for The Study of Vibration Control in Buildings by Use of TLCD and Soil-Structure Interaction Under Dynamic Loads. Technical Research Report - RTP-LBG2-04/2019. University of Brasilia-UnB, Faculty of Technology-FT, Department of Civil and Environmental Engineering-ENC, Postgraduate in Structures and Civil Construction-PECC, Structural Engineering, Group of Dynamics and Fluid Structure of UnB-GDFE.

Ghedini L. B., Freitas M. R. and Pedroso L. J. (2019). Study of Vibration Control Using TLCDs and Performed by the Software DynaPy in a Visual Way - XL Ibero Latin American Congress in Computational Methods in Engineering Natal, RN - Brazil. November 11-14, 2019. Paper Code: CILAMCE2019-6684; p. 15.

Gibert, R. J. (1988). *Vibrations des Structures - Interactions Avec les Fluids - Sources d'Excitation Aléatoires*. Collection de la Direction des Études et Recherches d'Électricité de France, Eyrolles Ed., Paris, França.

Gibert, R. J. (1989). *Flow Induced Vibrations in Liquid Metal Fast Breeder Reactors*. International Atomic Energy Agency, Vienna (Austria). Technical Reports Series No. 297.

Gosh, A. and Basu, B. (2004). Seismic vibration control of short period structures using the liquid column damper. *Engineering Structures* 26. Elsevier Ltd: 1905–1913. DOI: 10.1016/j.engstruct.2004.07.001

Gosh, A. and Basu, B. (2005). Effect of soil interaction on the performance of liquid column dampers for seismic applications. *Earthquake Engineering and Structural Dynamics* 34. John Wiley and Sons: 1375-1389. DOI: 10.1002/eqe.485

Gur, S., Roy, K. and Mishra, S. (2015). Tuned Liquid Column Ball Damper for Seismic Vibration Control. *Structural Control and Health Monitoring*, v. 22, pp. 1325-1342.

Hemmati, A., Oterkus, E. and Khorasanchi, M. (2019). Vibration suppression of offshore wind turbine foundations using tuned liquid column dampers and tuned mass dampers. *Ocean Engineering* 172 (September 2018). Elsevier Ltd: 286–295. DOI: 10.1016/j.oceaneng.2018.11.055

Hitchcock, P. A., Kwok, K. C. S., Watkins, R. D. and Samali, B. (1997). Characteristics of Liquid column vibration absorbers (LCVA) - I and II. *Engineering Structures*, 19(2).

Hochrainer, M. and Ziegler, F. (2006). Control of Tall Building Vibrations by Sealed Tuned Liquid Column Dampers. *Structural Control and Health Monitoring*, v. 13, 980-1002. DOI: 10.1002/stc.90

Huet, J. L. and Garcia, J. L. (1985). Note Technique DRE/STRE/LMA 85/685 (Bucle Claudia - Essais d'un clapet a battant bouvier DN150) - CEA - CEN/Cadarache - France 07/85.

Hunter, J. D. (2007). Matplotlib: A 2D Graphics Environment. *Computing in Science and Engineering* 9, n. 3, pp. 99–104. <https://doi.org/10.1109/MCSE.2007.55>

Kenny, A., Broderick, B. and McCrum, D. P. (2013). Optimization of a Tuned Liquid Column Damper for Building Structures. *Recent Advances in Structural Dynamics*, Pisa, Italy.

Ikago, K., Sugimura, Y., Saito, K. and Inoue, N. (2012). Seismic Control design of tall buildings using tuned viscous mass dampers. *CTBUH 9th World Congress Shanghai 2012 Proceedings*, 854–860.

Kwok, K. C. S. and Samali, B. (1995). Performance of Tuned Mass Dampers under Wind Loads. *Engineering Structures*, 17(9), 655–667. DOI: 10.1016/0141-0296(95)00035-6

La, V. D. and Adam, C. (2018). General on-off damping controller for semi-active tuned liquid column damper. *Journal of Vibration and Control* 24(23): 5487–5501. DOI: 10.1177/1077546316648080

Lago, A., Wood, A. and Trabucco, D. (2015). *Damping Technologies for Tall Buildings: New Trends in Comfort and Safety*. Elsevier, *Journals in Engineering - Special Issues*. Available at: <https://www.elsevier.com/physical-sciences-and-engineering/engineering/journals/dampingtechnologies-for-tall-buildings-new-trends-in-comfort-and-safety>. Accessed on July 12, 2022.

Lee, S. K., Min, K. W. and Lee, H. R. (2011). Parameter identification of new bidirectional tuned liquid column and sloshing dampers. *Journal of Sound and Vibration* 330. Elsevier Ltd: 1312–1327. DOI: 10.1016/j.jsv.2010.10.016

Lee, H. R. and Min, K. W. (2011). Reducing Acceleration Response of a SDOF Structure with a BiDirectional Liquid Damper. *Procedia Engineering*, 14, 1237–1244. DOI: 10.1016/j.proeng.2011.07.15520

Les Reacteurs Nucleaires à Caloporteur Sodium (2014). Une monographie de la Direction de l'énergie nucléaire. Commissariat à l'énergie atomique et aux énergies alternatives, CEA Saclay et Groupe Moniteur (Éditions du Moniteur). ISBN 978-2-281-11675-5. ISSN 1950-2672.

Liu, M.-Y., Chiang, W.-L., Hwang, J.-H. and Chu, C.-R. (2008). Wind-induced vibration of high-rise buildings with tuned mass damper including soil–structure interaction. *Journal of Wind Engineering and Industrial Aerodynamics*, 96(6-7), 1092–1102. DOI: 10.1016/j.jweia.2007.06.034

Lou, Y.K., Lutes, L.D. and Li, J.J. (1994). Active Tuned Liquid Damper for Structural Control. *Proceedings of the First World Conference on Wind Engineering*, Vol. I, Los Angeles.

Mendes, M. V. (2018). Análise Sísmica de Edifícios com Interação Solo-Estrutura e Atenuadores de Coluna Líquida Pressurizada. Dissertação de Mestrado, Departamento de Engenharia Civil e Ambiental, Universidade de Brasília, Brasília, Brasil.

Mendes, M.V., Freitas M.R. and Pedroso, L.J. (2018). Efeitos da interação solo-estrutura na análise sísmica de edificações com amortecedor de coluna líquida sintonizada – XXXVIII Jornadas Sudamericanas de Ingeniería Estructural, Lima, Perú. ID: XXXVIII JSIE-07-033.

Mendes, M. V., Ghedini, L. B., Batista, R. N. and Pedroso, L. J. (2023). A study of TLCD parameters for structural vibration mitigation. *Latin American Journal of Solids and Structures*, 20(1), e475. <https://doi.org/10.1590/1679-78257412>

Mendes, M. V., Ribeiro, P. M. V. and Pedroso, L. J. (2019). Effects of soil-structure interaction in seismic analysis of buildings with multiple pressurized tuned liquid column dampers. *Latin American Journal of Solids and Structures* 16(8). Brazilian Association of Computational Mechanics: 1–21. DOI: 10.1590/1679-78255707

Mensah, A. F. and Dueñas-Osorio, L. (2014). Improved reliability of wind turbine towers with tuned liquid column dampers (TLCDs). *Structural Safety* 47: 78–86. DOI: 10.1016/j.strusafe.2013.08.004

Min, K. W., Kim, H. S., Lee, S. H., Kim, H. and Ahn, S. K. (2005). Performance evaluation of tuned liquid column dampers for response control of a 76-story benchmark Building. *Engineering Structures* 27. Elsevier Ltd: 1101-1112. DOI: 10.1016/j.engstruct.2005.02.008

Moon, K. S. (2011). Structural Design of Double Skin Facades as Damping Devices for Tall Buildings. *Procedia Engineering*, 14, 1351–1358. DOI: 10.1016/j.proeng.2011.07.170

Moraes, M. V. G., Lopez, A. A. O., Martins, J. F. and Pedroso, L. J. (2020). Equivalent mechanical model of rectangular container attached to a pendulum compared to experimental data and analytical solution. *Journal of the Brazilian Society of Mechanical Sciences and Engineering (BMSE)*, v.42, p.143. <https://doi.org/10.1007/s40430-020-2232-7>

Naudascher, E., Rockwell, D. (2005). *Flow-Induced Vibrations: An Engineering Guide*. Dover.

Oliveira, L. F. C. (2021). Atenuação de vibrações em edifícios e torres utilizando coluna de líquido sintonizado (TLCD). Monografia de Projeto Final em Engenharia Civil, Departamento de Engenharia Civil e Ambiental, Universidade de Brasília, Brasília, DF, 90 p.

Park, B., Lee, Y., Park, M. and Ju, Y. (2018). Vibration Control of a Structure by a Tuned Liquid Column Damper with Embossments. *Engineering Structures*, v. 168, pp. 290-299.

Pedroso, L. J. (1983). The Nuclear Energy in France - Science and Technology. *Bulletin N°5. Embaixada Brasileira na França*, V.5, p.1 - 104.

Pedroso, L. J. (1986). Experimental Qualification of the Calculation Methods of Fluid-Structure Interactions in the Tube Circuits of Nuclear Reactors. Doctoral Thesis, 205 Pg. Centre d'Etudes Nucleaires de Saclay (CEA). Dept. des Etudes Mecaniques et Thermiques (DEMT) et Institut National des Sciences et Techniques Nucleaires (INSTN), Gif-sur-Yvette (France).

Pedroso, L. J. (1989). Analogia Mecânica para um Estudo de uma Coluna Oscilante de Fluido Incompressível Comportando Efeitos de Rigidez e Dissipação. UnB-FT/ENC. Brasília.

Pedroso, L. J. (1992a). Analogia Mecânica para um Estudo de uma Coluna Oscilante de Fluido Incompressível Comportando Efeitos de Rigidez e Dissipação. In: Nota Técnica. NT-LJP01-05/1992 - Universidade de Brasília - FT/ENC Vs. 01 - Brasília, DF.

Pedroso, L. J. (1992b). Dinâmica de Estruturas II. Notas de Curso e Apostila Didática, Programa de Pós-Graduação em Estruturas e Construção Civil - PPECC - Universidade de Brasília - FT/ENC - Brasília, DF.

Pedroso, L. J. (1992c). Interação Fluido-Estrutura. In: Notas de Curso e Apostila Didática, Programa de Pós-Graduação em Estruturas e Construção Civil - PPECC - Universidade de Brasília - FT/ENC Vs. 01 - Brasília, DF.

Pedroso, L. J. (1994). Análise e discussões dos resultados experimentais da Bancada Claudia - [Note Technique DRE/STRE/LMA 85/685 (Bucle Claudia - Essais d'un clapet a battant bouvier DN150) - CEA - CEN/Cadarache - France 07/85] - Nota técnica de pesquisa. UnB/FT, ENC.

Pedroso, L. J. (2000). Publicação Didática (Parte I) - Introdução a Dinâmica de Estruturas, Universidade de Brasília.

Pedroso, L. J. (2003a). Formulação das Equações de Movimento e Determinação das Frequências Naturais para SS1GL. UnB-FT/ENC. Brasília.

Pedroso, L. J. (2003b). Interação Fluido-Estrutura (Notas de Aula e Apostila Interna de Curso); versão preliminar, Universidade de Brasília.

Pedroso, L. J. (2015). Contribuições da Área Nuclear de Vertente Francesa no Domínio de Conhecimentos sobre TLCDS. In: Nota Técnica Bibliográfica. NTB-LJP01-07/2015. Programa de Pós-Graduação em Estruturas e Construção Civil - PPECC - Universidade de Brasília - FT/ENC Vs. 01 - Brasília, DF.

Pedroso, L. J. (2016). Controle de Vibrações em Estruturas com a Utilização de TLCDS. In: Notas de Curso e Apostila Didática de Dinâmica das Estruturas II - Programa de Pós-Graduação em Estruturas e Construção Civil - PPECC - Universidade de Brasília - FT/ENC - Brasília, DF.

Pedroso, L. J. and Gibert, R. J. (1987). Experimental study of the pressure drop of perforated plates in unsteady ducted flow. 9th International Conference on Structural Mechanics in Reactor Technology (SMIRT), Lausanne, Aug.17-21.

Pedroso, L. J. and Gibert., R. J. (1988). Experimental Investigation of The Pressure Loss Trough Perforated Structures in Unsteady Flow. *Journal of Structural Mechanics*. v.21, p.42-54. ISSN 0783-6104. <http://rmseura.tkk.fi/rmlehti/archive.html> (V.21, 1988, Number 1) http://rmseura.tkk.fi/rmlehti/1988/nro1/RakMek_21_1_1988_2.pdf

Pedroso, L. J. et al. (1990). Experimental study of the attenuation waves oriented to transients caused by the sodium-water explosive reaction in fast reactors. 6th Brazilian symposium on piping and pressure vessels (VI SIBRAT), Rio de Janeiro (Brazil), 4-7 Dec 1990. Vol.1, pp.303-321. Conference Proceedings. Available at National Technical Reports Library. U.S. Department of Commerce. Technical Report No. DE92624303 and NTIS Issue Number 199222.

Pedroso, L. J., Vital de Brito, J. L. and Barbosa, A. N. (1994). TRANS - A Computer Code for the Analysis of Transients in Nuclear Reactors Piping Networks - V General Congress on Nuclear Energy - Rio de Janeiro; 29/08-2/09/1994. Vol. I; pp.1-6; 411p; Available at the National Nuclear Energy Commission Library, RJ, BR.

Pestana, I. G. (2012). Controlo de Vibrações em Engenharia Civil - Amortecedor de Colunas de Líquido Sintonizado. Master's Thesis, Faculty of Science and Technology, New University of Lisboa, Lisboa, Portugal.

Saaed, T. E., Nikolakopoulos, G., Jonasson, J. E. and Hedlund, H. (2013). A state-of-the-art review of structural control systems. *Journal of Sound and Vibration* 21(5). Sage: 1–19. DOI: 10.1177/1077546313478294

Sakai, F., Takaeda, S. and Tamaki, T. (1989). Tuned liquid column damper-new type device for suppression of building vibrations. In: Proceedings of international conference on high-rise buildings., Nanjing, 1989, pp. 926–31.

Sarmiento, C. V. S., Pedroso, L. J. and Ribeiro, P. M. V. (2020). From Numerical Prototypes to Real Models: A Progressive Study of Aerodynamic Parameters of Nonconventional Concrete Structures with Computational Fluid Dynamics. *Revista Ibracon de Estruturas e Materiais*, v. 13, p. 628-643.

Sauvage, J. F. (2004). Phénix - 30 years of history: the heart of a reactor. Creys-Malville nuclear power plant. CEA & EDF, 241 Pgs. CEA Valrhô - BP 17171 - 30207 Bagnols-sur-Cèze cedex.

Shimizu, K. and Teramura, A. (1994). Development of vibration control system using U-shaped tank. Proceedings of the 1st International Workshop and Seminar on Behavior of Steel Structures in Seismic Areas, Timisoara, Romania, 7.25-7.34.

Shum, K. M., Xu, Y. L., Guo, W. H. (2008). Wind-Induced Vibration Control of Long Span Cable-Stayed Bridges Using Multiple Pressurized Tuned Liquid Column Dampers. *Journal of Wind Engineering and Industrial Aerodynamics*, v. 96, pp. 166-192. DOI: 10.1016/j.jweia.2007.03.008

Silva, A. C. (2018). Análise Numérica do Escoamento em Torno de Um Cilindro. Monografia de Graduação. Departamento de Engenharia Civil e Ambiental. Universidade de Brasília.

- Silva, A. C., Pedroso, L. J. and Oliveira, L. F. C. (2018). Estudo Numérico do Comportamento Dinâmico de uma Torre EÓLICA VIA CFD – XXXIX Ibero Latin American Congress in Computational Methods in Engineering. Paris/Compiègne, France. v.1 p. 386. ISBN: 978-2-9565961-0-3.
- Smith, R. J. and Willford, M. R. (2007). The Damped Outrigger Concept for Tall Buildings. *The Structural Design of Tall and Special Buildings*, 16(4), 501–517.
- Sonmez, E., Nagarajaiah, S., Sun, C. and Basu, B. (2016). A study on semi-active Tuned Liquid Column Dampers (sTLCDs) for structural response reduction under random excitations. *Journal of Sound and Vibration* 362. Academic Press: 1–15. DOI: 10.1016/j.jsv.2015.09.020
- Souza, R. A. (2003). Controle Passivo/Ativo das Oscilações de Estruturas Esbeltas por Meio de Dispositivos Fluido Dinâmicos. Doctoral Dissertation, COPPE, Federal University of Rio de Janeiro, Rio de Janeiro.
- Spencer, B. F. and Nagarajaiah, S. (2003). State of the Art of Structural Control. *Journal of Structural Engineering* 129. ASCE: 845-856.
- Tait, M. J. (2008). Modelling and preliminary design of a structure-TLD system. *Engineering Structures*, Volume 30, Issue 10, Pages 2644-2655, ISSN 0141-0296. <https://doi.org/10.1016/j.engstruct.2008.02.017>
- Tamura, Y., Fujii, K., Ohtsuki, T., Wakahara, T. and Kohsaka, R. (1995). Effectiveness of Tuned Liquid Dampers under Wind Excitation. *Engineering Structures*, 17(9), 609–621. DOI: 10.1016/0141-0296(95)00031-2
- Tatemichi, I., Kawaguchi, M. and Abe, M. (2004). A Study on Pendulum Seismic Isolators for High Rise Buildings. In CTBUH Conference, Seoul (pp. 182–189).
- Tedesco, J., McDougal, W., Ross, C. (1999). *Structural Dynamics: Theory and Applications*. Addison Wesley Longman.
- Thenozhi, S. and Yu, W. (2013). Advances in modeling and vibration control of building structures. *Annual Reviews in Control*, v. 37, p. 346-364.
- Velez, W., Pedroso, L. J. and Mendes, N. B. (2015). Simulação de Transientes de Pressão em Dutos de Usinas Hidroelétricas e Nucleares pelo Método das Características. In: XXXVI Iberian Latin American Congress on Computational Methods in Engineering, Rio de Janeiro.
- Vickery, B., Galsworthy, J. and Gerges, R. (2001). The Behavior of Simple Non-Linear Tuned Mass Dampers. In CTBUH 6th World Congress.
- Walt, S. V. D., Colbert, S. and Varoquaux, G. (2011). The NumPy Array: A Structure for Efficient Numerical Computation. *Computing in Science and Engineering* 13, n. 2, pp. 22–30. <https://doi.org/10.1109/MCSE.2011.37>
- Yalla, S. K. and Kareem, A. (2000). Optimum absorber parameters for tuned liquid column dampers. *Journal of Structural Engineering* New York, N.Y. 126(8). American Society of Civil Engineers: 906–915. DOI: 10.1061/(ASCE)0733-9445(2000)126:8(906)

Yamazaki, S., Nagata, N. and Abiru, H. (1992). Tuned active dampers installed in the Minato Mirai (MM) 21 landmark tower in Yokohama, *Journal of Wind Engineering and Industrial Aerodynamics* 43. 1937-1948. International Conference on Wind Engineering.

Yao, J.T.P. (1972). Concept of Structural Control, ASCE, *Journal of Structural Division*, 98, 1567-74.

Appendix

Where to download DynaPy

DynaPy can be downloaded for free on the GitHub webpages of both the original creator and of the author of this work. It is necessary to have Python installed in order to run it, along with other packages like Matplotlib and Numpy.

Python can be downloaded at <https://www.python.org/downloads>. The other packages can be downloaded and installed by running Python and then executing the pip install command (e.g. pip install Numpy).

DynaPy's Instructions Manual



Dynapy is composed of three main parts: pre-processing, processing and post-processing. The pre-processing part is where the user inputs all the data by interacting with the program interface. This includes steps such as the configurations of the analysis, the structure parameters, the TLCD parameters and the excitation parameters. The next figures show DynaPy's interface and all of the input data that it takes from the user.

First is the Structure tab. Here, the user can input structure parameters based on the geometry and properties of each story. After the properties are determined, the story can be added. If the building has stories with the same characteristics, the user can simply click on the "Add Story" button to quickly add stories.

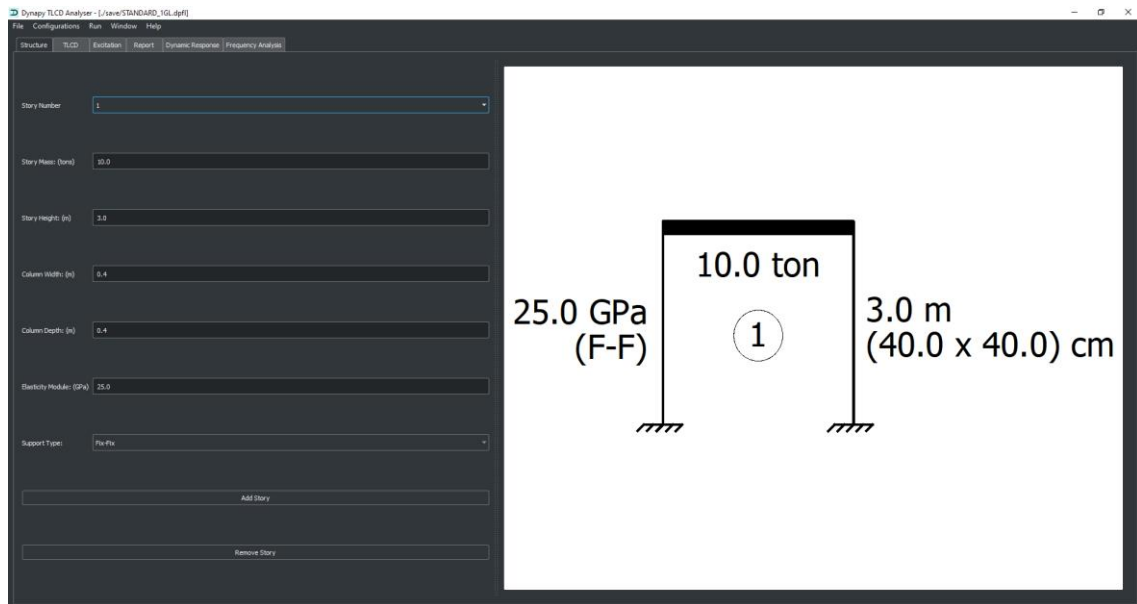


Figure A1 - Clicking on the "Add Story" button will add a story with the chosen parameters

To remove a story, it is necessary to remove all the stories above it first by selecting the story number and then clicking on the "Remove Story" button.

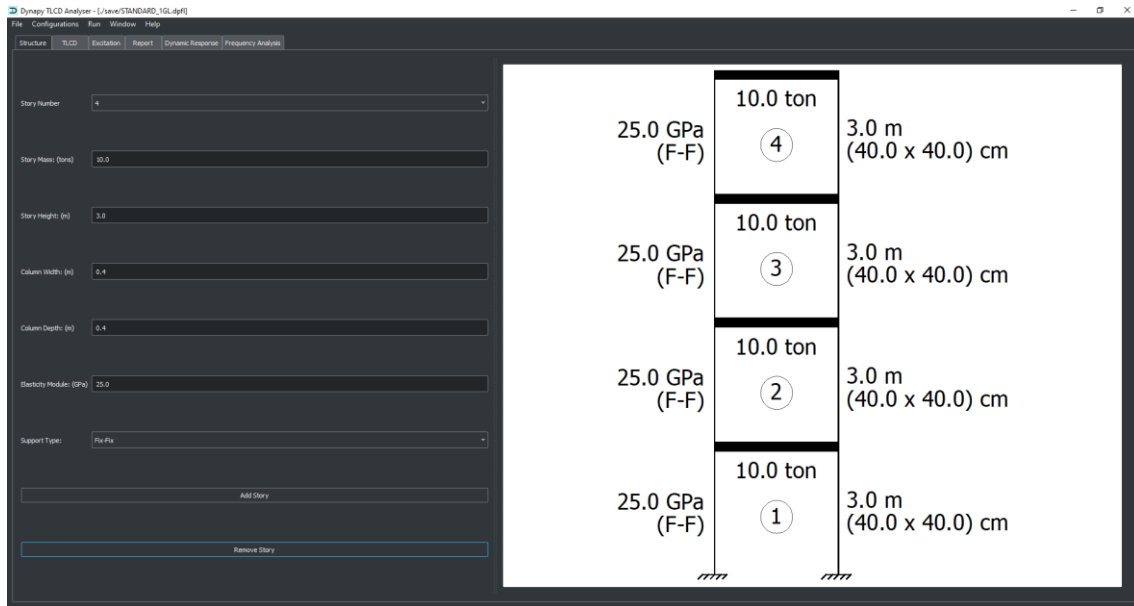


Figure A2 - Clicking on “Remove Story” button after selecting the last story number will remove it

Next is the TLCD tab. The user can choose to run an analysis with no TLCDs, with a single TLCD or with multiple TLCDs. It is also possible to choose a single or multiple PTLCDs. Just like the structure tab, it is necessary to define all the parameters before adding the TLCD by clicking on the “Confirm TLCD” button.

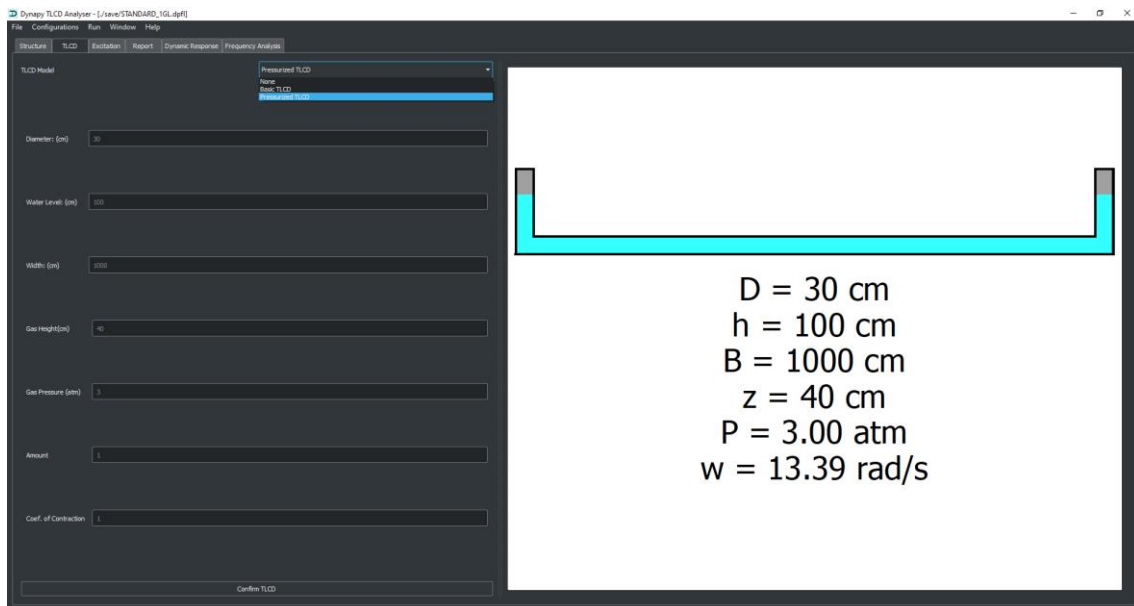


Figure A3 - Choosing and adding a PTLCD to the analysis

The final input screen is the Excitation tab. Here, the user can choose from two types of excitations - Sine Wave or General Excitation. The first one is defined by choosing relevant parameters, such as amplitude and frequency, while the second one can be manually created or uploaded from a formatted file by the user. The excitation duration and the analysis duration must be specified by the user for the Sine Wave, while for the General Excitation it comes from the data file itself.

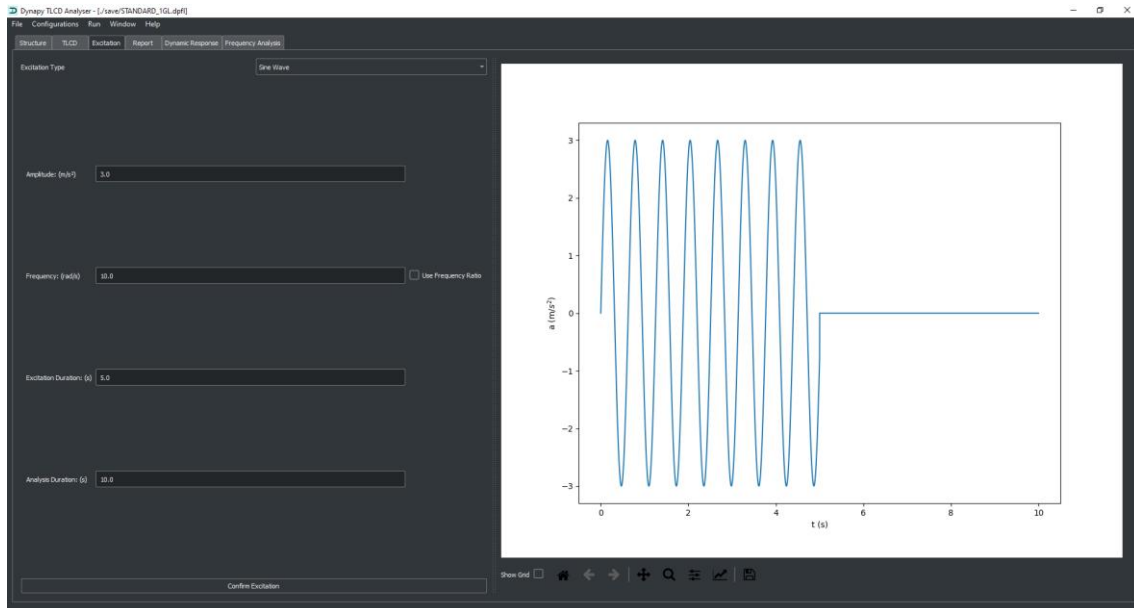


Figure A4 - Choosing and adding a Sine Wave with defined parameters to the analysis

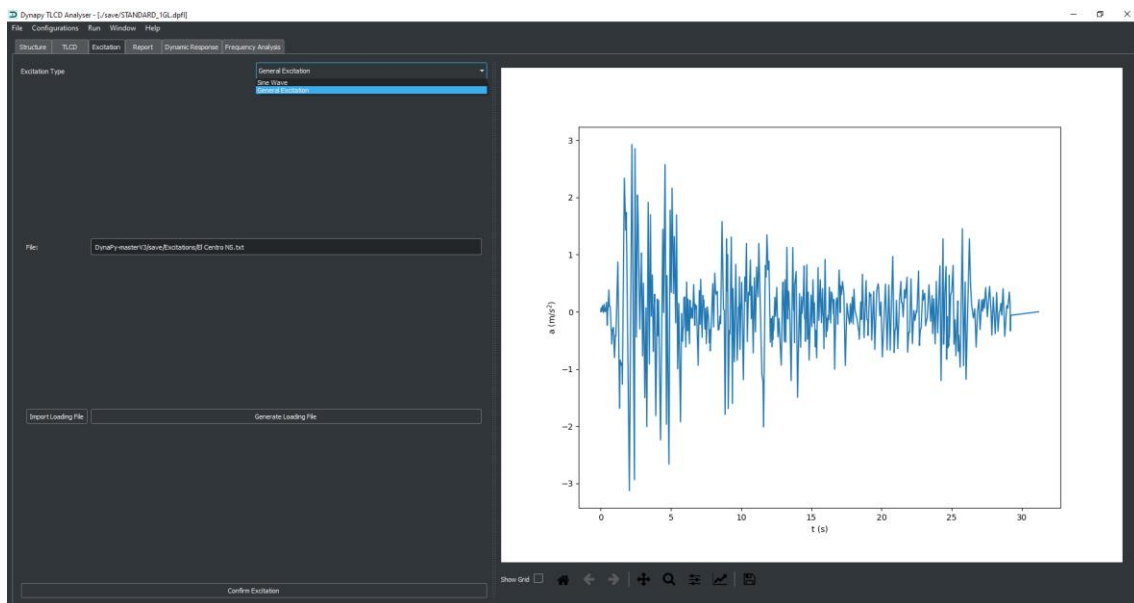


Figure A5 - Choosing and adding a General Excitation with data from the El Centro earthquake to the analysis

Finally, it is necessary to select and confirm certain analysis configurations before running a simulation. These include the solution method and the structure model, although the only currently available model for the structure is the shear building model. Other configurations are boundary conditions (initial conditions), fluid parameters, DMF (dynamic magnification factor) settings, step size and structure damping.

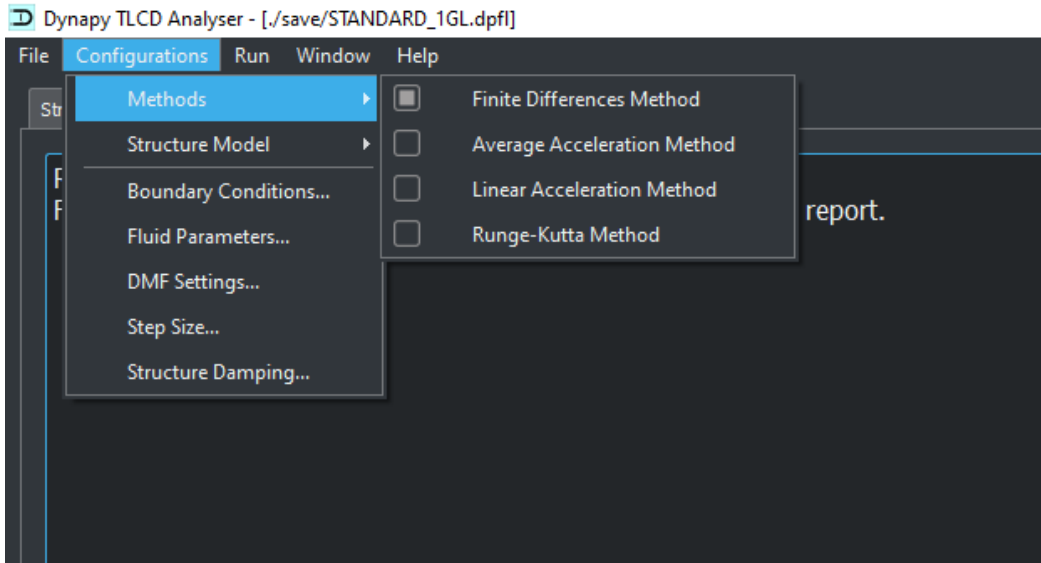


Figure A6 - Choosing a solution method for the analysis

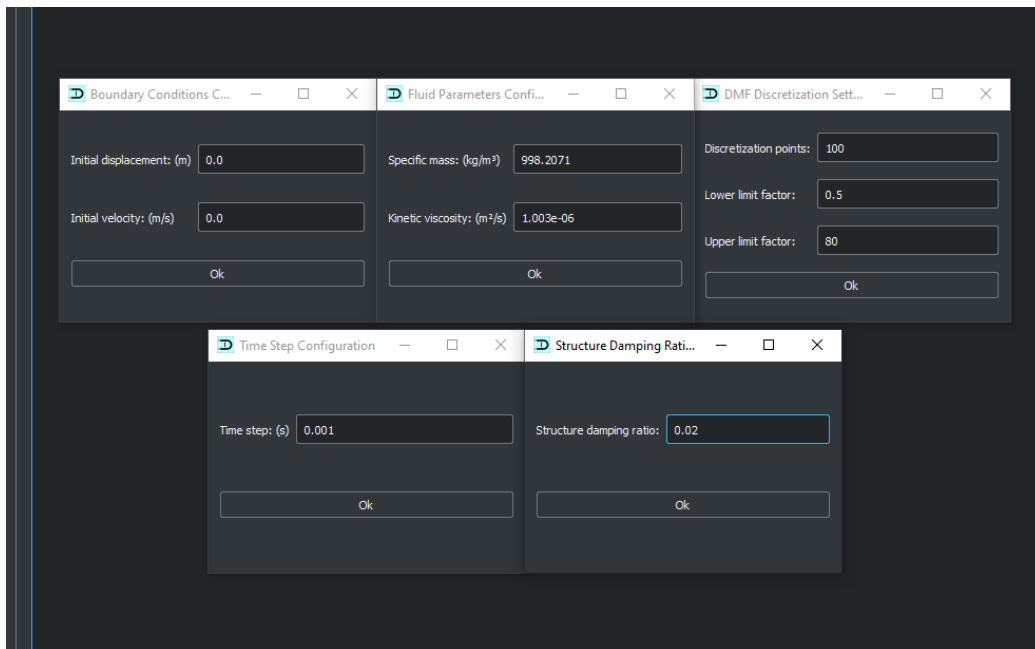


Figure A7 - Defining other settings for the analysis

After all the input parameters are filled out and the required configurations are defined, it is possible to run an analysis by clicking on the Run tab and then on the desired analysis. DynaPy currently has a Dynamic Response analysis and a Dynamic Magnification Factor analysis, but other analysis, such as a TLCD Response and a three-dimensional analysis, can be programmed and added to the software. Some options in the Run tab are greyed out and are currently unavailable (Optimization) or unavailable until a previous simulation is run (Step-by-Step Mode).

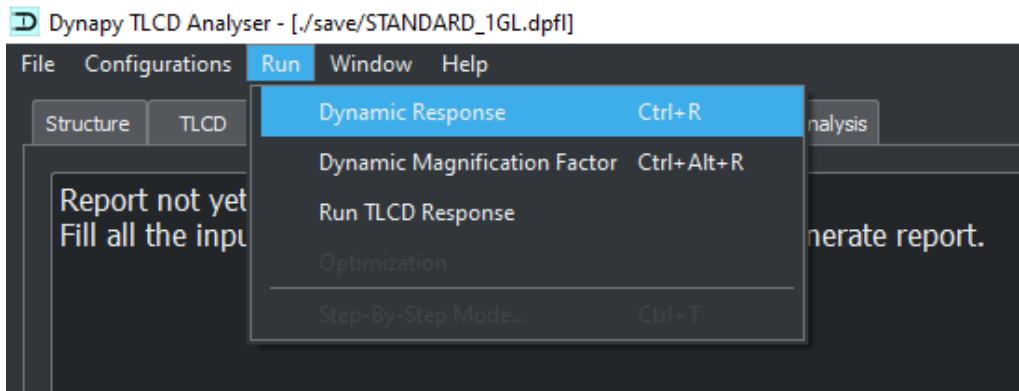


Figure A8 - Running a Dynamic Response

After running an analysis, DynaPy processes the data and presents the results to the user in the form of a report and in the form of plotted graphs. The report is not available until an analysis is performed first. It contains many important information of the analysis, such as structure, TLCD and excitation parameters, the chosen configurations, the values of all the matrices and vectors of the problem, among others.

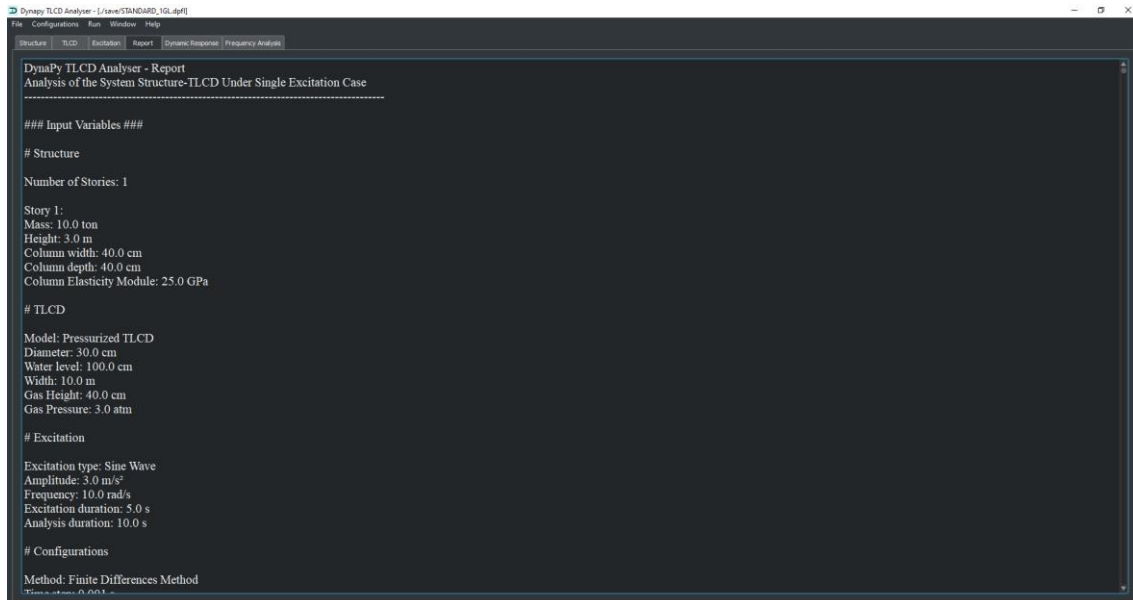


Figure A9 - Report tab containing important information of the analysis

The response data is available in the Dynamic Response tab and is presented to the user in the form of plotted graphs. The user can choose to plot specific degrees of freedom or all of them at the same time. The plot can be saved and its data can be exported to a CSV file by clicking on the corresponding buttons at the bottom right. The canvas where the graph was plotted on can be customized using the tools below it. It is also possible to choose from four different plot types.

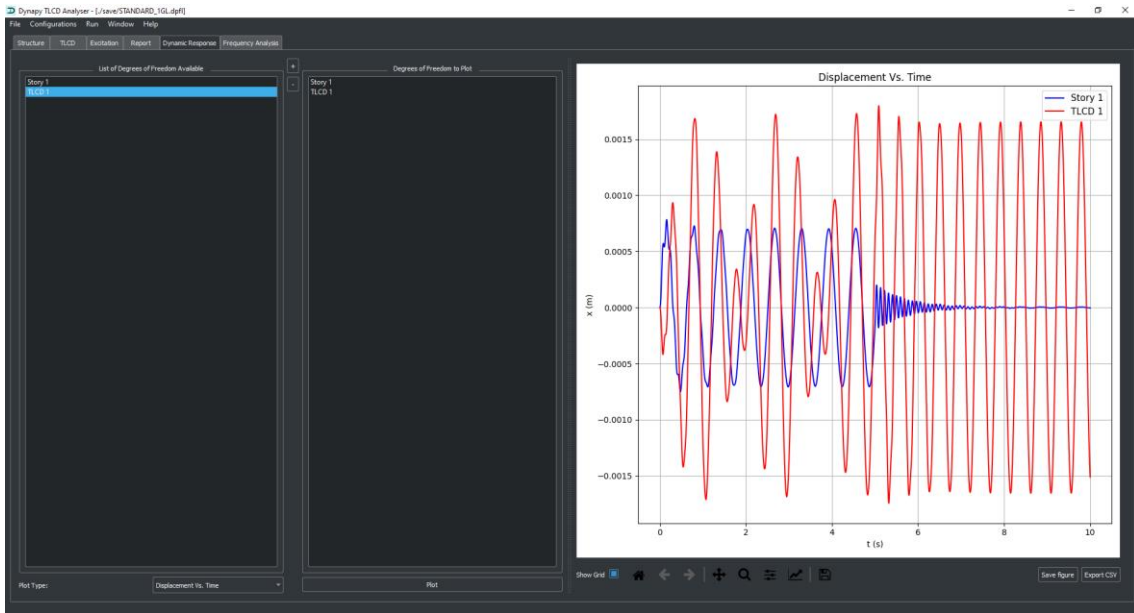


Figure A10 - Displacement vs time plot in the Dynamic Response tab

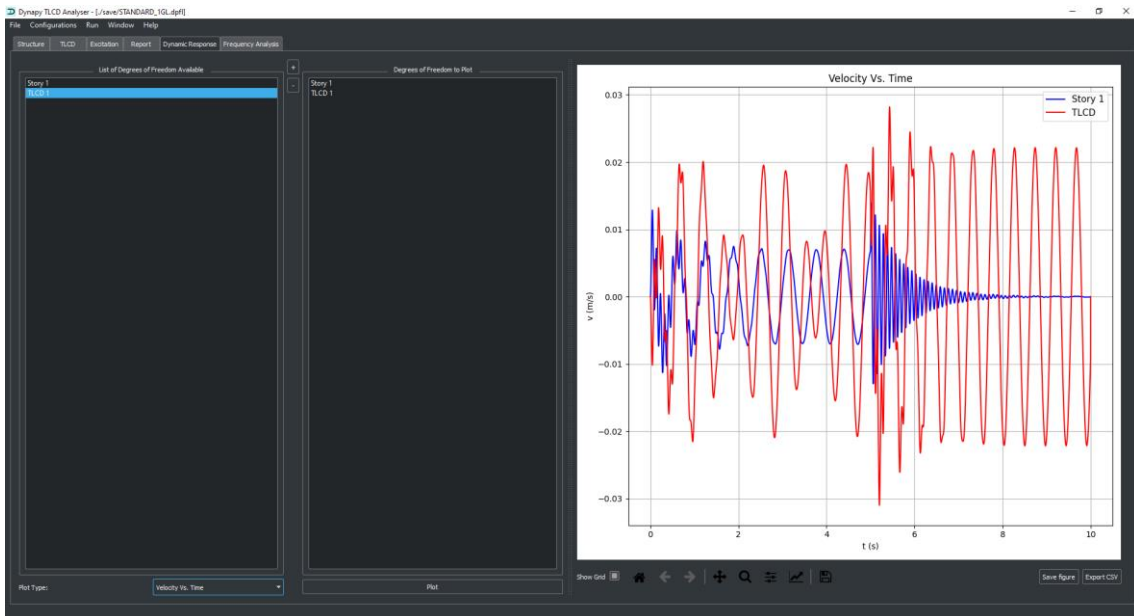


Figure A11 - Velocity vs time plot in the Dynamic Response tab

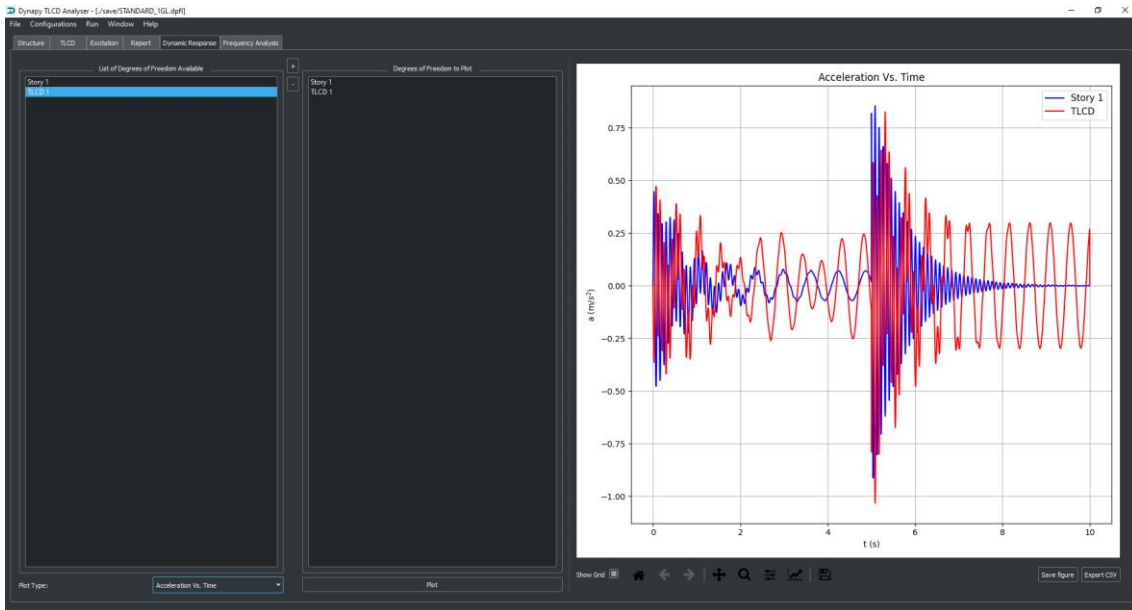


Figure A12 - Acceleration vs time plot in the Dynamic Response tab

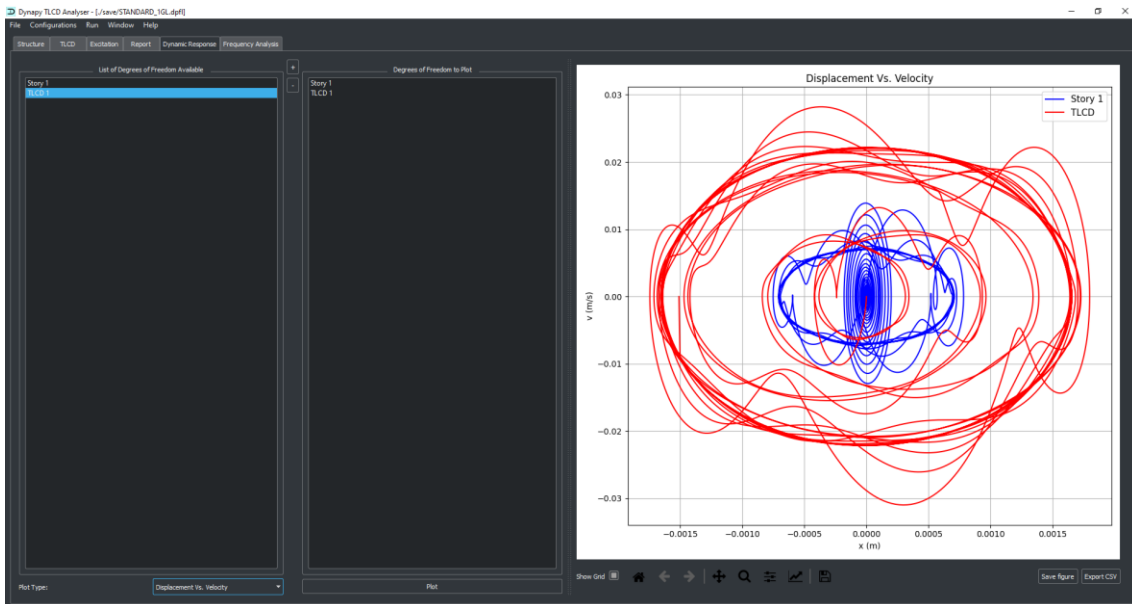


Figure A13 - Displacement vs velocity plot in the Dynamic Response tab

It is also possible to run a Dynamic Magnification Factor analysis, in which case the processed results are presented to the user in the Frequency Analysis tab. Just like in the Dynamic Response tab, the user can customize the canvas, export the plotted data and choose from the available plot type options. The results presented here are highly dependent on the DMF Settings chosen by the user in the Configurations tab, such as the number of points used in the discretization of the analysis.

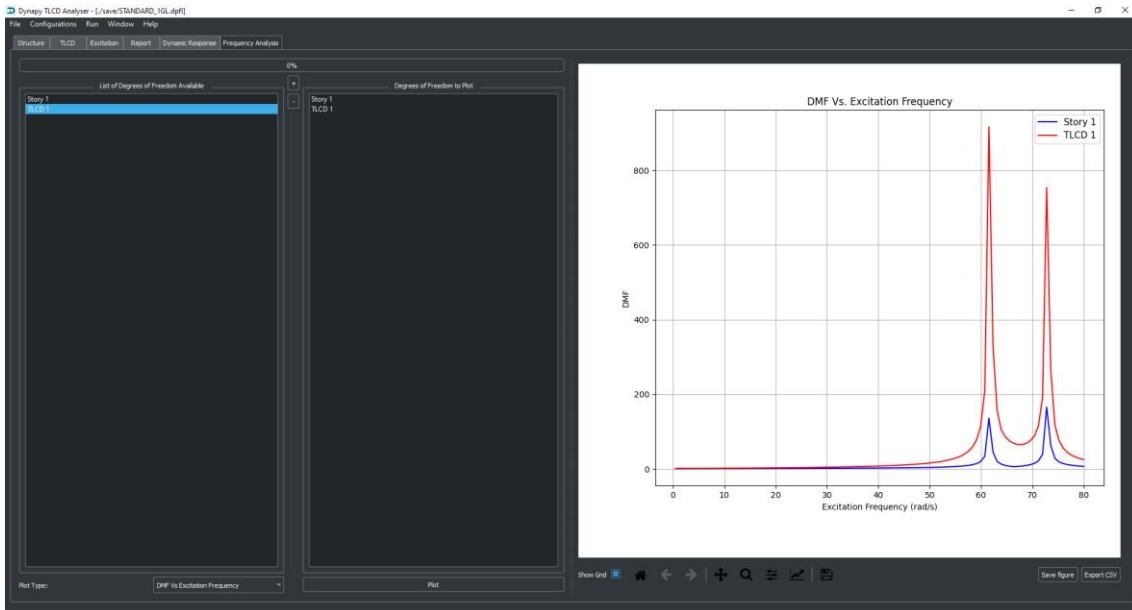


Figure A13 - Displacement vs velocity plot in the Dynamic Response tab

After a Dynamic Response is run, the Step-by-Step Mode option becomes available in the Run tab. It presents the results in a combined way and also shows the steps performed by DynaPy in the processing stage.

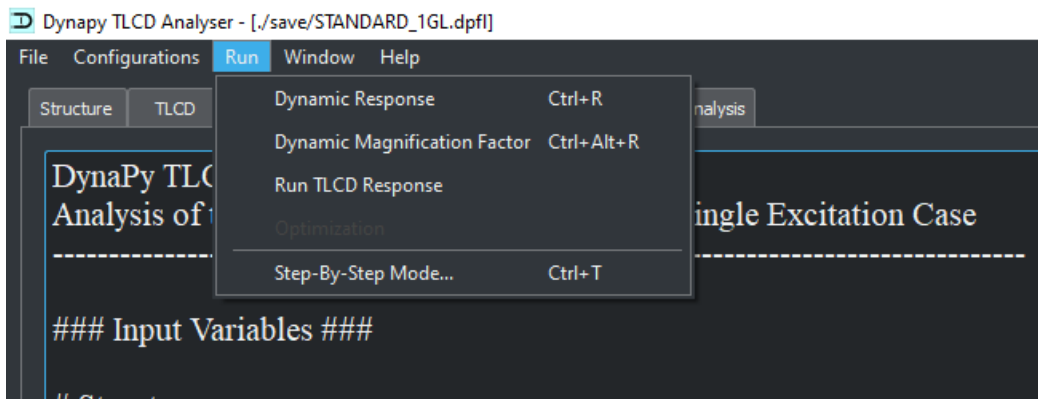


Figure A14 - The Step-by-Step Mode is no longer greyed out after a Dynamic Response is run

After clicking on the Step-by-Step Mode option, a new window opens up with three blank canvases located in the Inputs Summary tab. Clicking on “Load Results” displays the data from the pre-processing stage.

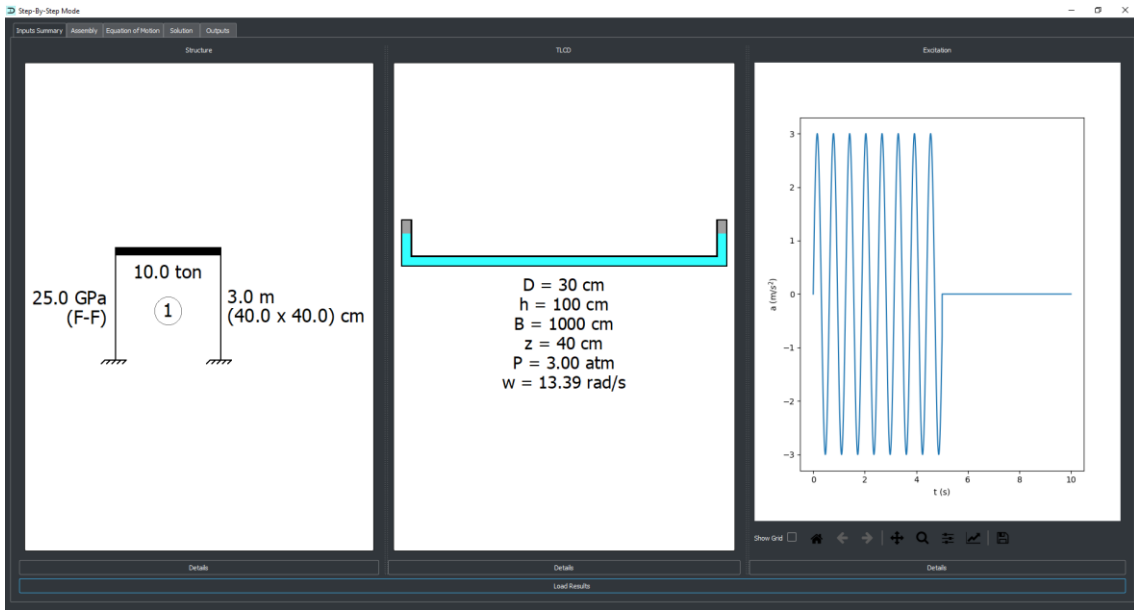


Figure A15 - Summary of the pre-processing stage in the first tab of the Step-by-Step Mode

Next, in the Assembly tab, the user can go through all the assembling of the matrices. The results can be displayed in a symbolic or in a numeric way



Figure A16 - Assembly tab of the Step-by-Step Mode

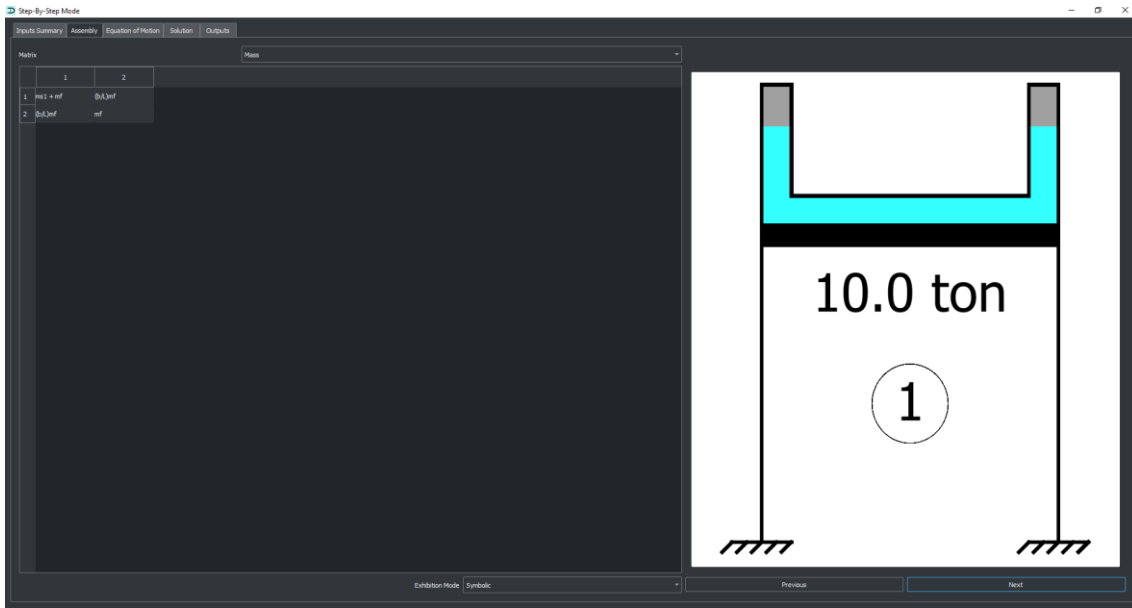


Figure A16 - Assembly of the mass matrix displayed in a symbolic way

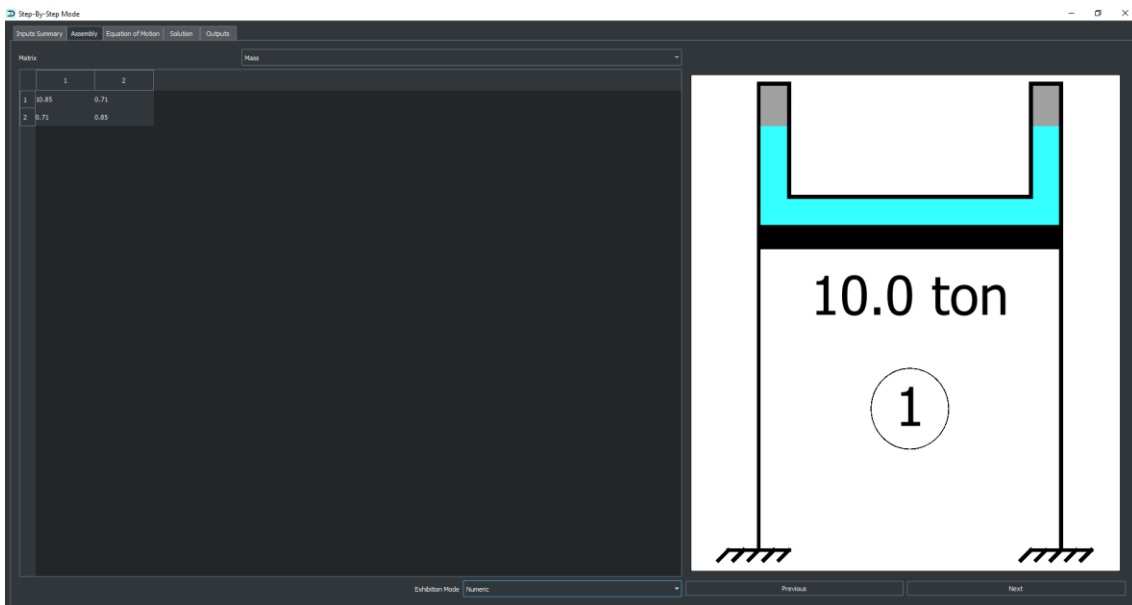


Figure A17 - Assembly of the mass matrix displayed in a numeric way

In the next step, the equations of motion are displayed in the Equation of Motion tab. They are a system of equations originating from the matrix equation and are displayed individually, line by line. Just like in the previous tab, it is possible to visualize them in a symbolic or in a numeric way.

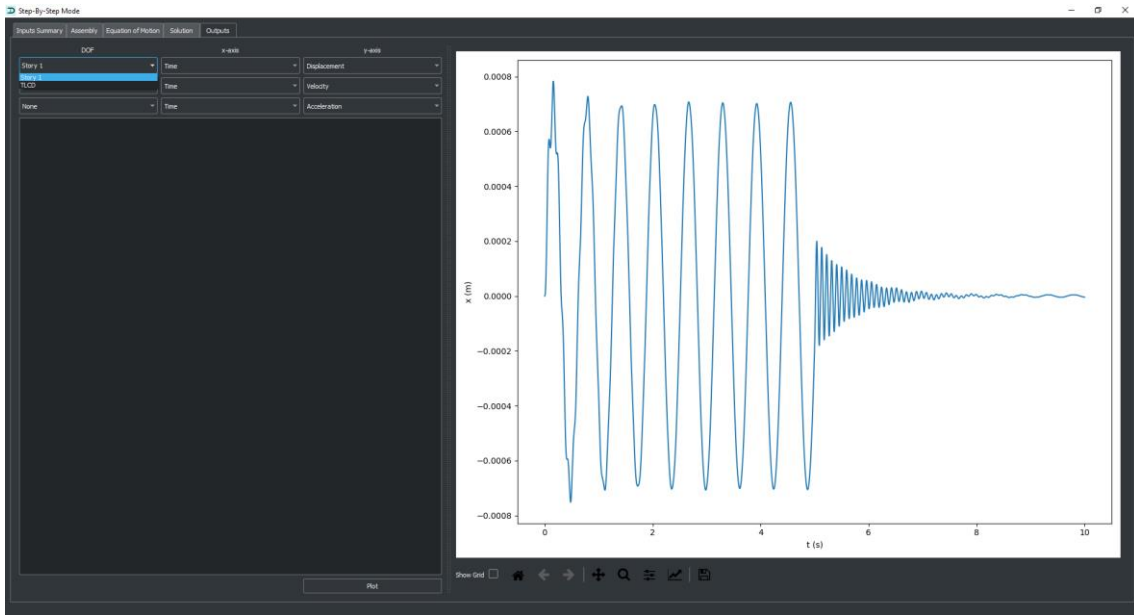


Figure A19 - Outputs tab with one plot

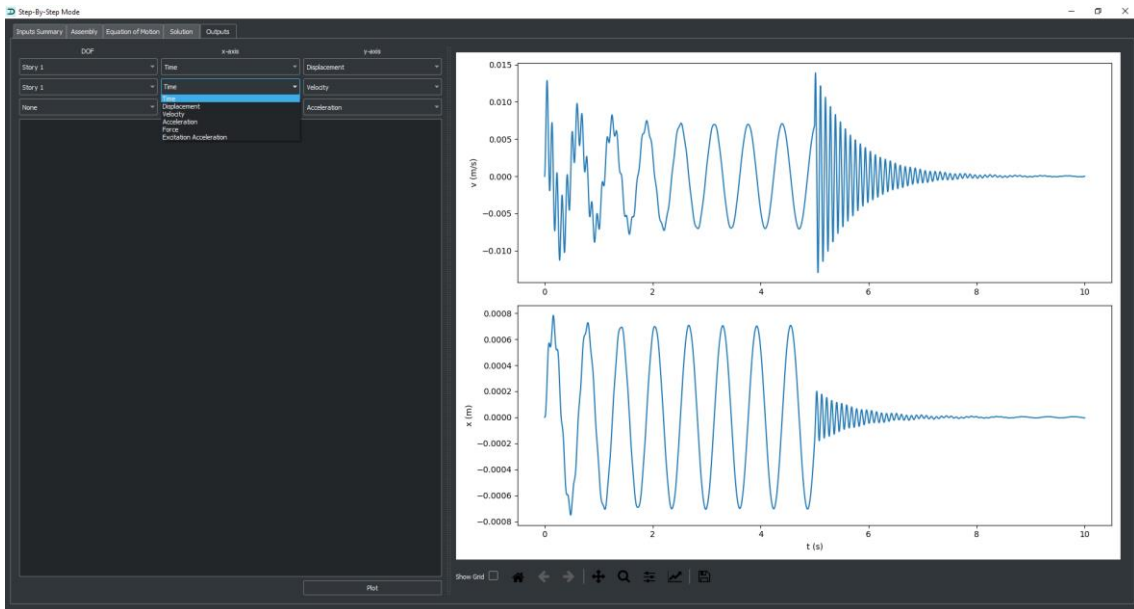


Figure A20 - Outputs tab with two plots

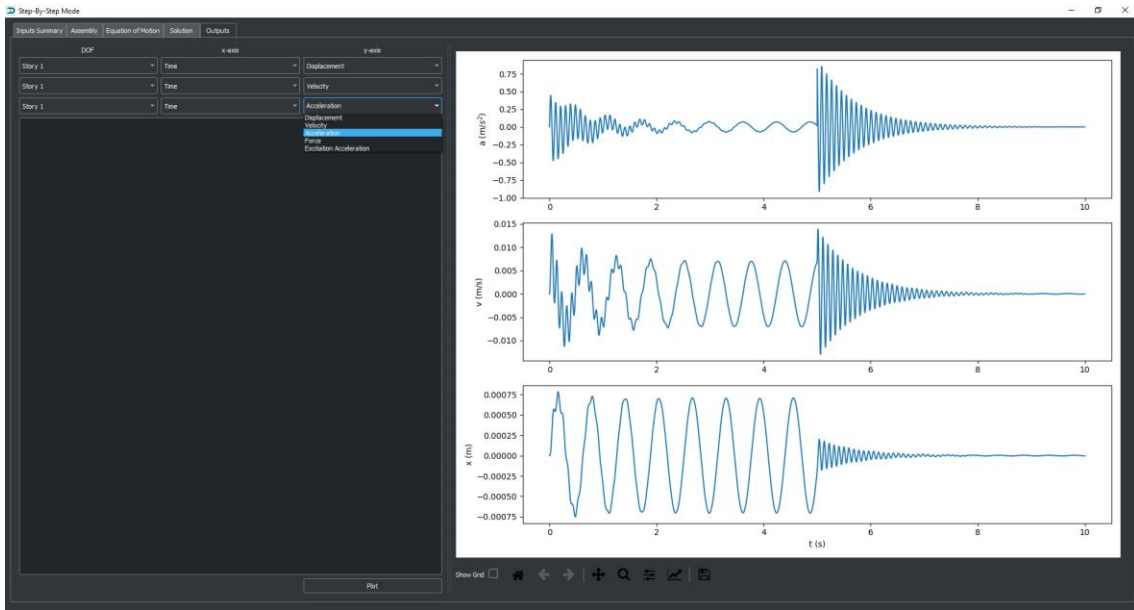


Figure A21 - Outputs tab with three plots

TAMARIS@CEA, SACLAY (FRANCE) A SYNERGY OF 4 SHAKING TABLES

TAMARIS (<http://www.tamaris.cea.fr/>) is a noble combination of Four Shaking Table (ST) Facilities (**Azalée**, **Tournesol**, **Mimosa** and **Vésuve**) was established in 1969 at Mechanical Seismic Studies Laboratory (EMSI) under the direction of Commissariat à l’Energie Atomique (CEA), Saclay, near Paris, France.

These ST Facilities are mainly dedicated to modeling and justification of infrastructures under dynamic loadings, deterministic and stochastic dynamics of nonlinear systems and interaction between fluid/soil with various infrastructures by utilizing sophisticated numerical tools (CAST3M, etc) within European collaborative research arena.

Specification	Azalée	Tournesol	Mimosa	Vésuve
Inauguration (Year)	1990	1976	1982	1969
Degrees of Freedom (DOF)	6	3	1	1
Payload	100 T	10 T	10 T	20 T
Test Platform (Area)	6x6 m (36 sqm)	2x2 m (4 sqm)	2x2 m (4 sqm)	3.8x3.1 m (11.78 sqm)
Maximum Ground Acceleration	1G	1G	4G	1.2G
Maximum Frequency	100 Hz	100 Hz	300 Hz	100 Hz



Array of 4 shaking tables



Silo containing sand on Vésuve



Model on Azalée